Politecnico di Torino

Master degree in civil engineering, infrastructure and transportation systems
A.a. 2023/2024
19/07/2024

Life Cycle Assessment on port pavements

Case study-Norvik Port

Supervisor:
Professor Maria Chiara Cavalli
Professor Lucia Tsantilis

Student:
Arianna Angelini

Index

Tables of figures 2
List of tables 4
Abstract 6
Introduction 7
1 Literature Review 9
1.1 Port Pavements 9
1.2 Materials employed in heavy duty pavements 12
1.2.1 Concrete overlays 18
1.2.2 Roller compacted concrete 19
1.3 Life Cycle Assessment (LCA) 22
1.3.1 Swedish methodology 25
1.3.2 UK methodology & case study 27
1.3.3 German case study, “cradle to cradle” methodology 29
2 Chapter 2 31
2.1 Norvik Port case study 31
3 Chapter 3 38
3.1 Structural design of port pavements 38
3.1.1 Application of the Heavy duty pavement manual to the case study 38
3.1.2 Application of AASHTO 1993 method to the case study 50
3.2 Life Cycle Assessment 65
3.2.1 Construction phase, concrete block pavements 66
3.2.2 Construction phase, rigid and flexible pavements 77
3.2.3 Maintenance phase 82
4 Chapter 4 84
4.1 Pavement designs 84
4.2 LCA results 88
4.2.1 Construction phase 88
4.2.2 Maintenance phase 96
4.3 Final results 100
5 Conclusions 100
Bibliography 103

Tables of figures

Figure 1.1.1: Suitability of pavements typologies based on various factors (Di Mascio et al., 2019) 10
Figure 1.2.1:Strcural design of an Interlocking concrete block pavement (Jamshidi et al., 2019) 13
Figure 1.2.2: Shapes of the concrete pavers (Jamshidi et al., 2019) 13
Figure 1.2.3: Example of load distribution on concrete block pavements (Jamshidi et al., 2019) 14
Figure 1.2.4: “LTE as a function of S/U” (Jamshidi et al., 2019) 15
Figure 1.2.5:Example of surface failure in ICBP (Jamshidi et al., 2019) 15
Figure 1.2.6: (c)grass germination, (b) surface dirt (Jamshidi et al., 2019) 16
Figure 1.2.7:construction costs of each pavement design (Di Mascio et al., 2019) 17
Figure 1.2.8:Example of pavement fatigue cracking after ATP testing (Sengun et al., 2024b) 20
Figure 1.3.1: Life Cycle Assessment(LCA) structure (Fastställd, 2006) 23
Figure 1.3.2: Total CO_2 emissions of the IVL report LCA analysis (Stripple, 2001) 26
Figure 1.3.3: Optimum LCA cycle (Huang et al., 2009) 27
Figure 1.3.4: 11 impact categories employed in the LCA methodology (Huang et al., 2009) 28
Figure 1.3.5: LCA cycle phases (Siverio Lima et al., 2021) 29
Figure 1.3.6:LCA results per category (Siverio Lima et al., 2021) 30
Figure 2.1.1: Norvik port aerial photo (J. D. Rodriguez Millan, 2024) 31
Figure 2.1.2: Detail of the composition of Norvik Port (J. D. Rodriguez Millan, 2024) 32
Figure 2.1.3:Plan details of the container terminal of Norvik Port (J. D. Rodriguez Millan, 2024) 33
Figure 2.1.4: Plan details of the Ro-Ro terminal of Norvik Port(J. D. Rodriguez Millan, 2024) . 34
Figure 2.1.5: Most damaged areas in Norvik port (J. D. Rodriguez Millan, 2024) 35
Figure 2.1.6:Handover spot in the container Terminal(J. D. Rodriguez Millan, 2024) 36
Figure 2.1.7: Ro-Ro terminal transit area (J. D. Rodriguez Millan, 2024) 36
Figure 2.1.8:Damage in the port area (J. D. Rodriguez Millan, 2024) 37
Figure 3.1.1:CBGM Base thickness design chart(Knapton, 2008) 39
Figure 3.1.2:Table 20 From Interpave manual(Knapton, 2008) 41
Figure 3.1.3: Container straddle carrier(Knapton, 2008) 41
Figure 3.1.4:Table19 from Heavy duty pavement manual, wheel proximity factor (Knapton, 2008) 42
Figure 3.1.5: Wheel spacing of the container straddle carrier(Knapton, 2008) 42
Figure 3.1.6: Container straddle carrier, subjected to the static wheel load 43
Figure 3.1.7: Table 17, Heavy duty pavements manual to calculate the dynamic factor (Knapton, 2008) 43
Figure 3.1.8: Base thickness of the container terminal pavement (Knapton, 2008) 46
Figure 3.1.9: base thickness of the Ro-Ro terminal (Knapton, 2008) 48
Figure 3.1.10:Composite modulus of subgrade reaction chart (AASHTO, 2001) 51
Figure 3.1.11: Chart to correct the composite subgrade modulus considering the presence of rigid foundation near surface (AASHTO,2001) 53
Figure 3.1.12: Loss of support values for different materials 54
Figure 3.1.13: Modulus of subgrade reaction corrected for loss of support (LS) (AASHTO, 2001) 54
Figure 3.1.14: Load transfer coefficient J (AASHTO, 2001) 55
Figure 3.1.15: Example of truck trafficking Norvik port (Knapton, 2008) 57
Figure 3.1.16:Example of trucks trafficking Norvik Port (Knapton, 2008) 57

Figure 3.1.17: Example of container straddle carrier (Liebherr Container Cranes Ltd., n.d.) 58
Figure 3.1.18:Table to evaluate the axle load equivalency factor, rigid pavements, single axles, pt equal to 3 (AASHTO, 2001) 60
Figure 3.1.19: Table to evaluate the axle load equivalency factor, rigid pavements, tridem/triple axles, pt equal to 3 (AASHTO, 2001) 61
Figure 3.1.20: Structural Number of the flexible pavement,(AASHTO, 2001) 64
Figure 3.2.1:Overview of the LCA of a generic road(Stripple, 2001) 65
Figure 3.2.2:display of the pavements currently used in port area(J. D. Rodriguez Millan, 2024) 66
Figure 3.2.3:Port pavements design(J. D. Rodriguez Millan, 2024) 67
Figure 3.2.4:LCA structure for the concrete blocks surface(Stripple, 2001) 67
Figure 3.2.5: structure of an LCA for a bituminous material(Stripple, 2001) 72
Figure 3.2.6: Structure of the LCA cycle of a generic unbound base of a road infrastructure(Stripple, 2001) 74
Figure 3.2.7:LCA cycle of a generic granular subbase (Stripple, 2001) 75
Figure 4.1.1: Distribution of concrete block pavements in Norvik port 85
Figure 4.1.2: Distribution of concrete block pavement in the container Terminal 85
Figure 4.1.3: Distribution of concrete block pavement in the Ro-Ro Terminal 86
Figure 4.2.1: Results of the LCA construction phase cycle on rigid pavements 89
Figure 4.2.2: Results of the LCA construction phase cycle on flexible pavements 89
Figure 4.2.3: Results of the LCA, construction phase on concrete block pavements 90
Figure 4.2.4: Results of LCA, construction phase of all pavement's designs 91
Figure 4.2.5: Results of the rigid pavements and the flexible pavements without a cement bound base 92
Figure 4.2.6: Results of the construction of concrete slabs and blocks 93
Figure 4.2.7: results of the construction of the asphalt layers 94
Figure 4.2.8: Results of the maintenance phase of flexible pavements 97
Figure 4.2.9: Results of the maintenance phase of concrete pavements 97
Figure 4.2.10: Results of the maintenance phase of concrete block pavements 98
Figure 4.2.11: Results of the maintenance phase of rigid, flexible and concrete block pavements 99
Figure 4.3.1: Results of the complete LCA cycle 100

List of tables

Table 3.1.1:Input data for the container straddle carrier 40
Table 3.1.2:dynamic wheel loads container straddle carrier 44
Table 3.1.3:Trucks input variables, container terminal 44
Table 3.1.4:input variable for the structural design of a container terminal pavement 45
Table 3.1.5:flexible pavement design 1, container terminal 46
Table 3.1.6: Flexible pavement design, full depth asphalt pavement, container terminal 47
Table 3.1.7:Rigid pavement design container terminal 47
Table 3.1.8:felxible pavement design in the Ro-Ro Terminal 49
Table 3.1.9: Full-depth asphalt pavement Ro-Ro terminal 49
Table 3.1.10:Rigid pavement design Ro-Ro Terminal 49
Table 3.1.11:Resilient moduli values [MPa] 51
Table 3.1.12: Input variables to calculate the slab thickness, D[inches], according to AASHTO 1993 55
Table 3.1.13:Loads in kips for each vehicle type 59
Table 3.1.14: Average passes of vehicles in each area (J. D. Rodriguez Millan, 2024) 59
Table 3.1.15: Total ESALs for the rigid pavement 62
Table 3.1.16: Rigid pavement design 1 AASHTO ‘93 62
Table 3.1.17: Rigid pavement design 2 AASHTO ’93 manual 62
Table 3.1.18:Input variables, flexible pavement, AASHTO 1993 63
Table 3.1.19:Final designs flexible pavements 64
Table 3.2.1:mix design of concrete used in the surface of the port pavements M1, M2, M3, M4 68
Table 3.2.2:Areas where the pavements are used, according to Figure 2.2.2 (J. D. Rodriguez Millan, 2024) 68
Table 3.2.3:Outflow data for the concrete block layer of the pavement(Stripple, 2001) 68
Table 3.2.4:Travel distance data used in the LCA cycle calculations (Stripple, 2001) 69
Table 3.2.5: $CO2$outflow concrete block pavements 70
Table 3.2.6:$CO2$ outflow for the LCA cycle of the sand layer (Stripple, 2001) 71
Table 3.2.7: Characteristics of the sand layer 71
Table 3.2.8: $eq.CO2$ outflow for the LCA cycle of the bituminous layers (Stripple, 2001) 73
Table 3.2.9:Travel distances covered in the LCA cycle for bituminous layers (Stripple, 2001) ... 73
Table 3.2.10: $CO2$ eq. outflow for concrete block pavements, asphalt layers 73
Table 3.2.11:Input data for a generic unbound base(Stripple, 2001) 74
Table 3.2.12:Charcteristics of the base layer (Balieu, 2022; J. D. Rodriguez Millan, 2024) 75
Table 3.2.13: Input data for a generic granular subbase (Stripple, 2001) 75
Table 3.2.14: Characteristics of the subbase layer(Balieu, 2022; J. D. Rodriguez Millan, 2024) 75
Table 3.2.15: $CO2$ eq. total outflow for concrete block pavements 76
Table 3.2.16: Flexible pavement in the Ro-Ro Terminal, Heavy duty pavement manual design 1 77
Table 3.2.17: Flexible pavement Ro-Ro terminal, Heavy duty pavement manual design 2 77
Table 3.2.18:Rigid pavement in the Ro-Ro Terminal, Heavy duty pavement manual design 77
Table 3.2.19:Rigid pavement Ro-Ro terminal, AASHTO ‘93 manual design 1 77
Table 3.2.20: Rigid pavement Ro-Ro terminal, AASHTO ‘93 manual design 2 77
Table 3.2.21:Flexible pavement Container terminal, Heavy duty pavement manual design 1 77
Table 3.2.22:Flexible pavement Container terminal, Heavy duty pavement manual design 2 78
Table 3.2.23:Rigid pavement Container terminal, Heavy duty pavement manual design 78
Table 3.2.24:Rigid pavement Container terminal, AASHTO 93 manual design 1 78

Table 3.2.25:Rigid pavement Container terminal, AASHTO 93 manual design 2 78
Table 3.2.26: Container and Ro-Ro areas..... 78
Table 3.2.27: Flexible pavement Container area, Heavy duty pavement manual design 1..... 79
Table 3.2.28:Flexible pavement container area, Heavy duty pavement manual design 2 79
Table 3.2.29:Rigid pavement total outflow container area, Heavy duty pavement manual design 79
Table 3.2.30: Rigid pavement container terminal, AASHTO ‘93 manual design 1..... 80
Table 3.2.31: Rigid pavement container terminal, AASHTO ‘93 manual design 2..... 80
Table 3.2.32:Fleixble pavement total outflow Ro-Ro terminal, heavy duty manual design 1..... 80
Table 3.2.33: Flexible pavement container terminal, Heavy duty pavement design 2..... 80
Table 3.2.34:Rigid pavement total outflow Ro-Ro terminal, Heavy duty pavement manual design 1..... 80
Table 3.2.35: Rigid pavement total outflow Ro-Ro terminal, AASHTO 93 manual design 1..... 81
Table 3.2.36: Rigid pavement total outflow Ro-Ro terminal, AASHTO 93 manual design 2..... 81
Table 3.2.37: $CO2$ eq. outflow flexible pavements 83
Table 3.2.38: $CO2$ eq. outflow concrete block pavements..... 83
Table 3.2.39: $CO2$ eq. Concrete block pavements 83
Table 4.1.1: Rigid pavement Heavy duty pavement manual design 86
Table 4.1.2: Flexible pavement design 1, Heavy duty pavement manual..... 86
Table 4.1.3: Flexible pavement design 2, Heavy duty pavement manual..... 86
Table 4.1.4: Rigid pavement design 1, AASHTO 1993 manual 87
Table 4.1.5: Rigid pavement design 2, AASHTO 1993 manual 87
Table 4.1.6: Flexible pavement design, AASHTO '93 manual 87

Abstract

There is an urgent need to develop sustainable infrastructure solutions. Considering this, it is of great importance to conduct LCA analysis due to the overall impact of the construction sector, which is around 30% of the energy consumption worldwide. Furthermore, the transport sector accounts for 24% of the total CO_2 emissions.

In light of this, the ELISA project, to which this thesis refers to, aims at improving the sustainability of infrastructures, by reducing energy and resource consumption, and creating a platform where it is possible to share knowledge and information, obtained using various technologies (J. D. Rodriguez Millan, 2024).

The main objective of this thesis is to evaluate the environmental impact of port pavements, through the use of the Life Cycle Assessment. In order to achieve that a concrete block pavement, employed at Norvik port, Sweden, is analysed and compared with two other design solutions, a concrete and a flexible pavement. Therefore the design of the two alternative pavements is assessed.

The pavements are designed referring to the Heavy duty pavement manual, by Jhon Knapton, published by Interpave, which provides a methodology to design port pavements. Subsequently, just for the sake of comparison, the designs are re-evaluated with the AASHTO ’93 manual, a commonly used method to design highway pavements.

To compare the rigid and flexible pavements to the concrete block ones, a Life Cycle Assessment is conducted considering both the construction and the maintenance phase. A Life Cycle Inventory is carried out, collecting all the necessary data for each step of the LCA from the “Life Cycle Assessment of roads”, realised by the IVL Swedish Environmental Research Institute. The functional unit adopted is one square meter of pavement, and the environmental impact is assessed through CO_2 equivalents (eq.).

The outcomes suggest that the construction phase has a more significant adverse environmental impact, when compared to the maintenance phase. The most crucial design, in terms of carbon footprint, is the concrete pavement. This is due the “production of cement”, which is the most crucial step in the construction phase, even when compared to the “production of bitumen”. Therefore the more environmentally friendly design, among those considered, is the fully flexible pavement. At the same time, the concrete block pavements have higher CO_2 eq. emissions, with respect to emissions of the flexible design solution, because of the concrete block surface.

Introduction

This thesis assesses the environmental impact of three different port pavements, by applying the Life Cycle Assessment (LCA) method. The chosen pavement designs are rigid, flexible and concrete block pavements designs. The last pavement technology mentioned is employed in Norvik Port, in the Southern part of Stockholm, Sweden, which is an important reference in this thesis.

As previously mentioned there is an urgent need to improve resilience and sustainability of critical nodes, such as ports. This comes as a consequence of the carbon footprint of the infrastructure field, which includes maintenance operations (J. D. Rodriguez Millan, 2024). Often this results in an inefficient process, due to lack of funding and updated data of the current infrastructure state, which lead to a damaged structure (J. D. Rodriguez Millan, 2024). This poses a risk to sustainability and efficiency of the node itself. Therefore it is necessary to use new methods to collect quality data, and estimate the future damage of the pavement, without relying entirely on a threshold system, which notifies us only when the infrastructure is already damaged (J. D. Rodriguez Millan, 2024). Once the new technologies have been put into place, it is necessary to find a way to implement them, in order to increase the efficiency of the system. These tasks have been further analysed in the PhD thesis "Smart pavement maintenance infrastructure operation through digital twins, case study of Norvik Port, Sweden" by (J. D. Rodriguez Millan, 2024). This study is a part of the ELISA project, which aims at improving the sustainability of infrastructures, by reducing energy and resource consumption, and creating a platform where it is possible to share knowledge and information, obtained using various technologies (J. D. Rodriguez Millan, 2024).

The present thesis work makes use of the data resulting from the traffic analysis and FEM model, in the PhD thesis by (J. D. Rodriguez Millan, 2024), to design alternative pavements solutions. Thereafter the designs are compared to the concrete block pavements in use, evaluating their carbon footprint through a Life Cycle Assessment (LCA).

The initial task is to design the rigid and flexible pavement designs using the Heavy duty pavement designs, and then re-evaluate them with the AASHTO '93 manual, a commonly used methodology to design highways pavements. This allows the analysis and comparison of two design methodologies.

Norvik port is composed of two functional areas, a container terminal and a Ro-Ro terminal. (J. D. Rodriguez Millan, 2024). The pavement's structural design is conducted making use of the traffic analysis performed in the PhD thesis "Smart pavement maintenance infrastructure operation through digital twins, case study of Norvik Port, Sweden" by (J. D. Rodriguez Millan, 2024). This analysis considers the presence of the terminals, and the operations of different vehicles within them. This results in various pavement designs, differentiated for the container terminal and the Ro-Ro terminal.

Whereas the concrete block pavements include a total of four designs, the differences between them are due to the various subgrade types they are laid on.

The main aim is to compare the CO_2 equivalent emissions of the presently employed concrete block pavement with the two alternative designs, a rigid and flexible one.

To compare these pavements a Life Cycle Assessment is conducted considering both, the construction and the maintenance phase. A Life Cycle Inventory has been carried out, collecting all the necessary data for each step of the LCA from the "Life Cycle Assessment of roads" realised

by the IVL Swedish Environmental Research Institute. The functional unit adopted is one square meter of pavement, the environmental impact is assessed through CO_2 equivalent, expressed in g/m^2.

1 Literature Review

This chapter commences with a description of ports, and the pavements technologies most used in those areas. Then it addresses the methods to improve resilience of flexible pavements, particularly for applications in port areas. It includes a description of a concrete pavement commonly used in heavy duty pavements. Lastly, it features a chapter dedicated to the Life Cycle Analysis (LCA), including various LCA case studies from around the globe.

1.1 Port Pavements

A port is a critical node where different activities are carried out, which require special areas. (Di Mascio et al., 2019). A port can be considered as an intermodal infrastructure where different modes of transportation take place, such as ocean freight, railways and roads. Moreover within the port it is possible to identify several functional areas, where different vehicles are working, such as (Di Mascio et al., 2019):

- Pedestrian areas, where safety requirements must be guaranteed under operating conditions (Di Mascio et al., 2019).
- Parking areas that can be divided into two categories:
    - Areas where only light vehicles can park. In this case the major risk for the deterioration of pavements is the solar radiation, which affects thermo-sensible pavements, or the long parking time, which can cause permanent deformations (Di Mascio et al., 2019).
    - Areas for heavy vehicles, where the loads applied on the pavements are significant and can lead to viscous phenomena (Di Mascio et al., 2019).
- Internal roads, used by both heavy and light vehicles (Di Mascio et al., 2019).
- Handling areas, where two different vehicles handle cargo. One is an unconstrained guides such as lift trucks, while the other is constrained such as an overhead traveling cranes (Di Mascio et al., 2019). The loads applied on the pavement can be considered analogous to the ones induced by airplanes however, dynamic loads are significant, and need to be accounted in the design phase (Di Mascio et al., 2019).
- Container storage, this area can be considered like a parking space for containers. Usually to optimize space the containers are parked in parallel rows (Di Mascio et al., 2019). It is very common to stack containers, generally up to three or four on top of each other. This means that the load spread on the pavement can reach 1000 kN on a square surface with a side of 61 cm^2 (Di Mascio et al., 2019).

Due to the composition of the port infrastructure, the design of the pavements is a crucial aspect (Di Mascio et al., 2019). This step needs to involve both an economical and technical analysis of the site, as the pavement's costs can lead up to 25% of the total construction cost (Di Mascio et al., 2019). The analysis should also include environmental consideration of the entire infrastructure, as the transport sector is responsible for 24% of the total CO_2 emissions worldwide(J. D. Rodriguez Millan, 2024). Further the overall impact of the construction sector is around 30% of the global energy consumption worldwide (J. D. Rodriguez Millan, 2024). Therefore, there is an urgent need to mitigate those numbers, and this is achieved only by the development of reliable, sustainable, high quality and resilient infrastructures (J. D. Rodriguez Millan, 2024). This will not only benefit the operations of critical nodes, which directly impacts the supply chain network, but the well-being of humans (J. D. Rodriguez Millan, 2024). Pavements play a crucial role in transportation and infrastructure sector, as a temporary damage of them can

lead to delays, and increase costs in the network. Therefore, the selection of materials is essential to guarantee the smooth work in specific infrastructures, like ports (J. D. Rodriguez Millan, 2024).

Specifically, four type of pavements are used in ports to accomplish all the tasks described previously:

- Flexible pavements where the surface is made with asphalt concrete. This material often experiences rutting and cracking due to longitudinal and shear stresses. The other layers are called base and subbase. The base is a cement or binder bound base, because the loads are significantly heavier than low volume roads or highways (Di Mascio et al., 2019). The subbase is usually composed of a granular material(Di Mascio et al., 2019).
- Rigid pavements where the wearing course is a concrete slab (Di Mascio et al., 2019). This can be laid on cement bound subbase or granular mixture (Di Mascio et al., 2019). The subbase layers can be one or two. Concrete slab can be reinforced, and it usually has a square pattern. (Di Mascio et al., 2019)
- Semi-rigid pavement, composed like flexible pavements with a cement bound layer. Usually they have a design life of 20 years. (Di Mascio et al., 2019)
- Concrete block pavements, the wearing course is usually composed of concrete blocks, laid over a bedding layer, a granular base and a subbase. (Di Mascio et al., 2019)

As previously mentioned the suitability of these pavements differs on various factors, those can be summed up in the following table Figure 1.1.1 (Di Mascio et al., 2019):

Type of Area	Type of Pavement		
	Semi-Rigid and Flexible	**Concrete**	**Modular Pavers**
Access and internal roads	😐 Suitable for light vehicles	😐 LCCA needs	😐 LCCA needs
Parking lots for heavy vehicles	☹ Avoid in presence of long period parking and oil spill	☺☺ Recommended solution	☺ Reasonable solution
Cargo handling	☹ suitable only for guided public transport	☺ reasonable solution	☺ suitable only for low-tangential stresses
Containers storage areas	☹☹ avoid if possible	☺ good solution	☺☺ recommended solution
Light vehicle parking	☺ reasonable solution	☺ suggested permeable concrete	☺ suggested vegetative and permeable blocks
Pedestrian	☺ even dirt road with anti-dusting bituminous layer	☹ LCCA needs	☺ reasonable solution

Figure 1.1.1: Suitability of pavements typologies based on various factors (Di Mascio et al., 2019)

As shown in Figure 1.1.1 flexible and semirigid pavements are not recommended in parking area, because of heavy loads, since this can lead to cracking and rutting of the pavement (Di Mascio et al., 2019). On the contrary rigid pavements do not experience rutting and are more prone to sustain high shear stresses and vertical loads (Di Mascio et al., 2019). However they tend to be more costly to maintain (Di Mascio et al., 2019). Moreover the production process of concrete is highly

resource demanding, as it produces 8250 Tons of CO_2 per kilometre (J. D. Rodriguez Millan, 2024).

1.2 Materials employed in heavy duty pavements

This sub-chapter describes and compares three pavements technologies widely used in port pavements; flexible, rigid and concrete block pavements. Then it addresses various ways to increase the resilience of asphalt pavements for heavy duty applications. Lastly, it includes a description of a widely used concrete pavement technology in heavy duty areas.

Interlocking concrete block pavements have been employed in heavy duty pavements for the first time in Northern Europe, specifically Rotterdam in the Netherlands (B.Shackel, 1990).

The history of segmental paving starts in the medieval era, because of the need to transport freight and people (B.Shackel, 1990). The first roads were made of stone stets, laid on a layer of coarse sand (B.Shackel, 1990). Stone stets provided a more even surface compared to cobblestones, previously used (B.Shackel, 1990). Since the early 19th century wood blocks started being used. Those were able to reduce noise coming from steel wheels and horses hoovers (B.Shackel, 1990). During the development of concrete blocks, two kinds of blocks were used:

1. The asphaltic blocks
2. The concrete blocks

In the first case, the blocks were realized as a mixture of bitumen and aggregates (B.Shackel, 1990). The concrete blocks developed quickly in Holland, where after World War II, there was a huge increase in population, which led to the need for new housing (B.Shackel, 1990). Therefor there was a shortage of bricks to use for pavements, and engineers resulted to concrete blocks (B.Shackel, 1990). Concrete block paving ended up being produced for 40% of the production cost of bricks, because of increasing mechanization and energy consumption (B.Shackel, 1990). Germany decided to shape the blocks like stone stets (B.Shackel, 1990). Concrete block pavements were more cost-effective and more versatile because of the different shaped units in the market (B.Shackel, 1990).

Nowadays the concept of pavement needs to adapt to consider new challenges, such as climate change and population growth (Jamshidi et al., 2019). These new infrastructures are referred to as Post Modern Pavement (PMP), in other words pavements that account for structural, sustainability and social-psychological requirements (Jamshidi et al., 2019). A study was conducted in Japan with the aims of considering Interlocking Concrete Block Pavements (ICBP) as PMP (Jamshidi et al., 2019).

This pavement type developed in Japan because of:

1. The oil crisis in the 1970s, which increased the asphalt price (Jamshidi et al., 2019)
2. The rise in the use of this material in Germany and western Europe, with satisfactory response (Jamshidi et al., 2019)
3. The economic growth of Japan, which resulted in an increase rate of car ownership (Jamshidi et al., 2019)

The pavement is usually structured as shown in Figure 1.2.1:

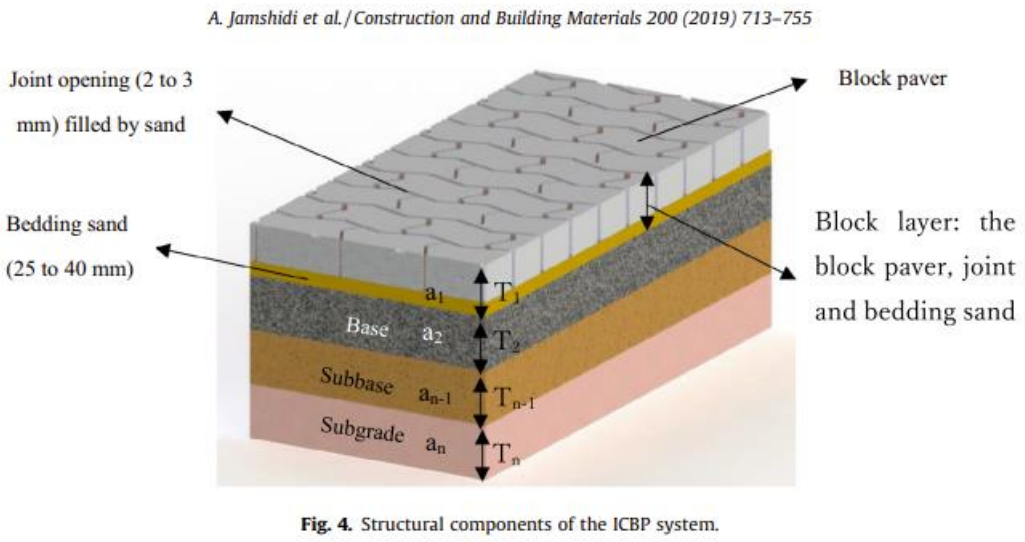

Figure 1.2.1:Strcural design of an Interlocking concrete block pavement (Jamshidi et al., 2019)

The paving blocks can have different shapes (Jamshidi et al., 2019):

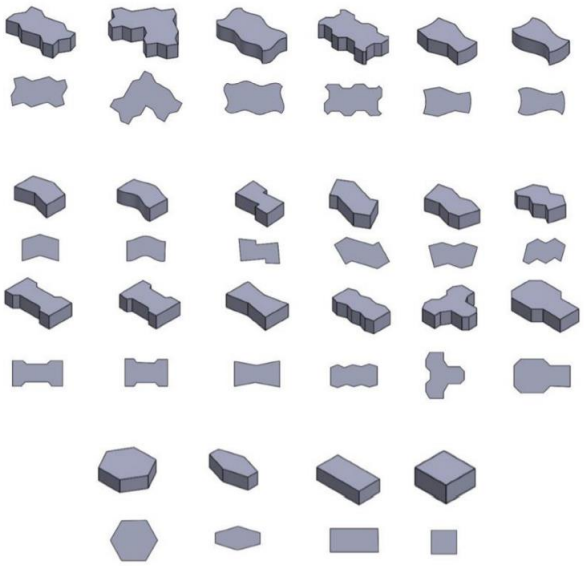

Figure 1.2.2: Shapes of the concrete pavers (Jamshidi et al., 2019)

The pavers in concrete block pavements have specific requirements, usually they have a length of 200mm – 250mm, a width of 100 mm – 120 mm, and thickness between 60 mm – 100 mm (B.Shackel, 1990). The bedding layer is usually sand and its thickness varies between 20 – 40 mm (Jamshidi et al., 2019). When using this type of pavement, there are several advantages compared to other types of pavements, such as (B.Shackel, 1990):

1. The manufacture is less expensive
2. It doesn't rely on the availability of petroleum
3. The equipment needed to lay them is less expensive
4. Concrete block pavement resists to loads and horizontal shear forces
5. They have a life span of 40 years, with full scale repairs every 20 years
6. During maintenance 90-95% of the original blocks can be reused

7. Excellent performance properties in heavy load areas
8. Able to withstand changing temperature and spillage of fuel

When designing ICBP there are different variables to consider, among which the interlocking phenomena is the most important (Jamshidi et al., 2019). The Japan Intellectual Property Association (JIPEA) has characterized the interlocking phenomena quantitatively with the Load Transfer Efficiency (LTE) (Jamshidi et al., 2019):

Equation 1.2.1:Load Transfer Efficiency (Jamshidi et al., 2019)

$$LTE = \frac{D_2}{D_1} \times 100$$

Where:

- D_1 is deflection at the edge of the block under a loaded condition of the block paver (Jamshidi et al., 2019)
- D_2 is the deflection at the edge of the block under an unloaded condition (Jamshidi et al., 2019)
- Assuming that D_0 is the deflection at the loading point (Jamshidi et al., 2019)

As shown in Figure 1.2.3:

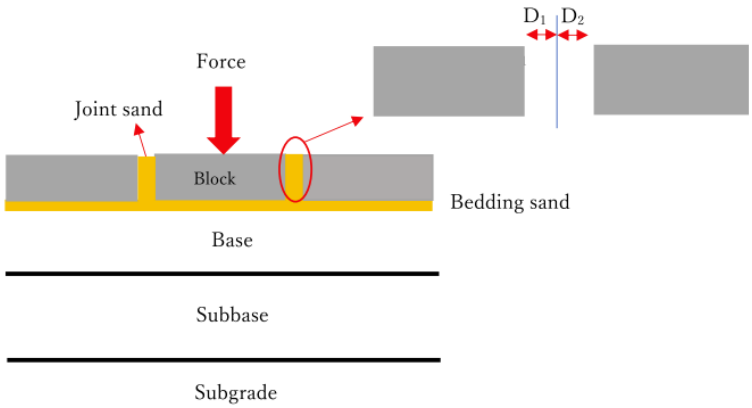

Figure 1.2.3: Example of load distribution on concrete block pavements (Jamshidi et al., 2019)

It is also possible to compare the behaviour of a concrete block to a concrete flag, analysing their LTE, as shown in Figure 1.2.4:

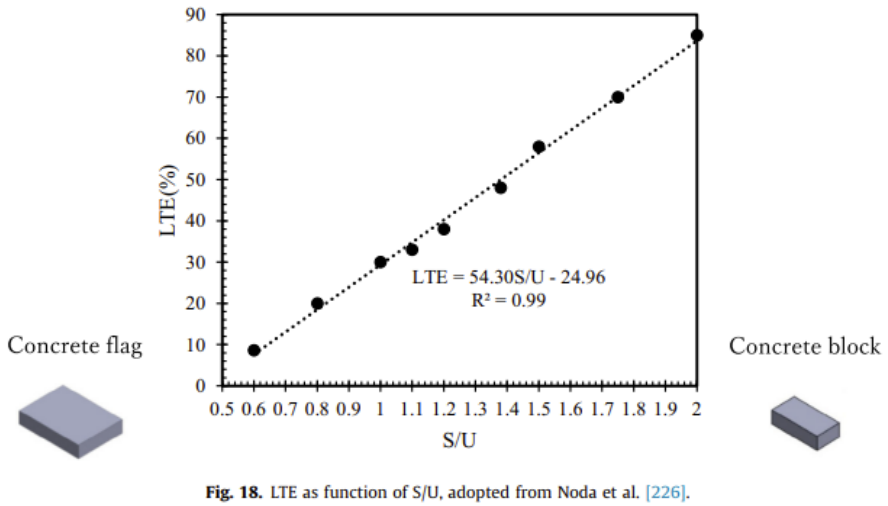

Fig. 18. LTE as function of S/U, adopted from Noda et al. [226].

Figure 1.2.4: "LTE as a function of S/U" (Jamshidi et al., 2019)

Where:

- (S) is the side area (Jamshidi et al., 2019)
- (U) is the upper surface area (Jamshidi et al., 2019)

It can be seen that the LTE increases linearly as the ratio increases, which means that the block pavers can develop interlocking owing to their higher LTE compared to concrete flags (Jamshidi et al., 2019). Therefore, it is safe to assume that the shape and dimensions of the concrete block are crucial.

Other characteristics of these pavements are that they tend to have a higher stiffness. (Jamshidi et al., 2019). As a consequence, they are ideal in low speed areas (Jamshidi et al., 2019). Moreover, the ICBP has lower noise emission when compared to concrete pavements (Jamshidi et al., 2019). It is also considered a safe pavement because of the block shape surface, which captures the driver's attention because of the block shapes, and it has a higher skid resistance when compared to asphalt pavements, both in wet and dry conditions (Jamshidi et al., 2019).

These pavements can be subjected to two different kinds of failures :

Figure 1.2.5:Example of surface failure in ICBP (Jamshidi et al., 2019)

As shown in Figure 1.2.5 one failure is characterised by cracking, chipping abrasion wear or joint sand loss. The other one is the structural failure due to cracking rutting or creep (Jamshidi et al., 2019). Compared to both flexible pavements and concrete pavements the ICBP have a more rapid maintenance (Jamshidi et al., 2019). This is due to the absence of binding materials, but critical issues can arise due to:

1. Grass germination (Jamshidi et al., 2019)
2. Surface dirt (Jamshidi et al., 2019)
3. Block laying process (Jamshidi et al., 2019)

Examples of the first two cases are shown in Figure 1.2.6:

(c) Grass germination

(d) Surface dirt and joint sand loss on the block layer

Figure 1.2.6: (c)grass germination, (b) surface dirt (Jamshidi et al., 2019)

When laying the blocks it is crucial to respect the joint tolerances (Jamshidi et al., 2019). This is a very labour intense task and it can be helpful to use the aid of a mechanical tool for installation (Jamshidi et al., 2019). This system has been employed in Kawasaki port, in Japan, where a sequence of 36 blocks per cycle were laid (Jamshidi et al., 2019).

In research interlocking concrete block pavements have been compared to rigid and flexible pavements in order to gain better understanding of their advantages and disadvantages, when applied in critical nodes, such as ports. In this research three pavement typologies have been designed using three different methods (Di Mascio et al., 2019):

1. Asphalt Institute method
2. The structural design of heavy duty pavements for ports and other industries manual
3. The Portland cement association method (PCA)

The objective of the research was to design three different pavements typologies and compare them under an economical and structural point of view. Usually flexible or semi-flexible pavements are not suitable to withstand heavy loads, as they trigger creep deformations (Di Mascio et al., 2019). Moreover those pavements are subjected to continuous deformation due to the change in temperature, and the rheological characteristics of bitumen lead to rutting and tangential stresses (Di Mascio et al., 2019). On the other side those pavements can be maintained easily (Di Mascio et al., 2019). On the contrary rigid pavement's maintenance and construction are expensive, but those pavements don't suffer from rutting (Di Mascio et al., 2019). Lastly block pavements are

suitable to sustain heavy loads for a long period of time, but it is better if they have rounded edges (Di Mascio et al., 2019).

Lastly an economic evaluation has been conducted, considering unit prices of construction and maintenance costs common in Northen Italy, as shown in table, Figure 1.2.7:

Type of Pavement	Construction Cost (€/m²)
Asphalt pavement	86.80
Concrete pavement	74.55
Concrete block pavement	58.52

Figure 1.2.7:construction costs of each pavement design (Di Mascio et al., 2019)

The economic analysis shows that the rigid pavement is the best economic option, although it is very close to the concrete block pavement, therefore a small change in the maintenance costs can alter the results (Di Mascio et al., 2019).

Although asphalt pavements didn't result to be the optimal solution, under the technical and economical point of view, studies have been conducted in order to improve their resilience (Sol-Sánchez et al., 2020). Several ports have been realized using flexible pavements, such as Hamburg Port, Germany. In certain situations this solution compared to the concrete pavement might be more cost-effective and versatile (Sol-Sánchez et al., 2020). In the majority of cases the type of asphalt mixture used is a High Modulus Asphalt Mixture (HMAM), usually made of aggregates of size 22mm–25mm, a hard binder and polymers, to improve mechanical performance (Sol-Sánchez et al., 2020). In research 5 mixtures of HMAM, in order to evaluate their properties when exposed to heavy loads (Sol-Sánchez et al., 2020). Those mixtures were then compare to a concrete sample, taken as reference (Sol-Sánchez et al., 2020).

Those mixtures were subjected to 3 laboratory tests:

1. Resistance to static punching stress due to storage of container (Sol-Sánchez et al., 2020)
2. Punching impact due to unloading actions of containers (Sol-Sánchez et al., 2020)
3. Resistance to rutting due to a combination of fuel leaks and heavy traffic (Sol-Sánchez et al., 2020)

Overall the results show that the type of bitumen used makes a difference in the sample's behaviour (Sol-Sánchez et al., 2020). Mixtures with conventional bitumen tend to present long deformation, and they have a higher susceptibility, as the stress increases. Whereas the HMAM with modified bitumen have a susceptibility comparable to concrete (Sol-Sánchez et al., 2020). Therefore the bitumen type is a critical component in the test (Sol-Sánchez et al., 2020). However in the second and third test the concrete sample shows the lowest deformation (Sol-Sánchez et al., 2020). In the third test, where the resistance to fuel and rutting is tested, concrete performs better than the asphalt mixtures, regardless of the type of bitumen.

In conclusion the study demonstrate that the type of bitumen plays an essential role in the asphalt mixtures (Sol-Sánchez et al., 2020). Furthermore the modified binder performed better when the level of load was increasing, resulting in a deformation which was 30% compared to concrete (Sol-Sánchez et al., 2020). Meanwhile the conventional bitumen mixtures registered a 60% deformation in reference to concrete (Sol-Sánchez et al., 2020). Therefore it concludes that the modified bitumen mixtures are a valid solution to be used as wearing course of a flexible pavement, in a critical node, as an alternative to the concrete slab (Sol-Sánchez et al., 2020).

1.2.1 Concrete overlays

Other ways to increase the resilience of flexible pavements, in the events of extreme weather conditions, such as flooding, are concrete overlays (King & Taylor, 2023). A research group has conducted a study in Australia, Queensland, comparing the behaviour of a flexible and a rigid pavement, considering data before and after a major flooding event (King & Taylor, 2023). The rigid pavement behaved in a more resilient way, because asphalt tends to transfer loads to the subgrade, therefore it needs a strong foundation (King & Taylor, 2023). Meanwhile concrete tends to distribute stresses over a wide area to the foundation (King & Taylor, 2023). Studies show that concrete overlays over asphalt pavements represent the most cost-effective solution, to improve resilience of existing pavements, without having to reconstruct the foundation (King & Taylor, 2023). A research has been conducted applying concrete overlay on flexible pavement after the flood in Iowa, United States of America, in 2008 (King & Taylor, 2023). Two design solutions were implemented:

1. Concrete overlay of asphalt (COA-B)., where the two are bonded (King & Taylor, 2023) The first solution was applied on two areas:
    a. The first where three inches of asphalt were milled (COA-B1) (King & Taylor, 2023).
    b. The second where asphalt was milled to a greater depth (COA-B2) (King & Taylor, 2023).
2. An unbounded concrete overlay of asphalt (COA-U), which requires a thicker concrete layer (King & Taylor, 2023)

These three solutions have been compared with the option of rehabilitation of the original flexible design, using a Life cycle Cost Analysis (LCCA) (King & Taylor, 2023). The conclusions of the study points out that the concrete overlay design is unaffected by flooding, meanwhile the opposite occurs in the flexible pavement (King & Taylor, 2023). Specifically, the first option COA-B1 was better suited for collector streets (King & Taylor, 2023). Meanwhile the COA-B2 becomes the most cost-effective strategy when the probability of annual flooding is between 5% and 25% (King & Taylor, 2023). Lastly the CAO-U design becomes a viable option at the event of an annual flood's, probability rate between 0 and 5%. However all three designs perform extremely well for high flood probability, in addition cost savings reach up to 350.000$ per mile, compared to rehabilitation strategy (King & Taylor, 2023).

1.2.2 Roller compacted concrete

When it comes to rigid pavements, the most used technique for industrial applications, is roller compacted concrete (RCC) (Sengun et al., 2024a). The mix design differs from the one of Portland Cement concrete (PCC) because it has a larger amount of fine aggregates and a lower water to cement ratio (Sengun et al., 2024b). Furthermore, the content of cement is lower, compared to regular concrete mixtures, with the different minimum value in the various countries (Sengun et al., 2024b). For example in the United States (US), the minimum content of cement to be employed is 270 kg/m^3, whereas in the European Union is 300 kg/m^3 (Sengun et al., 2024b). The mix design gives specific properties to the concrete. The higher presence of small aggregates helps in achieving a closed surface, whereas the use of larger size aggregates develops the interlocking process between aggregates, and it improves the load distribution at joints (Sengun et al., 2024a). Therefore it is crucial to define the main purpose of the mixture, in order to determine its composition (Sengun et al., 2024a). Further as reported by (Sengun et al., 2024a) the mechanical and durability characteristics of RCC are influenced by different parameters (Sengun et al., 2024a):

- binder content
- chemical and cementitious materials
- workability
- aggregates quality
- moisture content
- compaction level

Generally the flexural strength of RCC ranges from 4 MPa to 7 MPa, while the compressive strengths ranges from 30 MPa to 60 MPa. The Flexural stress can induce fatigue, and this is a crucial point when considering the thickness of the design. Recent studies suggest that RCC has a higher flexural strength and fatigue resistance than any other conventional concrete pavements. Another important phenomenon is the fracture mechanism, which influences the crack widths and their propagation (Sengun et al., 2024b). Although research in this field is still ongoing, the available studies suggest that RCC's fracture performance is comparable to conventional concrete. Another significant aspect is the shear-bonding strength between layers in multi-layer RCC pavements exceeding 25 cm. The main factor influencing fracture performance is placement delay. It can lead to a gradual reduction in RCC's fracture toughness and energy, resulting in a pavement vulnerable to crack propagation, under minimal loads. In this case it may be useful to employ fiber-reinforced RCC to reduce the section thickness and enhance fracture properties though crack bridging and shear load support. (Sengun et al., 2024b).

Therefore the RCC technology offers:

- rapid construction
- reduced traffic disruptions
- lower maintenance costs

All of those characteristics, together with the performance of those pavements, make them ideal design solutions for industrial areas, such as ports. However RCC has received limited attention when it comes to structural design, where the current methods seem to be conservative, and don't account for specific characteristics of critical nodes, such as ports (Sengun et al., 2024b).

According to the World Association for Waterborne Transport Infrastructure (PIANC,2015) heavy duty pavement's characteristics include. (Sengun et al., 2024b):

- Greater wheel loads due to heavy industrial equipment, than those encountered on highways
- Slow-moving handling equipment, which can result in deformation of flexible surfaces
- The presence of predetermined pathways along which vehicles move across
- The tires of industrial equipment tend to have higher pressure than those used in highway vehicles
- Wheel loads are amplified by dynamic movements, such as accelerating or braking
- Container resting on pavements contribute to deformation of softer surfacing materials.

A study has been conducted by the Louisiana Transportation research centre Teams (LTRC) to evaluate the performance and failure mechanism of RCC pavements. Six pavements sections, with RCC technology were realized, each of 20 meters length and 4 meters width, and an accelerated pavement testing (ATP) device simulating heavy vehicle loads was used. The results of the study highlighted how the cracks started to form on the RCC's surfaces on the spots where the tires were pressing. As the vehicles kept driving the cracks increased, and eventually they led to the pavement braking due to fatigue. This confirms that the pavements in heavy duty areas are likely to break down as a consequence of traffic stresses. (Sengun et al., 2024b)

Examples of pavement's fatigue cracking after accelerated pavement testing is shown in Figure 1.2.8:

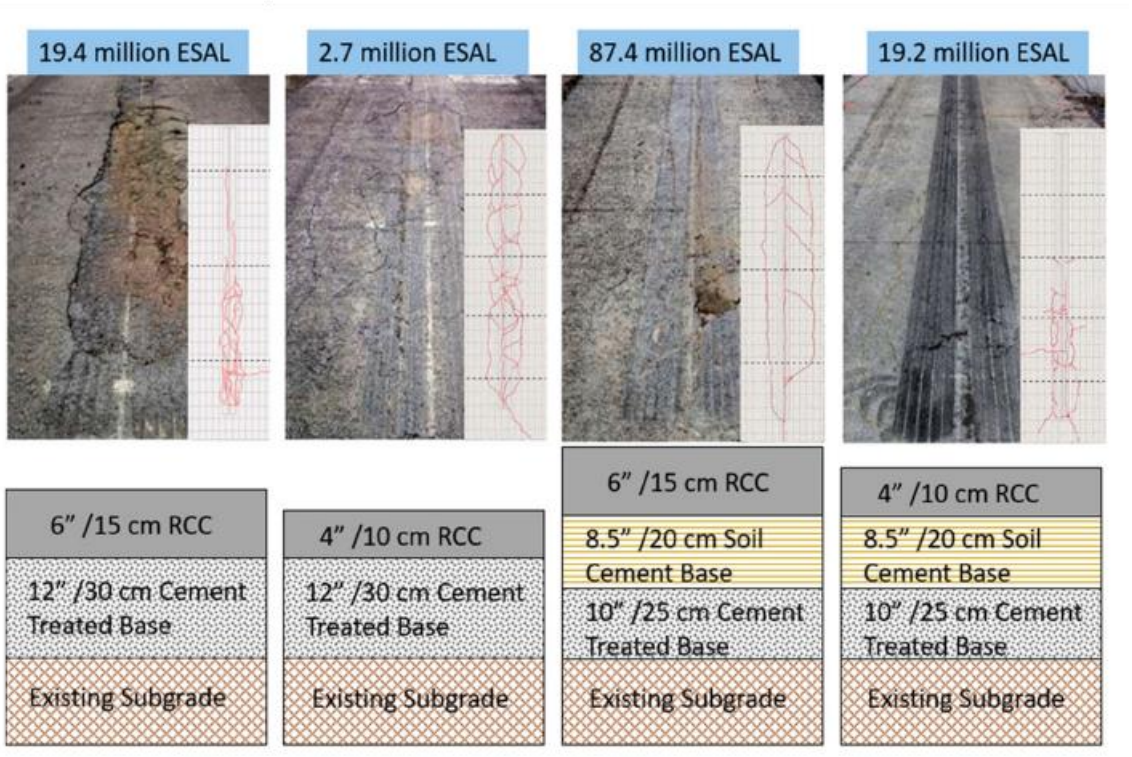

Figure 1.2.8:Example of pavement fatigue cracking after ATP testing (Sengun et al., 2024b)

Furthermore, when designing port pavements it is crucial to consider the presence of containers in the storage areas. To cum up, to understand the amount of stress on the ground it is essential to know how heavy the loads are, how they are spread out, and where they are in contact with the ground. In the design of rigid pavements the spots of interest are edges and corners, because those

places take the most strain. Therefore it is possible to conclude that it is fundamental to develop specific methods to account for the structural design of heavy duty pavements, such as ports. Moreover it is necessary to distinguish the material's properties of RCC to the ones of Plain Cement Concrete (PCC), as those affect greatly the pavement's performance. (Sengun et al., 2024b)

1.3 Life Cycle Assessment (LCA)

This chapter addresses the Life Cycle Assessment (LCA), a methodological framework to assess the environmental impacts associated with all stages of a products life. This chapter presents case studies from various parts of the world.

The Life cycle Assessment "addresses the environmental aspects and potential environmental impacts through a product's life cycle from raw material acquisition through production, use, end-of-life treatment, recycling and final disposal."(Fastställd, 2006) This approach is also referred to as "cradle to grave".

The concept of LCA was defined for the first time by the Resource Environmental Profile Analysis (REPAs)in the 1960s the concept of LCA was defined for the first time by the Resource Environmental Profile Analysis (REPAs). In the 1970s due to the scarcity of oil, there was the need to look for new sources of energy (Wintruff & Fernandes, 2023). As a result the LCA application was extended to different products. The LCA became popular in the United Sates in 1990s, and shortly expanded throughout the world. The International Organization for Standardization (ISO) has released two standards, the ISO 14040, and ISO 14044, with the scope to regulate the requirements and give guidance on how to conduct and LCA analysis (Wintruff & Fernandes, 2023). The LCA is generally divided into four parts (Wintruff & Fernandes, 2023):

1. Define the aim of the analysis
2. Do an inventory analysis
3. Evaluate the environmental impact of the product
4. Discuss the results

The first phase is focused on assessing the goal of the study, and the reasons behind it. It should comprehend the definition of the product system, which is the sum of the unit processes, each of them with a specific and defined function, that are used to model the LCA. Therefore it is necessary to define the unit processes, with their functional units, the system boundaries and the impact categories. Functional units are useful to identify a reference unit to which input and outputs, in the LCA, are related to. Whereas system boundaries define the unit processes that are comprised in the product system. Unit processes vary depend on the product the LCA is based on, however, they usually comprehend: raw materials, transportation, maintenance or use of substances, disposal operations and recovery.(Fastställd, 2006)

The second phase requires a Life Cycle Inventory (LCI), also referred to as inventory analysis, this is the step during which data is collected and the calculations are developed. The data refers to each unit process identified, and it includes: energy of raw materials inputs, products waste, emissions to air or the release of water. The calculation process includes the verification of the data collected. Then the data is related to the unit process it refers to, and, ultimately it is related to the functional unit of the LCA. (Fastställd, 2006)

The third step involves the development of the Life Cycle Impact Assessment (LCIA). This phase includes the assessment of environmental impacts of the LCA, and the association with the inventory data. This steps addresses only the impacts related to the environment and specified in the aim. There are several limitations to this phase, which are due to the presence of uncertainty in the collected data, the presence of limiting system boundaries that exclude some unit processes, and limited data to refer to.

Finally the last step is related to the discussion of results, it involves a report, which includes the relationship between the LCIA and the LCI data, the impact categories addressed, a description of the data used.

Overall the LCA should be structured as shown in:

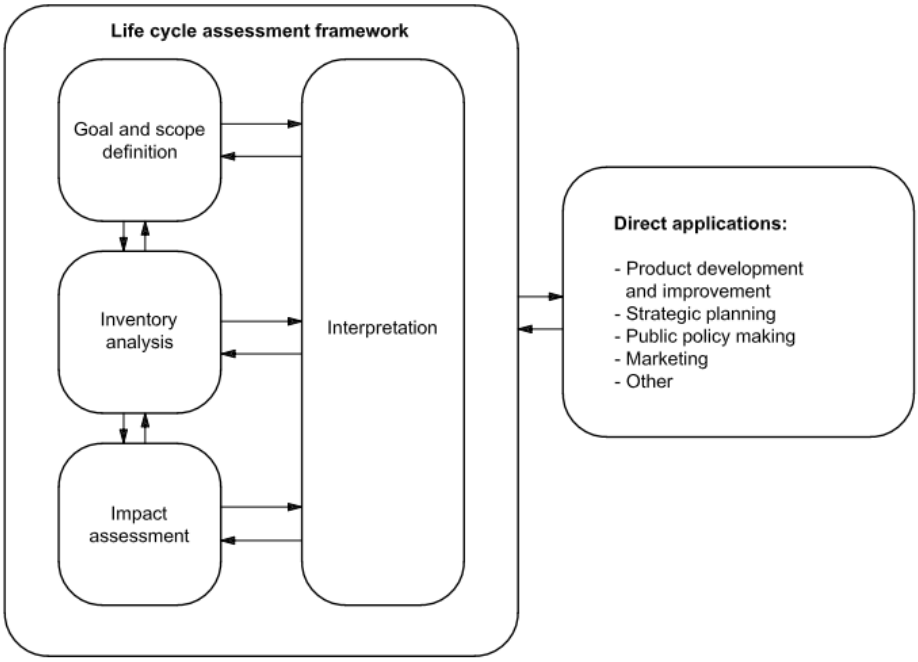

Figure 1.3.1: Life Cycle Assessment(LCA) structure (Fastställd, 2006)

The ISO recognize two types of studies, the LCI and the LCA, where the first one excludes the LCIA phase. (Fastställd, 2006)

The LCA has both strengths and weaknesses. It is comprehensive as it allows the evaluation of the product's impact across its life, it is an extremely valuable tool when it comes to decision making. It can be used to find the opportunity to improve a specific area that is characterized by a high environmental impact (Wintruff & Fernandes, 2023). On the other hand it is extremely important to have reliable data, otherwise the results may be inaccurate, it can be difficult to be implemented by non-experts, as it requires specific software and structure (Wintruff & Fernandes, 2023). In the infrastructure field LCA is a valuable tool as the environmental impact of pavements is enormous. The LCA covers a variety of factors, for example, the destruction of wildlife habitats as a result of clearing operations, and, the use of heavy vehicles in the construction and maintenance stages, which not only contributes to CO_2 emissions, but to noise pollution.

The main limits of the LCA on pavements is that it doesn't account for all the steps (Wintruff & Fernandes, 2023). For example often time earthworks are omitted, but those alone contribute to 60 – 85% of the emissions in the construction stage (Wintruff & Fernandes, 2023). Nevertheless Life Cycle Assessment (LCA) has proven to be a valid tool when it comes to decision making, especially when coupled with performance criteria, in the infrastructure sector. This course of action allows to conduct a comprehensive analysis of the possible design solutions, in order to evaluate the optimal one.

The subsequent chapter includes a short description of the most common LCA methodologies employed in Europe, among which the first LCA database example for road construction and maintenance, issued by the Swedish institute. This is followed by a short description of other common database in Europe, and a description of a UK LCA model, which includes the presence of recycled materials in asphalt pavements. Lastly, a German case study, which employs the "cradle to cradle" LCA methodology.

1.3.1 Swedish methodology

One of the first Life Cycle Inventory for the construction and maintenance of a concrete or asphalt road has been released by the IVL Swedish Institute. This institutes developed a model composed of process units, which can be added up to dynamically simulate the different road systems. This methodology follows the Society of Environmental Toxicology and Chemistry (SETAC) guidelines.

Generally an LCA cycle is composed of four steps (Stripple, 2001):

1. Goal definition
2. Inventory Analysis
3. Impact assessment
4. Improved assessment

Although the last category is not included in the IVL report.

Once the aim of the study is defined it is necessary to conduct an inventory analysis to define the data that need to be used. The methodology used by this report is referred to as “cradle to grave”. Therefore all inflows need to be referred back to the “cradle”, such as the extraction of raw materials, and the outflows to the “grave”, which is the end of life of the material. The inventory analysis collects inflows and outflows, and relates them to a functional unit, which is a reference unit used in the analysis. The third category involves the classification of the inflows and outflows. The main impact categories to be referred to are (Stripple, 2001):

1. Resource consumption
2. Health effects
3. Ecological effects
4. Inflows traced back to the cradle
5. Outflows traced to the grave

Then the flows need to characterized. Therefore the contributions from each flow are combined to provide a total impact for the specified category. (Stripple, 2001)

The aim of this report is to produce an LCA cycle for the construction and maintenance phase of concrete and flexible roads. The functional unit used is 1km of road length, and width of 13m. The model is composed of a number of sub-components, that are summed up to calculate the final environmental impact of the construction or maintenance of the pavement’s layers. Therefore the report collects all the data necessary to structure the cycle in each phase. The Appendix contains a database accounting for energy and resource consumption, specification for the road object and for the process. The data accounts for different pavement designs, a concrete road, a hot method asphalt road and a cold method one. The environmental impact is assessed through several indicators, among which the total energy use, and emissions of NO_x , SO_2, CO_2. Regarding the carbon footprint of the road surfaces analyzed, the report concludes that the construction process has the highest environmental impact in all the designs. Overall the most crucial case is the concrete road, as it is shown in the figure below: (Stripple, 2001)

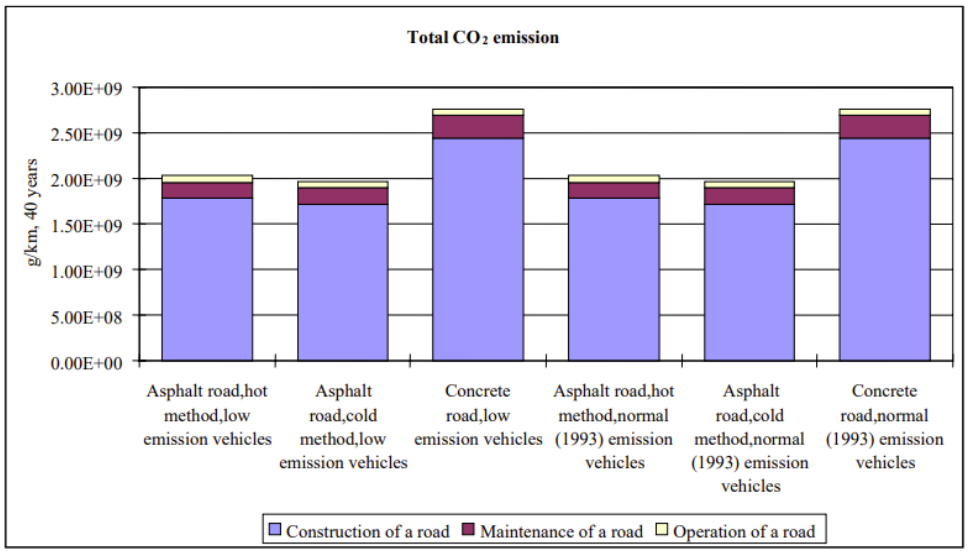

Figure 1.3.2: Total CO_2 emissions of the IVL report LCA analysis (Stripple, 2001)

1.3.2 UK methodology & case study

As previously mentioned the LCA is a powerful tool when it comes to decision making. It is accepted in the infrastructure and transportation industry globally, especially in the pavement sector. However the technologies used to realize pavements have evolved throughout time. Especially when it comes to asphalt pavement the use of recycled, and secondary material has increased rapidly, in the last years. Therefore there is an urgent need to account for the carbon footprint of these new designs, using the LCA analysis. (Huang et al., 2009)

The LCA is a common tool in Europe, the European LCA HUB holds a list of resources to refer to, such as books, journals and software. Since the 1990s the LCA started to develop rapidly throughout Europe, the first Life Cycle Inventory (LCI) was released by the Swedish Environmental Research Institute (IVL). This manual contains a procedure to account for environmental impacts of road construction and maintenance in both rigid and flexible designs. In 1998 an LCI study was released by the European Asphalt Pavement Association (EAPA), which included the use of Reclaimed Asphalt Pavement (RAP). The Technical Research Centre of Finland (VTT) released in 1996 a study comparing environmental impacts of rigid and flexible pavements. Shortly after, in 1998 the UK published the Built Research Establishment (BRE), which includes a database accounting for the environmental impact of the performance of materials used in buildings. The Technical University of Denmark followed with the publishment of an LCA methodology to construct roads using solid waste incineration, in 2005. (Huang et al., 2009)

However recently a new LCA model has been released by a research group in the United Kingdom (UK), and it has been applied to the realization of an asphalt pavement at London Heathrow (LHR) airport, Terminal 5. The aim of the research study was to obtain an LCA model that was accounting for the use of recycled materials in the pavement, referring to a UK database, fully compliant with the ISO 14040 standard, and easy to access. (Huang et al., 2009)

The optimal LCA should be developed as shown in Figure 1.3.3:

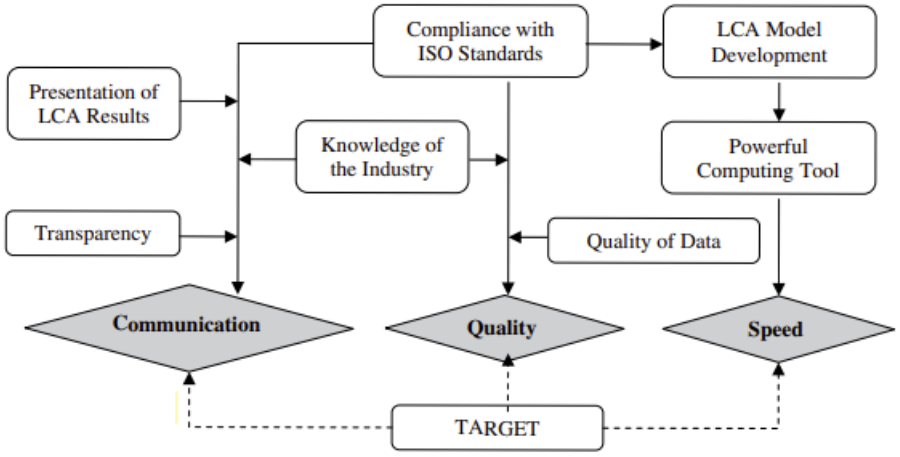

Figure 1.3.3: Optimum LCA cycle (Huang et al., 2009)

This model uses Microsoft Excel for the calculation and the representation of the results of the LCA. The software is divided into 5 worksheets:

1. Process parameters

2. Pavement parameters
3. Unit inventory
4. Project inventory
5. Results

The first category includes data on transport distance, expressed in km, energy efficiency of vehicles (litre/km), and the energy used to produce materials (MJ/t), and pavement construction (MJ/m^2). The data is taken from European studies, and UK contractors. The second category accounts for dimensions and materials used in pavements, and it includes mix designs recipes. There are three main groups of data: pavement dimensions, materials recipes and pavement lifetime. The data is usually collected from national material suppliers. The third category is aimed at applying an environmental input and output to the unit process. The fourth category is referencing all the data collected to the unit, used in the project. (Huang et al., 2009)

Lastly, the final point is involving the characterization of results, this is conducted taking into account 6 impact areas. Based on the data from the Refined bitumen Association (RBA), Quarry Products Associations (QPA), and Highway Agency in the UK, 11 impact categories are set for this model, and they are displayed in Figure 1.3.4:

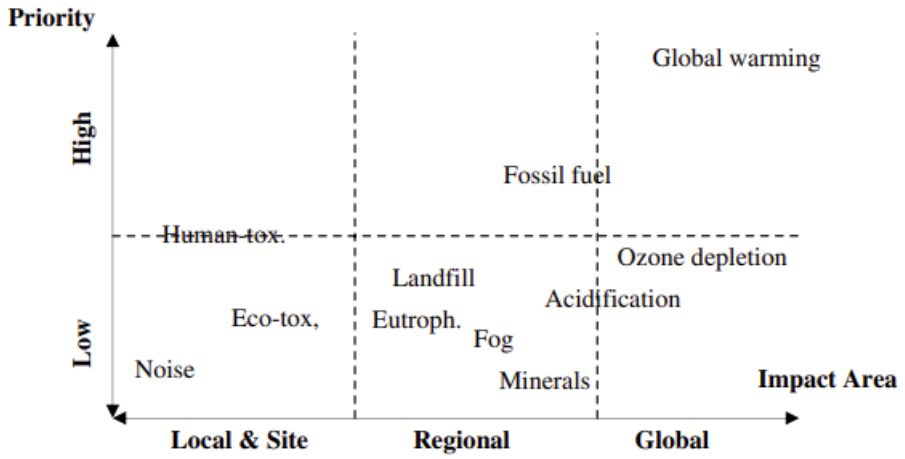

Figure 1.3.4: 11 impact categories employed in the LCA methodology (Huang et al., 2009)

This method has been applied to study the environmental impact of the London Heathrow terminal 5 asphalt pavement. In this study natural aggregates are replaced with RAP and glass incinerator bottom (IBA). The model is structured as explained before, therefore the first inputs are the process parameters and pavement ones, which involve the asphalt mix design used. The environmental inputs include raw materials and energy and the outputs are emissions to air water and solid waste. The functional unit used is 30 000 m^2 of asphalt surface. One of the main environmental indicator is CO_2 emissions. The results show that the production of bitumen and asphalt mix contribute the highest to the environment. Lastly, the study stresses that it is crucial to have an LCA model that is able to account for different asphalt mix designs, the presence of different recycled material in flexible pavements designs, and different techniques, such as hot mix or cold mix. (Huang et al., 2009)

1.3.3 German case study, "cradle to cradle" methodology

There are different methodologies to conduct LCA analysis. Usually the most common one is referred to as "cradle to grave" approach, where the materials are processed in the LCA until their end of life. Whereas in this case study the "cradle to cradle" with a closed loop recycling is employed (Siverio Lima et al., 2021). This means that 100% of the materials are recycled in the production chain (Siverio Lima et al., 2021).

This methodology is applied for the LCA of the city of Münster, Germany, in order to understand how to improve the environmental impact of the road pavements.

The raw material, in the cycle, are obtained from different locations in Europe, and then transported to the construction site, whereas the reclaimed asphalt pavement (RAP) is a result of the milling process of the city's pavements, and it needs to be treated before being used (Siverio Lima et al., 2021). The steps included in the LCA cycle are shown in the figure below (Siverio Lima et al., 2021):

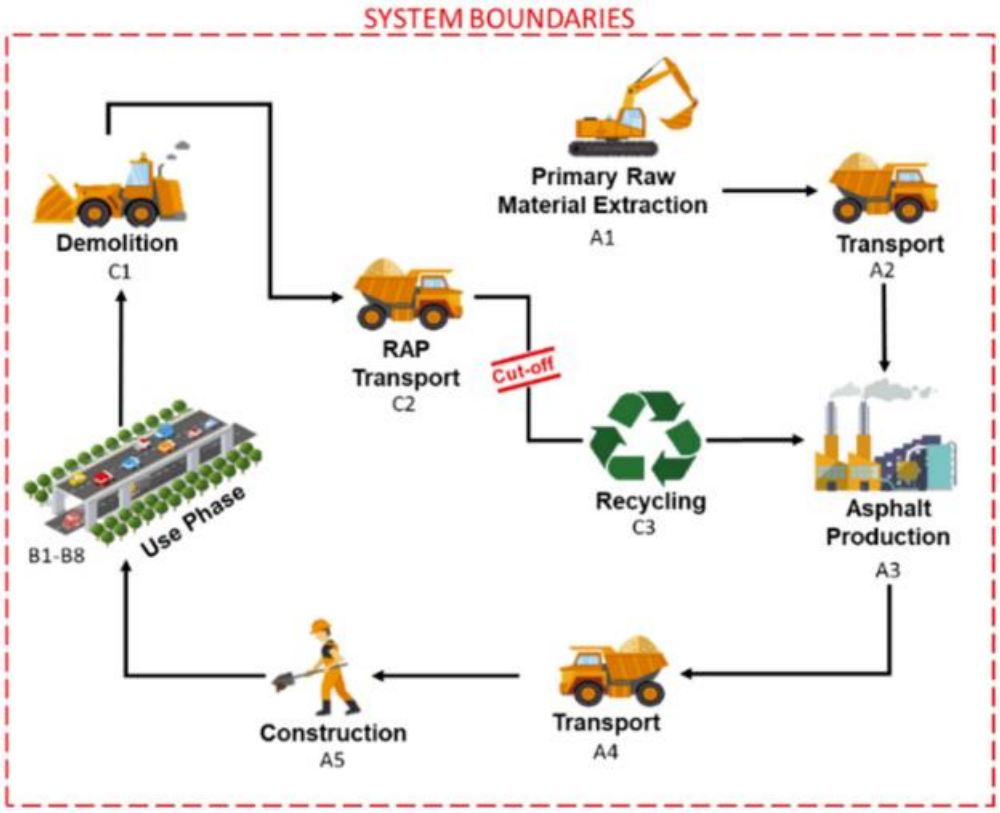

Figure 1.3.5: LCA cycle phases (Siverio Lima et al., 2021)

The functional unit is 1 m^2 of pavement (Siverio Lima et al., 2021). The results of the LCA analysis show that overall the modified pavements show a lower environmental impact (Siverio Lima et al., 2021). The longer the life span of the pavement the higher is the environmental benefit of using RAP in flexible pavements (Siverio Lima et al., 2021). The analysis has been carried out for different life spans; 20, 50, 80, and a 100 years (Siverio Lima et al., 2021). Furthermore the analysis takes into account the environmental impact in the form of Global warming production (GWP) estimating the kg of CO_2 eq., and the non-renewable cumulative energy demand (nr-CED) (Siverio Lima et al., 2021).The pavements strategies in use are two different, and they are referred to as "A" or "B", and depend on the period in which the operation is carried out (Siverio Lima et

al., 2021). The results per category show that the more impacting stages are (Siverio Lima et al., 2021):

- Production, covering the 78% of the overall nr-CED results, and 55% of the GWP ones
- Transportation, covering 20% in the nr-CED, and 36% in the GWP

As it is shown in the figure below (Siverio Lima et al., 2021):

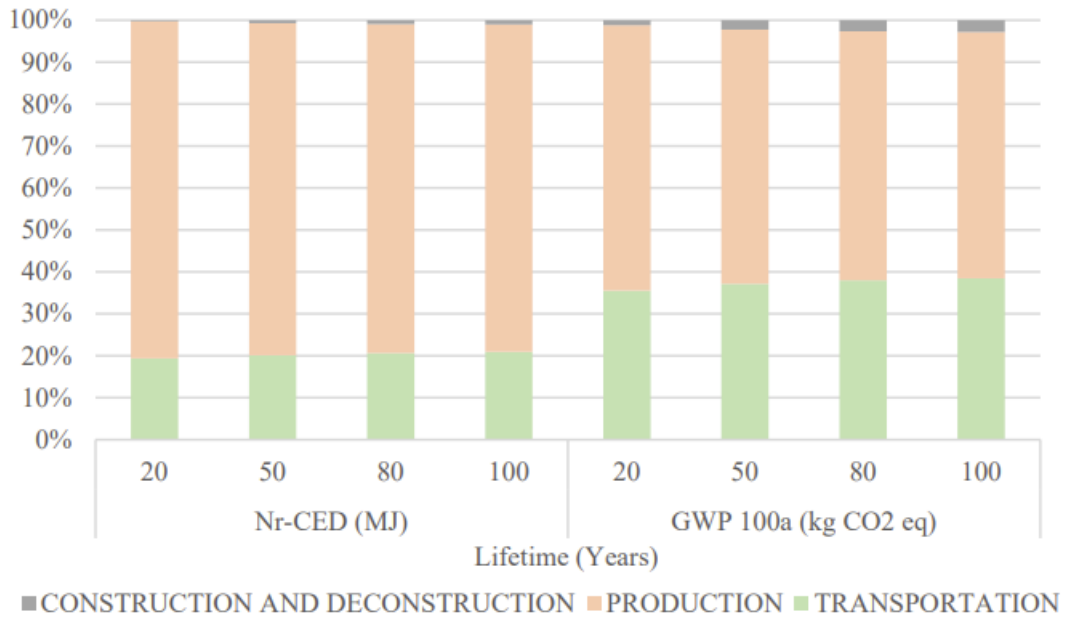

Figure 1.3.6:LCA results per category (Siverio Lima et al., 2021)

The transportation category has such a high impact in terms of CO_2 eq. emissions because the distances between the asphalt mixing plant and the suppliers of the various materials, are high, in the case of aggregates it is around 205 km, bitumen 112 km and filler 205 km (Siverio Lima et al., 2021). Overall 98% of the environmental impact is covered by those two categories (Siverio Lima et al., 2021). The results show that adding 30% of RAP in the surface layer, and 60% in the base might save 252 MJ of energy and 26.5 kg of CO_2 per meter square of pavement (Siverio Lima et al., 2021)

2 Chapter 2

This chapter presents the Norvik Port case study, on which this thesis study is based. It also assesses the aim of thesis and its objective.

2.1 Norvik Port case study

As mentioned previously, concrete block pavements have been employed in heavy duty areas for quite some time. A recently constructed port in Sweden, Norvik port, makes use of this pavement technology. It is located in the southern part of Stockholm.

Figure 2.1.1: Norvik port aerial photo (J. D. Rodriguez Millan, 2024)

As shown in the figure above, the port is small in size, but due to its geographical position in the Baltic sea, it is expected to have a central role in the Northern part of Europe (J. D. Rodriguez Millan, 2024).

A railway system and a motorway surround the port, which connect it to the region nearby. The node is active since 2020 and it is composed of two major areas (J. D. Rodriguez Millan, 2024):

1. Container terminal, that has a capacity of 500 thousand containers of 20 foot per year. Moreover there are plans to expand its current capacity using an adjacent terrain
2. Roll on – Roll off (Ro-Ro) terminal, with a capacity of 200 thousands vehicles each year

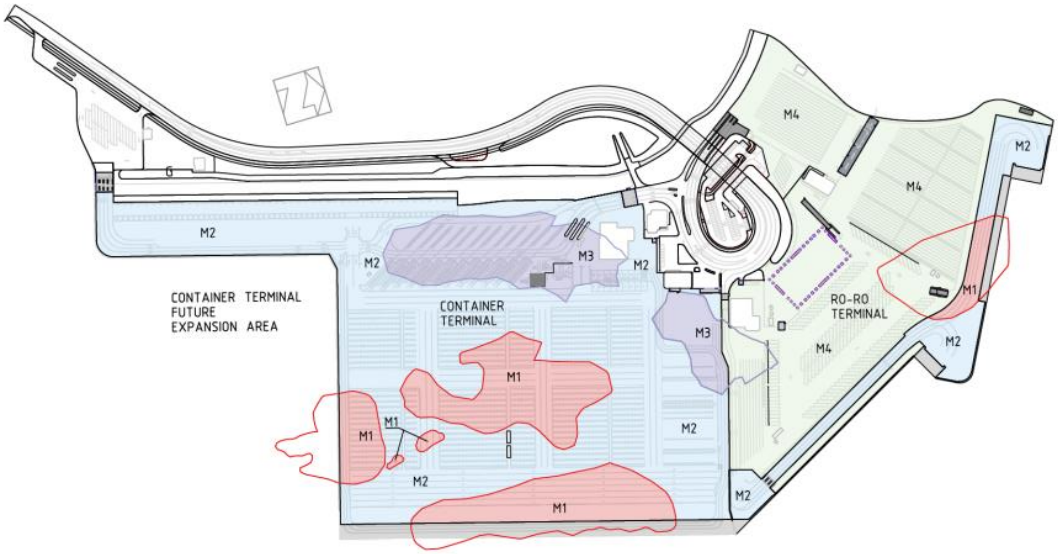

Figure 2.1.2: Detail of the composition of Norvik Port (J. D. Rodriguez Millan, 2024)

As it is shown in Figure 2.1.2, M1 M2 M3 M4 are the different concrete block pavement structures in use, both the container and the Ro-Ro terminal have access to the sea and to the infrastructure connecting them to the outer region (J. D. Rodriguez Millan, 2024). The container terminal has four functional areas (J. D. Rodriguez Millan, 2024):

1. The seaside where the cargo is loaded or unloaded from the ships
2. The container yard, where the cargo is stored
3. The truck roadway, where vehicles can handle cargo and transit
4. The railway system, where the cargo is moved to the rest of the region

Whereas in the Ro-Ro terminal has two major functional areas (J. D. Rodriguez Millan, 2024):

1. The seaside, where cargo is loaded and unloaded from ships
2. The truck area, including waiting zones, parking areas for trailers, and transitioning areas for vehicles.

The container terminal is composed as shown in Figure 2.1.3:

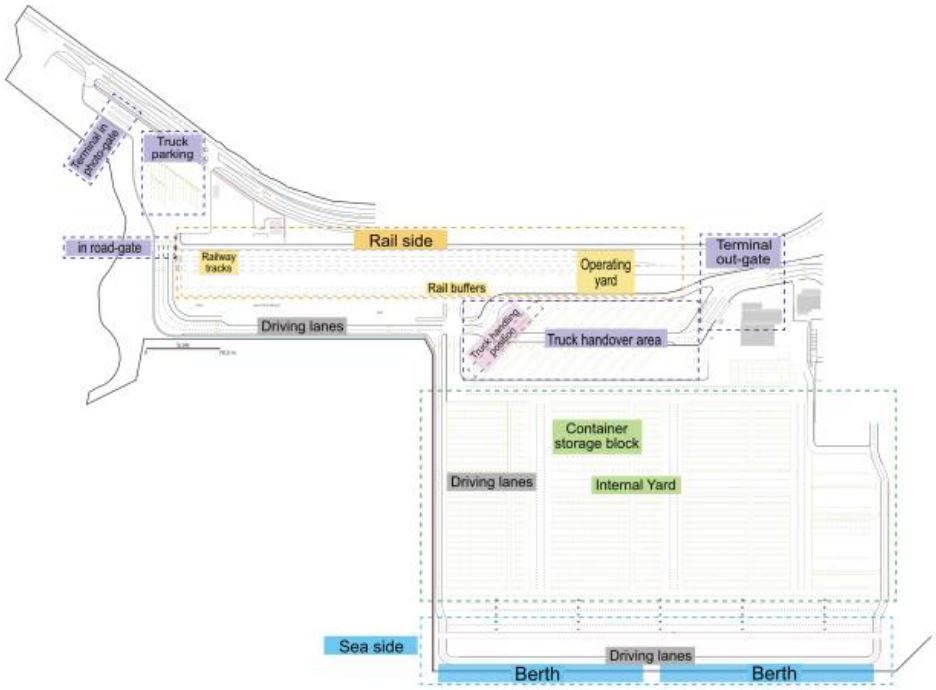

Figure 2.1.3:Plan details of the container terminal of Norvik Port (J. D. Rodriguez Millan, 2024)

The ships come into contact with the port infrastructure in the berth positions. There the container straddle carriers proceed to load or unload the cargo from the ships to the container storage block. Then the containers are parked in the truck handover area, which is one of the busiest areas in the port, into one of the twelve parking spots. The trucks then proceed to carry the cargo outside the port infrastructure into the roads or railway system nearby.

The Ro-Ro terminal is organized as shown in Figure 2.1.4:

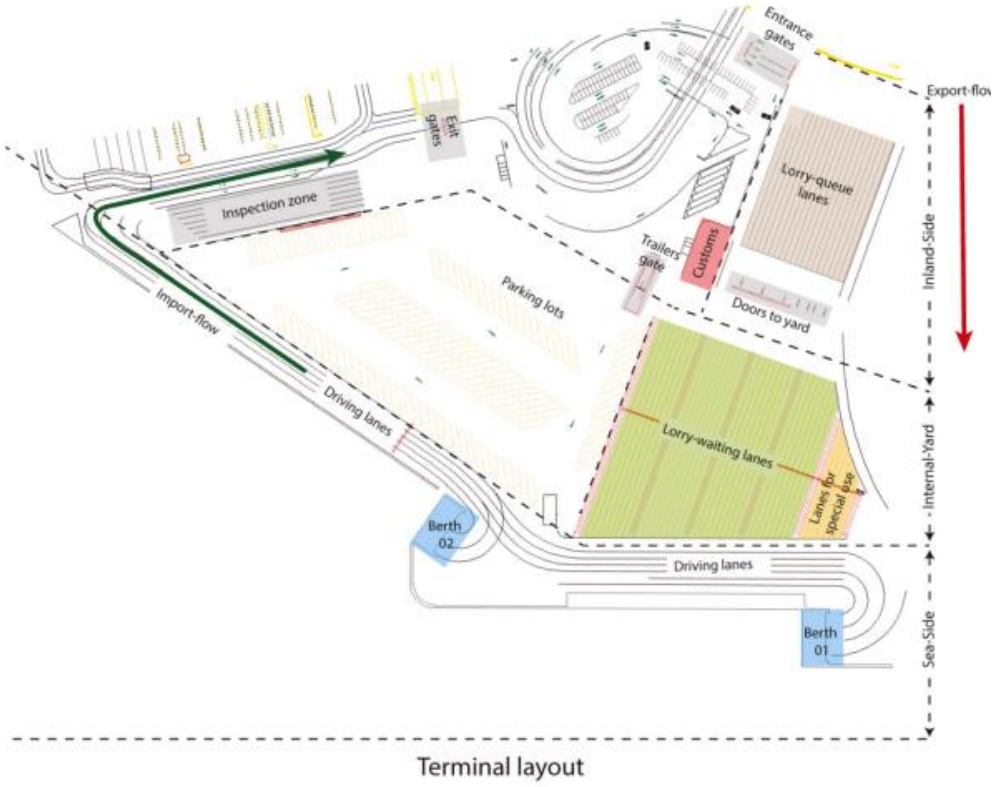

Figure 2.1.4: Plan details of the Ro-Ro terminal of Norvik Port(J. D. Rodriguez Millan, 2024)

This area is trafficked only by trucks. Two main systems to handle cargo are in place:

1. Cargo mode: where the trucks with the cargo enter the lorry waiting lanes through the door to yard, and then proceed to load the ships through berth 01 or berth 02.
2. Trailers only: in this case the trucks enter the parking lots area, and leave the cargo to other trailers that are going to load the ships in berth 01 or berth 02.

Different areas of Norvik port have been analysed for damage, and it has been divided into six areas, as shown in Figure 2.1.5:

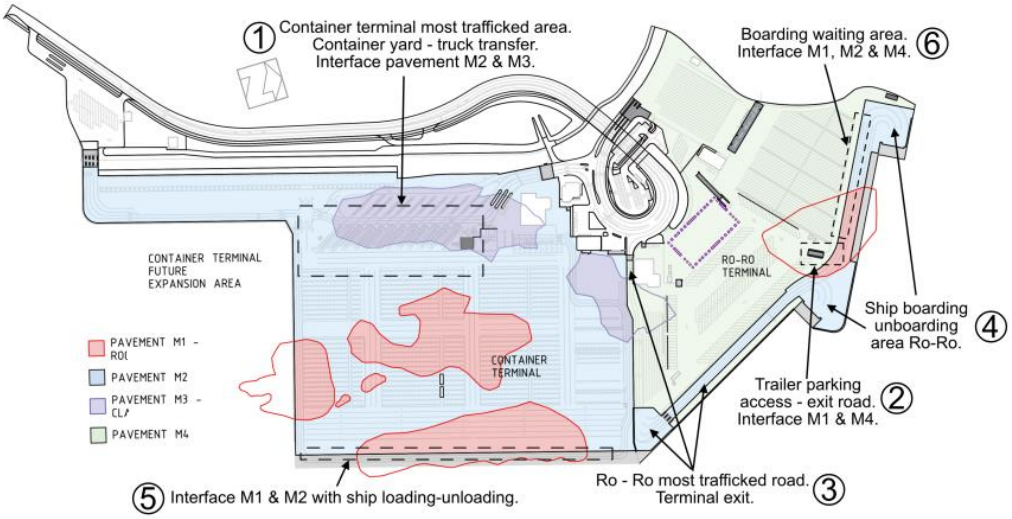

Figure 2.1.5: Most damaged areas in Norvik port (J. D. Rodriguez Millan, 2024)

The most trafficked and damaged area in the port is the handover spot, in the container terminal area, and the transit area in the Ro-Ro Terminal, which correspond to area 1 and area 4 (J. D. Rodriguez Millan, 2024). The details of those areas are shown in Figure 2.1.6 and Figure 2.1.7:

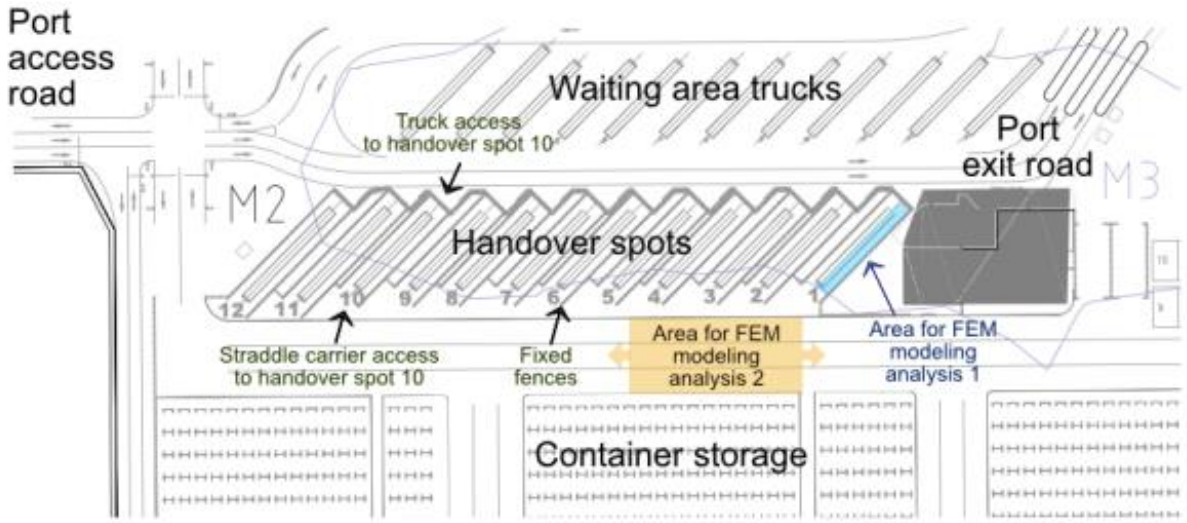

Figure 2.1.6:Handover spot in the container Terminal(J. D. Rodriguez Millan, 2024)

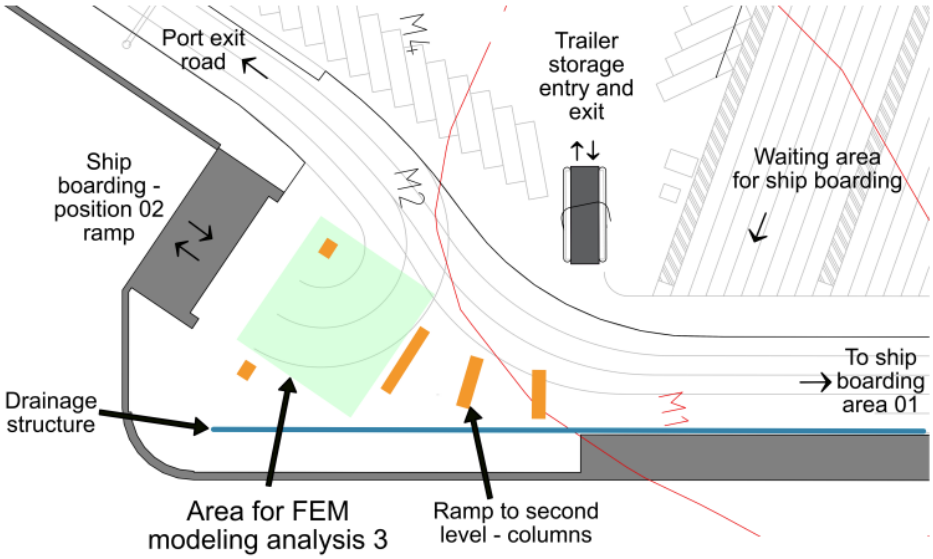

Figure 2.1.7: Ro-Ro terminal transit area (J. D. Rodriguez Millan, 2024)

Examples of the level and type of damage on the port pavement are shown in Figure 2.1.8:

(a) Rutting at handover spots in the container terminal.

(b) Rutting at straddle carrier parking spots in the container terminal.

(c) Pavement damage due to turning vehicles in Ro-Ro terminal.

(d) Lost of joint sand and movement on paving blocks.

(e) Deterioration at the entry of the trailer parking (Figure 4.5 - area 2).

(f) Paving block deterioration and rutting near drainage structures.

Figure 2.1.8:Damage in the port area (J. D. Rodriguez Millan, 2024)

In particular most of the damage in area four is due to the presence of trucks turning with heavy cargo (J. D. Rodriguez Millan, 2024)

The remaining area of the port includes the terminal exit, where there is a trailer inspection location and the exit lanes (J. D. Rodriguez Millan, 2024).

3 Chapter 3

This chapter three commences with a description of two methods used in road design, then it describes the Life Cycle Assessment of the pavements designed.

3.1 Structural design of port pavements

3.1.1 Application of the Heavy duty pavement manual to the case study

This chapter presents a short description of the Heavy duty pavement manual, and its use to develop rigid and flexible pavement designs applied to case study of Novik port.

This method allows the structural design of pavements in heavy duty areas, it addresses specifically port pavements, in order to avoid failure of the pavement. This is due to four conditions environmental failure, structural failure, surface failure, operational failure. (Knapton, 2008):

The manual is based on a reference pavement composed by the following features (Knapton, 2008):

1. 80 mm thickness concrete paving blocks
2. 30 mm laying course material
3. Cement bound base
4. Crushed rock subbase
5. Capping layer if the subgrade CBR is less than 5%

In order to evaluate the thickness of the cement bound layer a chart has been developed. This was the result of an analysis using Finite Element method (Knapton, 2008). The chart's aim is to provide the base thickness that can withstand the heavy loads the pavement is subjected to. The chart used in the structural design of the pavements, and it is shown in Figure 3.1.12 (Knapton, 2008):

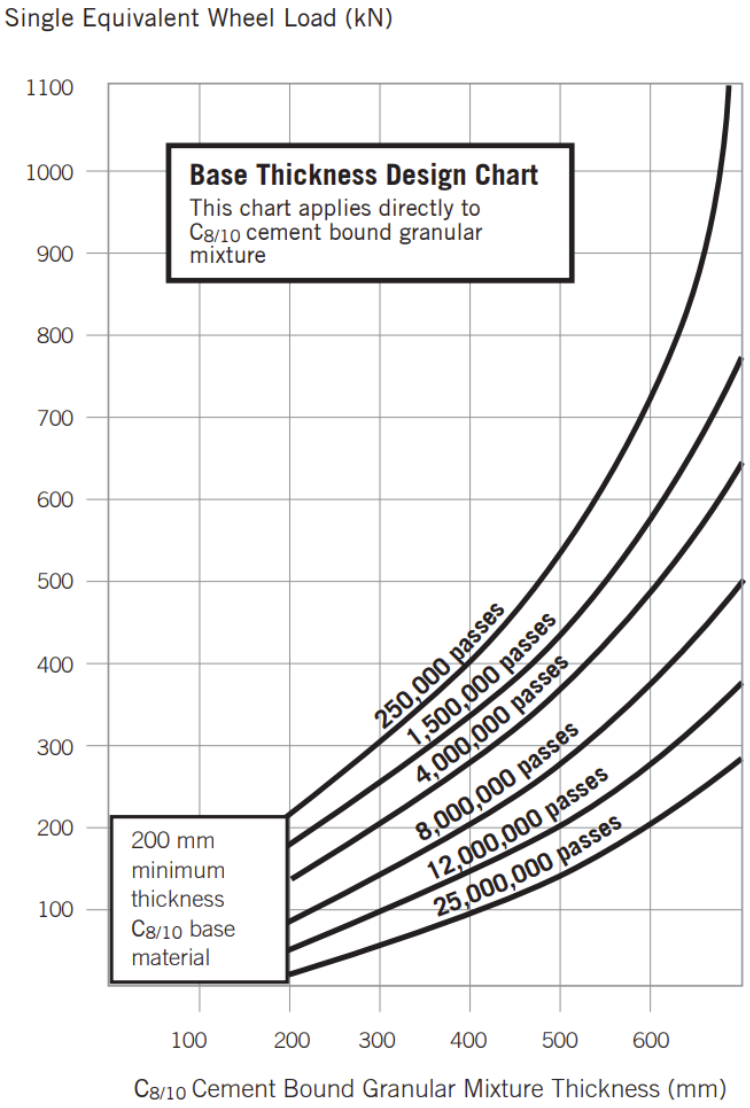

Figure 3.1.1:CBGM Base thickness design chart(Knapton, 2008)

The method allows to change materials in the pavement, using the Material equivalence factor (MEF), this is changing with the material itself, as shown in the tables in the manual (Knapton, 2008). The thickness of the new material layer can be evaluated using this formula (Knapton, 2008):

Equation 3.1.1:Relationship between the new layer thickness and the standard one (Knapton, 2008)

$$d_{new} = d_{stand} * (\frac{\sigma_{stand}}{\sigma_{new}})^{1/2}$$

Where:

- d_{new} is the revised base thickness for the alternative material
- d_{stand} is the design thickness of the cement bound granular material with $C_{8/10}$
- σ_{stand} is the tensile strength of $C_{8/10}$ CBGM
- σ_{new} is the tensile strength of alternative material

For the purpose of this study the pavements are composed in two different ways. The rigid pavement design consists of a concrete slab laid over a granular subbase. The flexible pavement comprises two designs, one with a Hot Rolled Asphalt (HRA) surface, a cement bound granular mixture (CBGM) base , and a granular subbase, the other with a Hot Rolled Asphalt (HRA) surface and a granular subbase. The subgrade is characterized by a 20% CBR, for all pavement's designs. This is calculated inputting the roadbed resilient modulus used in the AASHTO '93 calculations, in the following equation:

Equation 3.1.2:Conversio from CBR to roadbed resilient modulus in [MPa](Airport Engineering Division, 2010)

$$M_R = 10 * CBR$$

In order to obtain the base thickness of the pavement, it is necessary to use the chart in Figure 3.1.12. The inputs are the Single Equivalent Wheel Load (SEWL), and the average passes of the vehicles in the design life of the pavement. The only unknown is the SEWL for each vehicle type, in the two areas of interest, the container terminal and the Ro-Ro terminal. In the calculation of the SEWL the exercises "New pavement design, example 1, straddle carrier design" "Design example 3: distribution warehouse" in the heavy duty pavement manual have been taken as a reference (Knapton, 2008).

In the case of the container terminal the traffic is composed for 75% by container straddle carriers, and 25% by trucks (J. D. Rodriguez Millan, 2024). Therefore two different calculations need to be developed. Starting considering the container straddle carrier, the input data are:

Table 3.1.1:Input data for the container straddle carrier

Input data		
design life	10	years
CBR of the soil	20%	
subbase thickness	150	mm
number of axles	4	
number of wheels on plant	8	
Average number of passes (75%)	1.20E+05	

The design life of the pavement, the CBR of the subgrade and the number of axles in the vehicles, are known values, used in previous calculations. The average number of passes of the container straddle carrier, in a year, is equal to 75% of the total average passes in the container terminal area. Lastly the subbase thickness is 150mm, because the Heavy duty pavement manual states that when the CBR of the soil is 5% or higher the subbase thickness needs to be minimum 150mm, as it's shown in Figure 3.1.2 (Knapton, 2008):

CBR of Subgrade	Capping Thickness (mm)	Sub-base Thickness (mm)
1%	900	150
2%	600	150
3%	400	150
4%	250	150
5% and greater	Not required	150

Figure 3.1.2:Table 20 From Heavy duty pavement manual(Knapton, 2008)

The number of wheels of the container straddle carrier are 8, as there are two wheels for each axle, as shown in Figure 3.1.3:

Figure 3.1.3: Container straddle carrier(Knapton, 2008)

To compute the SEWL it is necessary to take into account the proximity factor of the wheels.

As stated previously the active design constraint, when dealing with cement bound granular bases, is the horizontal tensile stress in the base (Knapton, 2008). This occurs directly under the centre of the wheel, when only one is considered (Knapton, 2008). However when there are two wheels in close proximity, the other wheel might generate tangential stresses, those would be added to the radial stresses due to the primary wheel (Knapton, 2008). Therefore it is necessary to determine the proximity factor (Knapton, 2008). This takes into account the effective depth of the slab, as if it was made of subgrade material (Knapton, 2008). The effective depth can be calculated with the following equation (Knapton, 2008):

Equation 3.1.3:Effective depth of the slab (Knapton, 2008)

$$Effective\ depth\ [mm] = 300 * \sqrt[3]{\frac{35000}{CBR * 10}}$$

The CBR of the soil in this case is 20, therefore the effective depth of the slab is 1678mm. To evaluate the proximity factor it is possible to use the following table:

Wheel Spacing (mm)	Proximity factor for effective depth to base of:		
	1000mm	2000mm	3000mm
300	1.82	1.95	1.98
600	1.47	1.82	1.91
900	1.19	1.65	1.82
1200	1.02	1.47	1.71
1800	1.00	1.19	1.47
2400	1.00	1.02	1.27
3600	1.00	1.00	1.02
4800	1.00	1.00	1.00

Figure 3.1.4:Table19 from Heavy duty pavement manual, wheel proximity factor (Knapton, 2008)

The proximity factor is considered as the ratio of the sum of the radial stress, due to the primary wheel, and the tangential stress of the secondary wheel, to the radial tensile stress (Knapton, 2008). In order to determine it with the table, it is necessary to know the wheel spacing in the vehicle. This has been assumed equal to the one used in the exercise "New pavement design, example 1, straddle carrier design" page 55 of the Heavy duty pavement manual (Knapton, 2008), which is shown in Figure 3.1.5:

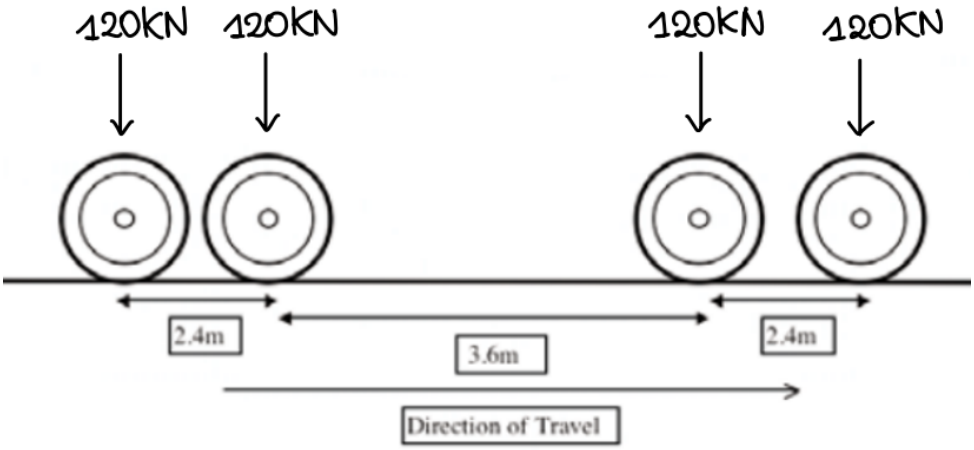

Figure 3.1.5: Wheel spacing of the container straddle carrier(Knapton, 2008)

The track width is considered equal to 4.5m, and the load on each wheel is equal to 120kN (J. D. Rodriguez Millan, 2024), as stated in previous calculations. The proximity factor can be interpolated from Figure 3.1.5 and it is equal to 1.1. Therefore the effective wheel load on each wheel is resulting from the product of the wheel load by the proximity factor, so 133kN. This is referred as the effective wheel load, considering the wheel proximity factor, as shown in Figure 3.1.4 (Knapton, 2008):

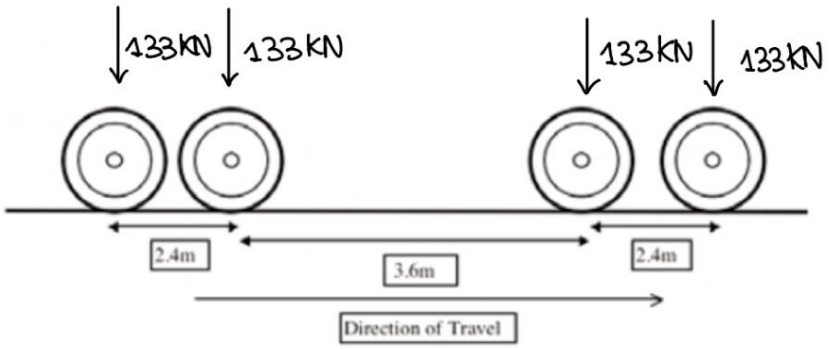

Figure 3.1.6: Container straddle carrier, subjected to the static wheel load

The manual accounts for dynamic loads, due to braking, accelerating, cornering and surface unevenness (Knapton, 2008). The dynamic factor f_d can be evaluated using the following table from the manual (Knapton, 2008):

Condition	Plant Type	fd
Braking	Reach Stacker/Front Lift Truck	±30%
	Straddle Carrier	±50%
	Side Lift Truck	±20%
	Tractor and Trailer	±10%
	Rubber Tyred Gantry Crane (RTG)*	±10%
Cornering	Reach Stacker/Front Lift Truck	40%
	Straddle Carrier	60%
	Side Lift Truck	30%
	Tractor and Trailer	30%
	Rubber Tyred Gantry Crane (RTG)*	zero
Acceleration	Reach Stacker/Front Lift Truck	10%
	Straddle Carrier	10%
	Side Lift Truck	10%
	Tractor and Trailer	10%
	Rubber Tyred Gantry Crane (RTG)*	±5%
Uneven Surface	Reach Stacker/Front Lift Truck	20%
	Straddle Carrier	20%
	Side Lift Truck	20%
	Tractor and Trailer	20%
	Rubber Tyred Gantry Crane (RTG)*	±10%

Table 17: Table of dynamic load factors (f_d). Static loads are increased by the percentage figures in the Table.

*Note: that multi-wheel RTGs, i.e. RTGs with say 16 wheels arranged in four undercarriages of four wheels each as shown in Figure 18 perform well over a pavement but for other wheel arrangements, wheel loads may be so great as to require piled runway beams.

Figure 3.1.7: Table 17, Heavy duty pavements manual to calculate the dynamic factor (Knapton, 2008)

The most adverse loading case is the braking one, for container straddle carriers. Therefore the effective load on each extreme front wheel is increased, and decreased in the rear wheel, by 50%. The inner wheels are subjected to an increment/decrement of load equal to 21%. This is because the distance from the wheel to central line needs to be accounted for. Therefore the outer wheels are 4.2m away from the centre, and the inner ones are 1.8 m away. Therefore the dynamic factor applied to the inner wheels is equal to:

Equation 3.1.4:dynamic factor of the inner wheels in a container straddle carrier

$$21\% = 50\% * \frac{1.8}{1.4}$$

The loads, as a result of the dynamic factor become:

Table 3.1.2:dynamic wheel loads container straddle carrier

front wheel	199.8	kN
back wheel	66.6	kN
inner front wheel	161.7	kN
inner back wheel	104.7	kN
SEWL	199.8	kN

The Single equivalent Wheel Load is the highest one, therefore 199.8kN, which can be approximated to 200kN. The four load values need to be expressed as an equivalent number of passes of the SEWL (Knapton, 2008). This can be done using the following equation:

Equation 3.1.5:Equivalence factor from Heavy duty pavement manual (Knapton, 2008)

$$Equivalence\ factor = \frac{W_i}{SEWL}^{3.75}$$

Where W_i is the dynamic load on the wheel considered, so for example for the inner front wheel, which is the second wheel from the front, the equivalence factor would be equal to :

Equation 3.1.6:Example of equivalence factor for container straddle carrier

$$0.45 = \frac{66.6^{3.75}}{200}$$

Which is equal to 0.45 passes of the wheel subjected to the heaviest load. All the equivalence factors obtained need to be summed up, the total equivalence factor is 1.56. Therefore considering that the average passes of the container straddle carriers in the container terminal is 1.2E+05, each time the vehicle passes in one spot and it brakes it applies 1.56 repetitions of the highest wheel load. So the passes in a year would be equal to the product of the average passes by the equivalence factor. The total passes, in the design life of the pavement, of the container straddle carrier correspond to 1.86 million passes of a load of 200kN.

Since the container terminal is trafficked by both container straddle carriers and trucks, it is necessary to evaluate the average passes in the design life of the pavement and the SEWL for the trucks as well.

The calculation procedure requires the following input variables:

Table 3.1.3:Trucks input variables, container terminal

Input Data Trucks		
Average passes in a year (25%)	3.99E+04	
design life	10	years
CBR of the soil	20%	
subbase thickness	150	mm
steering axle	1	

non-steering axles	4	
wheel proximity factor	1.1	
load on each non-steering axle	110	kN
load on each steering axle	65	kN

The wheel proximity factor is assumed equal to the one used in the exercise "New pavement design example 3, distribution warehouse pavements" page 64 of the Heavy duty pavement manual, as the trucks considered in the calculations are the same as the ones used in the exercise (Knapton, 2008). The total number of average passes in the container terminal of trucks, in one year, is equal to 3.99E+04. Therefore the number of passes of trucks in the design life of the pavement, 10 years, is 3.99E+05. Thus the number of passes of each non-steering axle, is the product of 3.99E+05 by 4, the number of non-steering axles. This is equal to 1.56E+06. Since the highest load is the one on the non-steering axle, it is necessary to compute the equivalent factor for the steering axle. This will be:

Equation 3.1.7:Equivalent factor for trucks

$$0.14 = \frac{65}{110}^{3.75}$$

Consequently the number of passes of the steering axle, expressed in terms of the non-steering axles, will be:

Equation 3.1.8: Average passes of the steering axle, in terms of the non steering axles

$$5.58 \times 10^4 = 5.58 \times 10^5 \times 0.14$$

This value shows that the impact of the steering axle is very low. The total average passes in the design life of the pavement is equal to the sum of the two values:

Equation 3.1.9: Total number of passes of a truck in the container terminal.

$$1.65 \times 10^6 = (1.59 \times 10^6) + (5.58 \times 10^4)$$

The SEWL is the highest one, so 110kN, but divided by two because for each axle there are two wheel, so the load on each wheel will be 55kN. This is the static load. It is necessary to multiply this load by the proximity factor and the dynamic factor. In this case the dynamic factors are the ones for braking and cornering. The total sum of the proximity factor and the dynamic ones is 1.5. Therefore the SEWL is 82.5kN.

In order to evaluate the base thickness using the chart, it is necessary to find the total average passes in the design life of the pavements of both vehicles, and the total SEWL. The input variable to use in the chart will be:

Table 3.1.4:input variable for the structural design of a container terminal pavement

Number of passes of both vehicles, in the design life	3.51E+06	
SEWL	282	kN

Using the chart the base thickness is equal to 360 mm of cement bound granular material, as shown in :

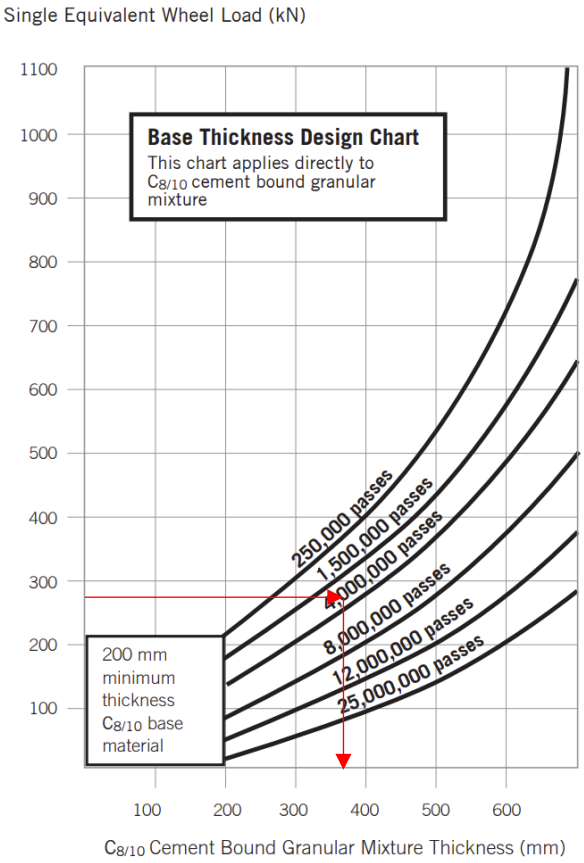

Figure 3.1.8: Base thickness of the container terminal pavement (Knapton, 2008)

Therefore the reference pavement is going to be:

- 80 mm of concrete blocks
- 30 mm of bedding layer
- 360mm of CBGM base
- 150 mm subbase

In order to obtain a flexible and a rigid pavement it is necessary to apply the Material Equivalence Factor from table 13 page 28 of the manual (Knapton, 2008). The MEF for the flexible pavement with a surface of HRA is 1.25, whereas for the rigid pavement it depends on the type of concrete used in the slab, considering a concrete $C_{25/35}$ the MEF is 0.65 (Knapton, 2008). Lastly for the granular subbase it is 3 (Knapton, 2008).

Therefore the flexible pavement design in the case of the container terminal will be:

Table 3.1.5:flexible pavement design 2, container terminal

Flexible pavement container terminal, design 2		
HRA surface	138	mm
Base	300	mm
Subbase	330	mm

A second design has been realized for the flexible pavement, structuring it as a full-depth asphalt pavement:

Table 3.1.6: Flexible pavement design, full depth asphalt pavement, container terminal

Flexible pavement container terminal, design 1		
HRA	588	mm
subbase	150	mm

The rigid pavement will be:

Table 3.1.7:Rigid pavement design container terminal

Rigid pavement container terminal		
Concrete surface	306	mm
Subbase	150	mm

This is the only plausible design for the rigid pavement, as with the presence of a base the thickness of the wearing course would have been less than 100 mm. This is not enough to withstand the heavy loads on the pavements, therefore design has been changed extending the concrete layer to cover both the surface layer and the base.

To compute the thickness of the layers it is sufficient to multiply the thickness of the surface of the reference pavement by the MEF. For example in the case of the HRA, the thickness of the surface layers in the reference pavement is 80+30=110mm. Therefore the thickness of the HRA surface is 110*1.25=138mm. The same applies to the concrete surface. The base thickness is chosen equal to 300mm. The remaining 60mm are then multiplied by MEF of 3, so they become 180mm of granular subbase, to which 150mm subbase need to added. Therefore the final subbase thickness is 330mm. In the case of the rigid pavement the concrete layer thickness has been obtained multiplying the thickness of the surface 80+30=110mm, summed up to the base thickness, 360, all multiplied by the MEF for concrete. Then subbase needs to be 150 mm minimum as the CBR value is greater than 20%.

The Ro-Ro terminal is trafficked only by trucks, the procedure to assess the SEWL and the average passes in the design life is the same as the one already explained. The only difference is the average pass in the terminal, which are 2.8E+05. This value is then used to calculate the total passes in the design life, following the same steps as before. The total passes in the design life of the pavement are, 11.6 million. The SEWL is 82.5kN, as the trucks are assumed to be the same as the ones used in the container terminal. Therefore the base thickness of this pavement is 250mm as shown below:

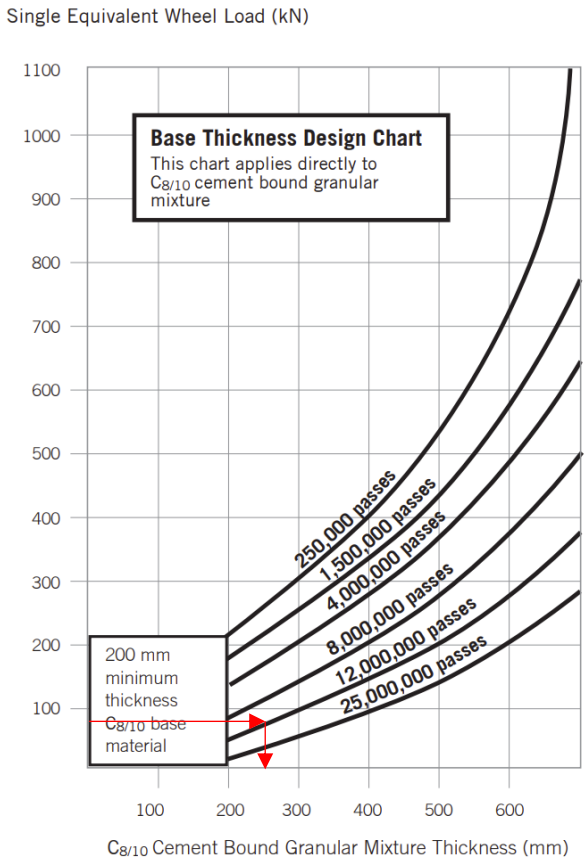

Figure 3.1.9: base thickness of the Ro-Ro terminal (Knapton, 2008)

The reference pavement in this terminal will be:

- 80 mm of concrete blocks
- 30 mm of bedding layer
- 250mm of CBGM base
- 150 mm subbase

The flexible pavement design is:

Table 3.1.8:Flexible pavement design in the Ro-Ro Terminal

Flexible pavement Ro-Ro terminal		
HRA surface	138	mm
Base	200	mm
Subbase	300	mm

The full depth design is:

Table 3.1.9: Full-depth asphalt pavement Ro-Ro terminal

Flexible pavement Ro-Ro terminal		
HRA surface	450	mm
Subbase	150	mm

The rigid pavement design is:

Table 3.1.10:Rigid pavement design Ro-Ro Terminal

Rigid pavement Ro-Ro terminal		
Concrete slab	234	mm
Subbase	150	mm

3.1.2 Application of AASHTO 1993 method to the case study

This chapter will present the use of AASHTO method for the case study of a flexible and rigid port pavement. It commences with a short description of the method and the variables used, then it continues assessing the calculations for the structural design of flexible and rigid pavements.

AASHTO 1993 is a design method used to determine the structural composition of pavements. In the manual chapter II is focusing on the requirements for the design of highways and low volume roads, meanwhile chapter III is based on the design procedure of both flexible and rigid highways. Therefore it is not specific for heavy duty pavements. The method requires specific input variables, but those are different from rigid pavements to flexible ones. In the case of rigid pavements the initial variables are (AASHTO, 2001):

1. Reliability, R
2. Concrete modulus of rupture, S'_c
3. Effective modulus of subgrade reaction, k
4. Concrete elastic modulus, E_c
5. Estimated future traffic, in terms of 18kip equivalent single axle loads (ESAL)
6. Desing serviceability loss, ΔPSI
7. Terminal serviceability index, p_t
8. Drainage coefficient, C_d
9. Load transfer coefficient, J
10. Overall standard deviation, S_0

Each one of these factors is extremely important. Reliability accounts for the credibility of the design solution in the analysis period. It considers changes in the traffic prediction and the performance prediction, and provides a level of certainty that the pavements will withstand the loads (AASHTO, 2001). AASHTO 1993 indicates specific values to use in Table 2.2 “suggested levels of reliability for various functional classifications”. For the purpose of this study the reliability value was taken from a previous exercise by (A.Guarin, 2023). The Present Serviceability Index (PSI), is a performance criteria, and it shows how the pavement withstands the traffic loads. It can range from 0 to 5, where 5 indicates the perfect road conditions (AASHTO, 2001). The change in PSI is considered as the design serviceability loss, ΔPSI, which is equal to:

Equation 3.1.10:Desing serviceability loss(AASHTO, 2001)

$$\Delta PSI = p_0 - p_t$$

where p_0 is the initial serviceability, and p_t is the terminal serviciability. This equation applies to both rigid and flexible roads, ΔPSI was also known (A.Guarin, 2023).

The roadbed resilient modulus, M_R , is determined through specific tests, which are seasonal, in order to evaluate the possible damage the pavement is undergoing throughout the year (AASHTO, 2001). The tests, such as AASHTO T 274, are conducted on samples of the roadbed material, and a combination of the values obtain are then used in the design process (AASHTO, 2001). In this case the roadbed resilient modulus is known, as it was characterized in previous studies in the PhD thesis by (J. D. Rodriguez Millan, 2024), and three different values are available (J. D. Rodriguez Millan, 2024). The most preventive value is used in the calculation. The final value is represented in Table 3.1.11:

Table 3.1.11:Resilient moduli values [MPa]

Subgrade modulus [MPa]
200

The roadbed resilient modulus is used in the structural design of flexible pavements. Whereas the effective modulus of subgrade reaction, k, is employed in the rigid pavement. This value can be determined using specific graphs listed in the AASHTO manual, where the roadbed resilient modulus M_R is used as an input.

The modulus of rupture is required only for rigid pavement and it is the mean value after 28 days of using the third point loading, as per AASHTO T 97, ASTM C 78 (AASHTO, 2001).

The load transfer coefficient accounts for the ability of rigid slabs to distribute loads in discontinuities like joints (AASHTO, 2001).

Drainage coefficients are usually describing the effects of drainage on pavement performance. In flexible pavements those are accounted for using the m_i value, which doesn't account for drainage effects on the asphalt surface. In rigid pavements recommended values from Table 2.5 AASHTO 1993 manual can be used (AASHTO, 2001).

The first step in the design of a rigid pavement is to determine the value of the composite modulus of subgrade reaction k_∞, this is achieved using the following graph:

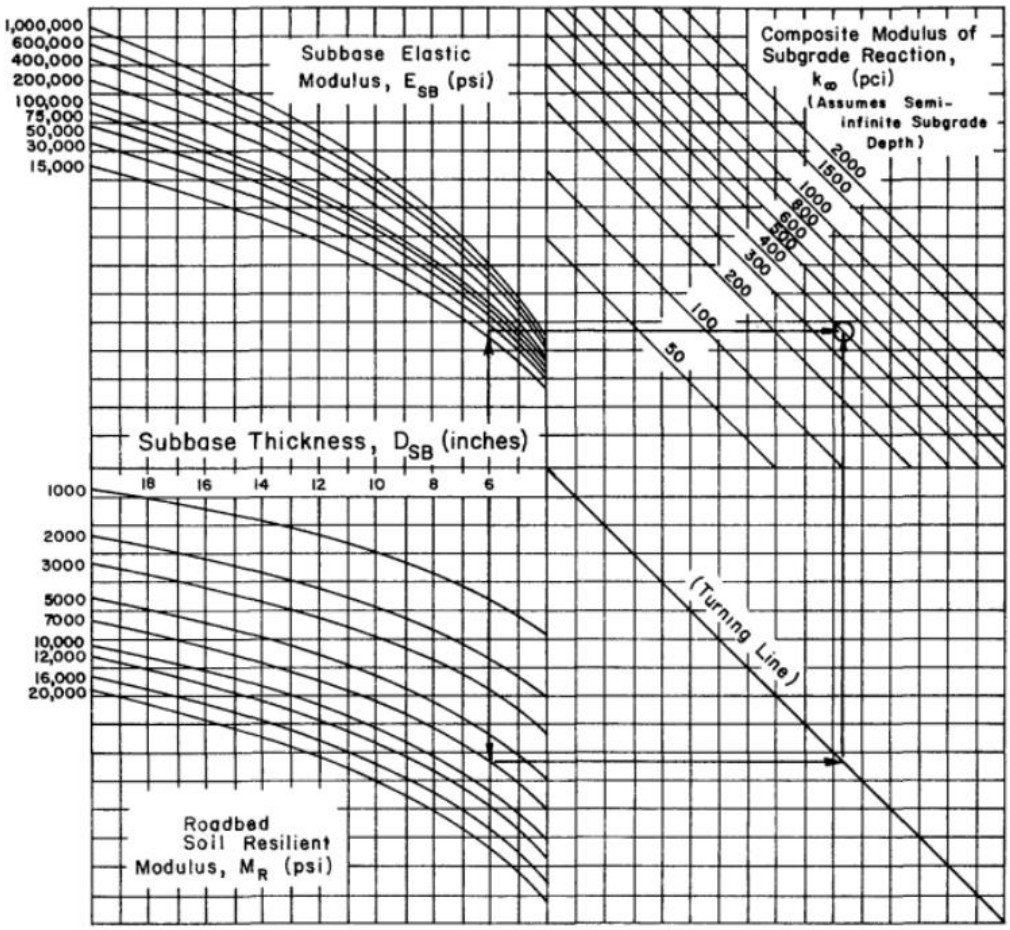

Figure 3.1.10:Composite modulus of subgrade reaction chart (AASHTO, 2001)

The input variables required by the AASHTO 1993 manual are:

- Thickness of the subbase and base layers, in inches
- Roadbed resilient modulus (M_R=29000 psi)
- Subbase elastic modulus, in psi

The rigid pavement has been designed in two different ways, one design considers the presence of a granular subbase of 150 mm, and the other has both a cement bound base of 210 mm and a granular subbase of 150 mm. Therefore two different values of k_∞ need to be evaluated. In the first case the input data are:

- Thickness of the granular subbase: 6 inches
- Roadbed resilient modulus (M_R=29000 psi)
- Subbase elastic modulus (E_B= 20000 psi)

The $k_{\infty,1}$ in this case is 900 pci.

Whereas in the second case, since the base is cement bound and the subbase is granular it is necessary to evaluate the equivalent thickness ($h_{eq.}$) of the subbase as if it was cement bound. This can be achieved using the following equation:

Equation 3.1.11: Equation to determine the equivalent thickness of the subbase layer

$$\frac{E_{SB}(D_{SB})^3}{(1-\upsilon)^2} = \frac{E_{SBc}(h_{eq.})^3}{(1-\upsilon)^2}$$

Where:

- E_{SB} is the elastic modulus of the granular subbase, 20 kpsi
- D_{SB} is the thickness of the granular subbase, 6 inches
- υ is the Poisson coefficient which is 0.35 for a granular subbase and 0.2 for the cement bound one
- E_{SBc} is the elastic modulus of a cement bound mixture, 500 kpsi
- $h_{eq.}$ is the equivalent thickness of the cement bound subbase, 2.4 inches

Once the equivalent thickness has been determined it is possible to insert the following parameters in the graph, and evaluate the k_∞:

- Thickness of the cement bound base and the subbase (12 inches)
- Roadbed resilient modulus (M_R=29000 psi)
- Elastic modulus of a cement bound mixture (E_{SB}= 500 Kpsi)

The $k_{\infty,2}$ is 2000 pci.

Since in some areas of the port there is a rock subgrade, it is necessary to correct the effective subgrade compositive values, using the following graph:

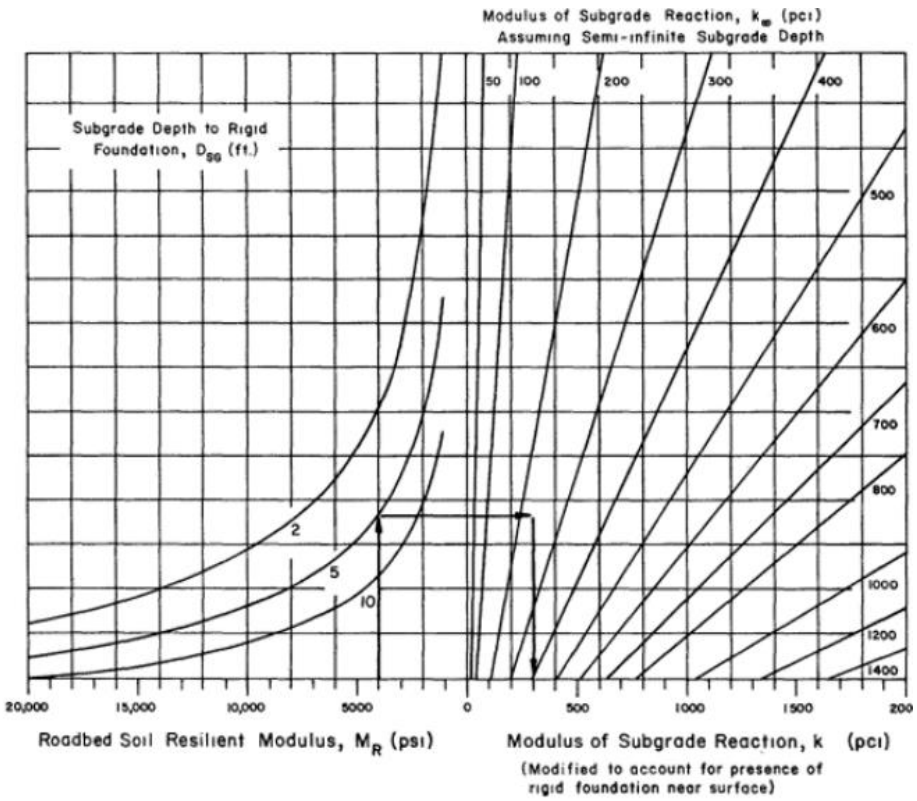

Figure 3.1.11: Chart to correct the composite subgrade modulus considering the presence of rigid foundation near surface (AASHTO,2001)

In the port area there are different subgrades, some of which are composed of rock material, and they are close to the surface, therefore in those cases the value of *k* needs to be corrected using the chart above. The following considerations are applied:

- $M_R = 29\ kpsi$
- $k_{\infty,1}$= 1000 psi and $k_{\infty,2}$= 2000 psi
- $D_{SG} = 2\ ft$

The corrected values of k are:

- k'_1= 1250 psi
- k'_2= 2000 psi

All four values need to be corrected considering the loss of support of the base and subbase layers. The loss of support (LS) is estimated using the table in Figure 3.1.12 in the AASHTO 1993 manual:

Type of Material	Loss of Support (LS)
Cement Treated Granular Base (E = 1,000,000 to 2,000,000 psi)	0 0 to 1 0
Cement Aggregate Mixtures (E = 500,000 to 1,000,000 psi)	0 0 to 1 0
Asphalt Treated Base (E = 350,000 to 1,000,000 psi)	0 0 to 1 0
Bituminous Stabilized Mixtures (E = 40,000 to 300,000 psi)	0 0 to 1 0
Lime Stabilized (E = 20,000 to 70,000 psi)	1 0 to 3 0
Unbound Granular Materials (E = 15,000 to 45,000 psi)	1 0 to 3 0
Fine Grained or Natural Subgrade Materials (E = 3,000 to 40,000 psi)	2 0 to 3 0

NOTE: E in this table refers to the general symbol for elastic or resilient modulus of the material

Figure 3.1.12: Loss of support values for different materials

In the case of the cement aggregate mixture the LS is considered equal to 1, and for the granular subbase mixtures the LS is considered equal to 2. Using the graph below it is possible to correct the four values estimated.

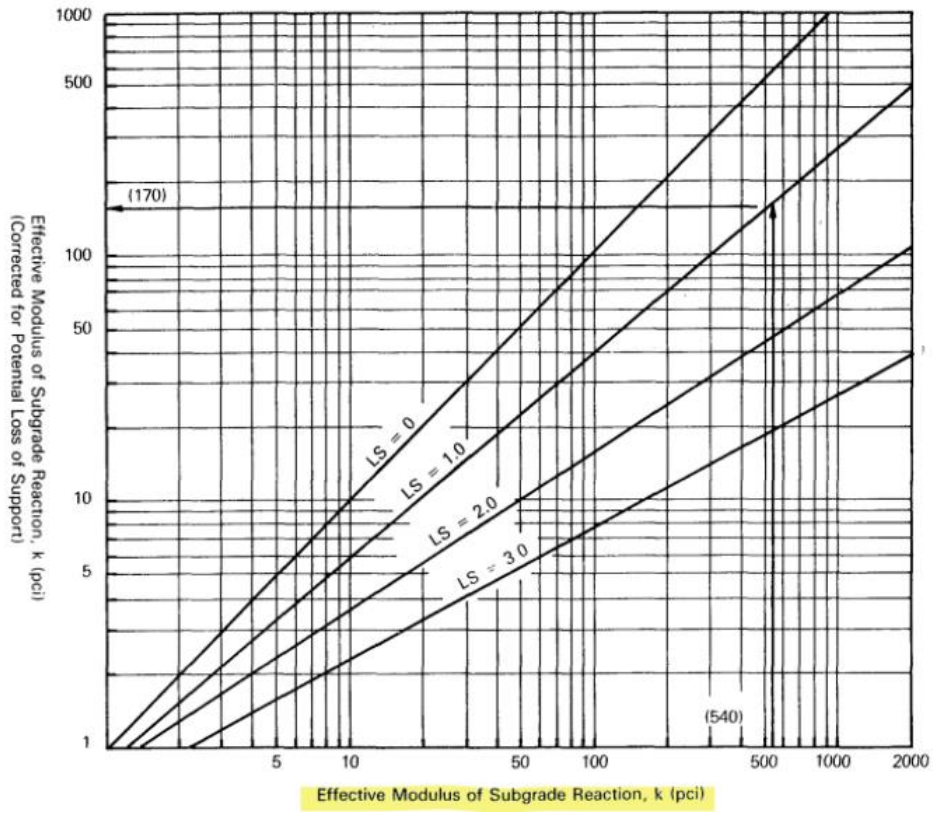

Figure 3.1.13: Modulus of subgrade reaction corrected for loss of support (LS) (AASHTO, 2001)

Entering the x-axis with the subgrade modulus values estimated, and then intercepting the correct LS line, it is possible to read on the y-axis the effective subgrade resilient moduli, which are:

- k_1 = 60 pci

- k'_1= 70 pci, with rock subgrade
- k_2 = 500 pci
- k'_2= 500 pci with rock subgrade

Not all the variables were known, therefore some assumptions had to be made. The elastic modulus of concrete and the modulus of rupture were assumed as indicated in Figure 3.7 "Design Chart for Rigid Pavements Based on Using Mean Values for Each Input Variable" Part. II, page 45-46 (AASHTO, 2001).

Whereas the load transfer coefficient, *J*, was estimated from a table listed in the AASHTO '93 manual:

Shoulder	Asphalt		Tied P.C.C.	
Load Transfer Devices	Yes	No	Yes	No
Pavement Type				
1 Plain jointed and jointed reinforced	3 2	3 8–4 4	2 5–3 1	3 6–4 2
2 CRCP	2 9–3 2	N/A	2 3–2 9	N/A

Figure 3.1.14: Load transfer coefficient J (AASHTO, 2001)

In this case the slab is made of plain jointed concrete, and no load transfer devices are used, therefore the range of *J* is 3.6 – 4.2, the value of 3.6 was used in the calculations.

Using the following equation it is possible to calculate an initial value of slab thickness. *D*:

Equation.3.1.12: Design Equation for rigid pavements (AASHTO, 2001)

$$\log_{10}(W18) = Z_R S_0 + 7.35\log_{10}(D+1) - 0.06 + \frac{\log_{10}[\frac{\Delta PSI}{4.5-1.5}]}{1+\frac{1.624*10^7}{(D+1)^{8.46}}} + (4.22-0.32p_t)*\log_{10}[\frac{s'_c * c_d[D^{0.75}-1.132]}{215.63*J[D^{0.75}-\frac{18.42}{(E_c/k)^{0.25}}]}]$$

The input variables used in Equation.3.1.12 are summed up in the table below.

Table 3.1.12: Input variables to calculate the slab thickness, D[inches], according to AASHTO 1993

k	60-70/500	pci
ESAL	1.00E+07	
R	90%	
S_0	0.29	
ΔPSI	1.5	
P_t	3	
Z_R	-1.282	
J	3.6	

Once all the input variables are known it is possible to calculate the initial slab thicknesses, for the two designs, based on an estimated ESAL value, which will be corrected once the load equivalent factor is known. The initial slab thicknesses are:

- D = 11 inches, with the presence of the granular subbase only
- D = 10 inches with the presence of a cement bound base and a granular subbase

By knowing the initial value of *D* it is possible to evaluate the real loads due to traffic, in terms of ESALs, using the tables in Appendix D of the AASHTO 1993 manual (AASHTO, 2001). The only remaining unknown is the axle composition of the vehicles in the port. The vehicles operating are trucks and container staddle carriers.

The trucks considered for the purpose of this analysis are similar to the ones represented in Figure 3.1.15 and Figure 3.1.16, that can be taken as reference:

Figure 3.1.15: Example of truck trafficking Norvik port (Knapton, 2008)

Figure 3.1.16:Example of trucks trafficking Norvik Port (Knapton, 2008)

Looking at the figures above it is possible to assume that the axles compositions are

I. Two single axles
II. Tridem axle group

The loads on each axle are distributed the following way (Knapton, 2008):

I. 65 kN on the single steering axle
II. 110 kN on the other single axle
III. 330 kN on the tridem group, therefore 110 kN on each of one of the three axles in the group.

The container straddle carrier is shown in Figure 3.1.17:

Figure 3.1.17: Example of container straddle carrier (Liebherr Container Cranes Ltd., n.d.)

This vehicle is composed of four steering axles (LIebherr Container Cranes Ltd., n.d.), and it is assumed that those are single axles. The loads on these axles are (J. D. Rodriguez Millan, 2024):

1. 120 kN on each wheel, considering two wheels on each axle, the load on each axle is equal to 240 kN

The traffic analysis has been differentiated between the two areas, container terminal and the Ro-Ro terminal. Therefore the vehicles and the traffic loads are different, this results in two distinct pavements designs.

The load values need to be converted into kips, in order to be used the tables in Appendix-D from AASHTO 1993 manual (AASHTO, 2001). The final load values are shown in Table 3.1.13.

Table 3.1.13:Loads in kips for each vehicle type

Loads		
vehicle	**axles**	**kips**
Trucks	single	15
	single	25
	tridem	75
container straddle carrier	single	54
	single	54
	single	54
	single	54

Since the maximum load, as shown in the Appendix-D tables for single axles (AASHTO, 2001), is 50 kips, the 54 kips of the container straddle carrier have been considered as 50 kips, in order to continue with the analysis. Once the loads are evaluated it is possible to determine the axle load transfer factor, and multiply it by the average passes per year on each area. This values are contained in Table 3.1.14:

Table 3.1.14: Average passes of vehicles in each area (J. D. Rodriguez Millan, 2024)

Average passes per year in the container terminal	**Average passes per year in the Ro-Ro terminal**
1549000	2809000

To evaluate the ESALs in each area it is enough to multiply the average passes by the axial load equivalent factor and by the design life of the pavement, which is 10 years (J. D. Rodriguez Millan, 2024). In order to evaluate the axial load factor it is sufficient to use the tables in Appendix-D for a rigid pavement, with a p_t equal to 3. An example of those tables is shown below:

Table D.16. Axle Load Equivalency Factors for Rigid Pavements, Single Axles and p_t of 3.0

Axle Load (kips)	Slab Thickness, D (inches)								
	6	7	8	9	10	11	12	13	14
2	0003	0002	0002	0002	0002	0002	0002	0002	0002
4	003	003	002	002	002	002	002	002	002
6	014	012	011	010	010	010	010	010	010
8	045	038	034	033	032	032	032	032	032
10	111	095	087	083	081	081	080	080	080
12	228	202	186	179	176	174	174	174	173
14	408	378	355	344	340	337	337	.336	336
16	660	640	619	608	603	600	599	599	599
18	1 00	1 00	1 00	1 00	1 00	1 00	1 00	1 00	1 00
20	1 46	1.47	1 52	1 55	1 57	1 58	1 58	1 59	1 59
22	2 07	2 06	2 18	2 29	2 35	2 38	2 40	2 41	2 41
24	2.90	2 81	3 00	3 23	3 38	3 47	3 51	3 53	3 54
26	4 00	3 77	4 01	4 40	4 70	4 87	4 96	5 01	5 04
28	5 43	4 99	5 23	5 80	6 31	6 65	6 83	6 93	6 98
30	7 27	6 53	6 72	7 46	8 25	8 83	9 17	9 36	9 46
32	9 59	8 47	8 53	9 42	10 54	11 44	12 03	12 37	12 56
34	12 5	10 9	10 7	11 7	13 2	14 5	15 5	16 0	16 4
36	16 0	13 8	13 4	14 4	16 2	18 1	19 5	20 4	21 0
38	20 4	17 4	16 7	17 7	19 8	22 2	24 2	25 6	26 4
40	25 6	21 8	20 6	21 5	23 8	26 8	29 5	31 5	32 9
42	31 8	26 9	25 3	26 0	28 5	32 0	35 5	38 4	40 3
44	39 2	33 1	30 8	31 3	33 9	37 9	42 3	46 1	48 8
46	47 8	40 3	37 2	37 5	40 1	44 5	49 8	54 7	58 5
48	57 9	48 6	44 8	44 7	47 3	52 1	58 2	64 3	69 4
50	69 6	58 4	53 6	53 1	55 6	60 6	67 6	75 0	81 4

Figure 3.1.18:Table to evaluate the axle load equivalency factor, rigid pavements, single axles, pt equal to 3 (AASHTO, 2001)

For example considering a slab thickness of 10 inches, and a vehicle, like the container straddle carrier, that is composed by all single axles, of 50 kips each, it is enough to input those values to find the axle load transfer coefficient for that vehicle. For the single axle the equivalent factor is 55.6, this needs to be multiplied by 4, as there are four axles. Then the overall load coefficient for the straddle carrier will be 222.4. The same method applies to the trucks, but in that case there are two single axles, and a tridem group. In this case the tables to use will be the one for the single axles and the one for the tridem one, shown in Figure 3.1.19:

Table D.18. Axle Load Equivalency Factors for Rigid Pavements, Triple Axles and p_t of 3.0

Axle Load (kips)	Slab Thickness, D (inches)								
	6	7	8	9	10	11	12	13	14
2	0001	0001	0001	0001	0001	0001	0001	0001	0001
4	0004	0003	0003	0003	0003	0003	0003	0003	0003
6	001	001	001	001	001	001	001	001	001
8	003	003	002	002	002	002	002	002	002
10	007	006	005	005	005	005	005	005	005
12	013	011	010	009	009	009	009	009	009
14	023	020	018	017	017	016	016	.016	016
16	039	033	030	028	028	027	027	027	027
18	061	052	047	045	044	044	043	043	043
20	091	078	071	068	067	066	066	066	066
22	132	114	104	100	098	097	097	097	097
24	183	161	148	143	140	139	139	138	138
26	246	221	205	198	195	193	193	192	192
28	322	296	277	268	265	263	262	262	262
30	411	387	367	357	353	351	350	349	349
32	515	495	476	466	462	460	459	458	458
34	634	622	607	599	595	594	593	592	592
36	772	768	762	758	756	756	755	755	755
38	930	934	942	947	949	950	951	951	951
40	1 11	1 12	1 15	1 17	1 18	1 18	1 18	1 18	1 18
42	1 32	1 33	1 38	1 42	1 44	1 45	1 46	1 46	1 46
44	1 56	1 56	1 64	1 71	1 75	1 77	1 78	1 78	1 78
46	1 84	1 83	1 94	2 04	2 10	2 14	2 15	2 16	2 16
48	2 16	2 12	2 26	2 41	2 51	2 56	2 58	2 59	2 60
50	2 53	2 45	2 61	2 82	2 96	3 03	3 07	3 09	3 10
52	2 95	2 82	3 01	3 27	3 47	3 58	3 63	3 66	3 68
54	3 43	3 23	3 43	3 77	4 03	4 18	4 27	4 31	4 33
56	3 98	3 70	3 90	4 31	4 65	4 86	4 98	5 04	5 07
58	4 59	4 22	4 42	4 90	5 34	5 62	5 78	5 86	5 90
60	5 28	4 80	4 99	5 54	6 08	6 45	6 66	6 78	6 84
62	6 06	5 45	5 61	6 23	6 89	7 36	7 64	7 80	7 88
64	6 92	6 18	6 29	6 98	7 76	8 36	8 72	8 93	9 04
66	7 89	6 98	7 05	7 78	8 70	9 44	9 91	10 18	10 33
68	8 96	7 88	7 87	8 66	9 71	10 61	11 20	11 55	11 75
70	10 2	8 9	8 8	9 6	10 8	11 9	12 6	13 1	13 3
72	11 5	10 0	9 8	10 6	12 0	13 2	14 1	14 7	15 0
74	12 9	11 2	10 9	11 7	13 2	14 7	15 8	16 5	16 9
76	14 5	12 5	12 1	12 9	14 5	16 2	17 5	18 4	18 9
78	16 2	13 9	13 4	14 2	15 9	17 8	19 4	20 5	21 1
80	18 2	15 5	14 8	15 6	17 4	19 6	21 4	22 7	23 5
82	20 2	17 2	16 4	17 2	19 1	21 4	23 5	25 1	26 1
84	22 5	19 1	18 1	18 8	20 8	23 4	25 8	27 6	28 8
86	25 0	21 2	19 9	20 6	22 6	25 5	28 2	30 4	31 8
88	27 6	23 4	21 9	22 5	24 6	27 7	30 7	33 2	35 0
90	30 5	25 8	24 1	24 6	26 8	30 0	33 4	36 3	38 3

Figure 3.1.19: Table to evaluate the axle load equivalency factor, rigid pavements, tridem/triple axles, pt equal to 3 (AASHTO, 2001)

In this case the load on each axle in the triple axles group is 25 kips, so a total of 75 kips, so the load equivalent factor needs to be interpolated between 74 and 76 kips. Lastly the overall axle load equivalent factor will be the sum of the ones obtained from the single axle table, and the one from the triple axel table. These considerations apply to the flexible pavement design, the tables will be different as both the surface material and the terminal serviceability are different.

The container terminal is trafficked by both vehicles typologies, therefore it is considered that the traffic is divided as it follows (J. D. Rodriguez Millan, 2024):

1. 75% container straddle carrier
2. 25% trucks

Therefore the total value of ESALs for each terminal is:

Table 3.1.15: Total ESALs for the rigid pavement

ESALs in the design life Container terminal	ESALs in the design life Ro-Ro terminal
2.73E+08	5.14E+07

It is now possible to use Equation.3.1.12, and compute the slab thickness for both areas.

Since the aim of the thesis work is to compare different design solutions to evaluate their environmental impact, two designs have been realized for the rigid pavement. As mentioned previously the AASHTO 1993 manual only helps in the direct calculation of the slab's thickness, the thickness of the base and subbase layers derive from experimental studies. In this case those values were assumed as there was no experimental data to refer to. Therefore the current slab thicknesses have been used to obtain two designs. The first one is shown in Table 3.1.16, the second in Table 3.1.17:

Table 3.1.16: Rigid pavement design 1 AASHTO '93

Container Terminal			Ro-Ro Terminal		
concrete slab	432	mm	concrete slab	356	mm
subbase	150	mm	subbase	150	mm

Table 3.1.17: Rigid pavement design 2 AASHTO '93 manual

Container Terminal			Ro-Ro Terminal		
concrete slab	432	mm	concrete slab	356	mm
Cement bound base	210	mm	Cement bound base	210	mm
subbase	150	mm	subbase	150	mm

The same traffic considerations have been applied to the flexible pavement. This can be designed following AASHTO 1993 manual, the steps are the same as for the rigid pavements, but the input variables change (AASHTO, 2001):

1. Estimated future traffic, in terms of 18kip equivalent single axle loads (ESAL)
2. Effective resilient modulus of roadbed material M_r, [psi]
3. Design serviceability loss ΔPSI
4. Overall standard deviation S_0
5. Terminal serviceability index, p_t
6. Drainage coefficient for base and subbase layers, m_i
7. Layer coefficient, for surface, base and subbase layers, a_i
8. Reliability, R

Using the following equation is possible to compute the structural number, *SN*, for the pavement, which is then used to evaluate the axial load equivalency factors, and ultimately correct the initial ESAL estimation.

Equation 3.1.13: Design equation flexible pavement (AASHTO, 2001)

$$\log_{10}(W18) = Z_R S_0 + 9.36\log_{10}(SN+1) - 0.20 + \frac{\log_{10}[\frac{\Delta PSI}{4.2-1.5}]}{0.40 + \frac{1094}{(SN+1)^{5.19}}} + 2.23 * \log_{10} M_r - 8.07$$

This equation can be solved graphically or analytically, considering the following variables as input:

Table 3.1.18:Input variables, flexible pavement, AASHTO 1993

ESAL 10 years	1.0E+07	
M_r subgrade	2.9E+04	psi
M_r subbase	4.35E+04	psi
M_r base cement bound	7.25E+05	psi
$a_i$asphalt	0.42	
$a_i$base	0.14	
$a_i$subbase	0.1	
$m_i$base	0.8	-
$m_i$subbase	0.7	
R	90%	
S_0	0.35	
ΔPSI	1.5	
p_t	2.7	

The subgrade modulus are the ones from Table 3.1.18, it is enough to convert the unit of measurement into pound per square inches [psi]. The values corresponding to the layer coefficient, the drainage coefficient and the ESAL are known (A.Guarin, 2023) .The same applies for the standard deviation, reliability and design loss and terminal serviceability. It is possible to refer to the tables in the Appendix-D of the AASHTO 1993 manual, in order to determine the axial load equivalent factor (AASHTO, 2001). These are very similar to the ones previously used, with the difference that instead of the slab thickness the input value is the SN of the whole pavement.

Once the axial load equivalent factor has been estimated for every vehicle type, it is possible to evaluate the ESALs, multiplying the average passes in each terminal, Table 3.1.14, by the design life of the pavement, ten years, and by the axle load equivalent factor. When the real value of ESALs is known, it is sufficient to solve Equation 3.1.5 for SN. Using Equation 3.1.14 it is then possible to determine the layer thicknesses:

Equation 3.1.14: Structural Number equation(AASHTO, 2001)

$$SN = a_1 D_1 + a_2 D_2 m_2 + a_3 D_3 m_3$$

It should be noted that the analysis is layered, therefore the structure of the pavement should be in accordance with Figure 3.1.20 (AASHTO, 2001):

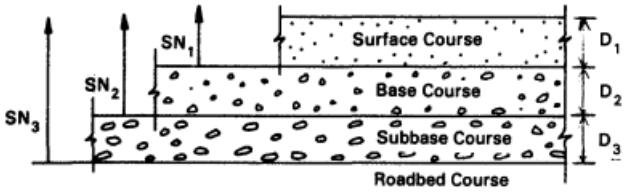

Figure 3.1.20: Structural Number of the flexible pavement,(AASHTO, 2001)

The structural number over the roadbed soil should be computed, then the one over the subbase layer, and finally the one over the base layer. Then rearranging Equation 3.1.14 into the following ones it is possible to compute the thicknesses of the layers:

1. $SN_1 = a_1 D_1$
2. $SN_2 = a_1 D_1 + a_2 D_2 m_2$
3. $SN_3 = a_1 D_1 + a_2 D_2 m_2 + a_3 D_3 m_3$

The final flexible pavements design is shown in Table 3.1.19:

Table 3.1.19:Final designs flexible pavements

Flexible pavement, container terminal		**Flexible pavement, container terminal**
layers	**mm**	**mm**
Asphalt concrete surface	88	52
base cement bound	687	467
subbase crushed stones	247	159

However the thickness of the asphalt concrete layer doesn't meet the minimum thickness requirement by the AASHTO 1993 manual, therefore the pavement cannot be used in the LCA calculation. This result could have been expect as both the loads and the resilient moduli exceed the recommended values. Consequently the design is atypical and cannot be used further.

3.2 Life Cycle Assessment

This chapter describes the Life Cycle Assessment methodology employed in the IVL report. Then it focuses on the Life Cycle Inventory (LCI) of the data, the assessment of the environmental impact, and the application of this method to the case study and the alternative pavements designed.

The life cycle assessment of the pavements, previously designed, has been conducted following the steps indicated by the Swedish Research Institute (IVL). They have developed a report, where there are detailed steps to follow when realizing an LCA cycle for both rigid and flexible roads. Those are summarized in Figure 3.2.1:

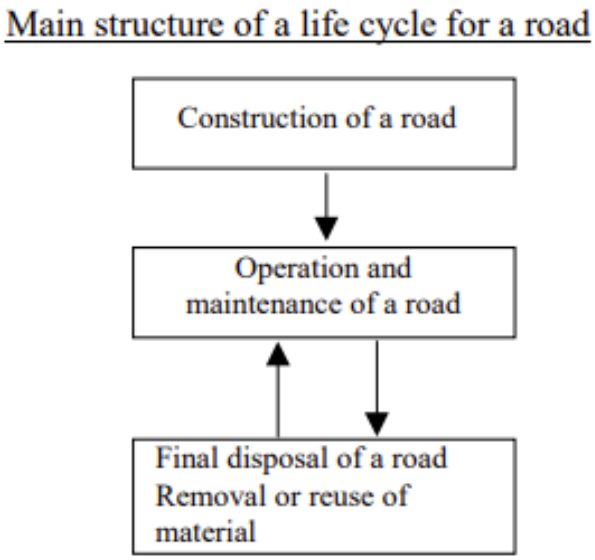

Figure 3.2.1:Overview of the LCA of a generic road(Stripple, 2001)

Generally Life Cycle Assessments have multiple phases, this thesis work is focusing on the construction and maintenance one. The functional unit used is a square meter $(m^2)$of pavement.

A life cycle assessment is "a tool which makes it possible to assess the environmental impact of a product, a process or an activity, through identifying and quantifying the flows of energy and material" (Stripple, 2001). In this case the object of analysis are port pavements, the block pavements used in Norvik port, and the rigid and flexible ones previously designed. The environmental impact of the construction and maintenance phases is expressed through equivalent (eq.) CO2 outflow in $[g/m^2]$.

3.2.1 Construction phase, concrete block pavements

The pavements currently used in port are a total of four different designs and they are referred to as:

- M1
- M2
- M3
- M4

It is possible to see how they are displayed in the port:

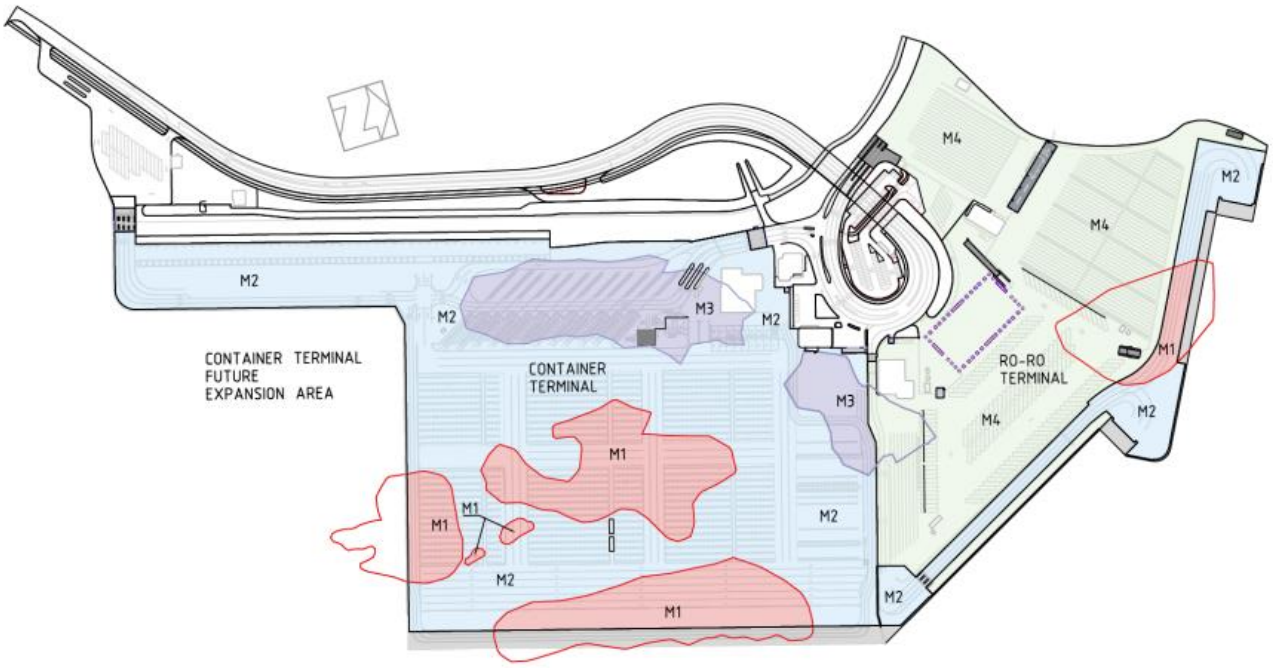

Figure 3.2.2:display of the pavements currently used in port area(J. D. Rodriguez Millan, 2024)

These pavements are designed as shown in Figure 3.2.3:

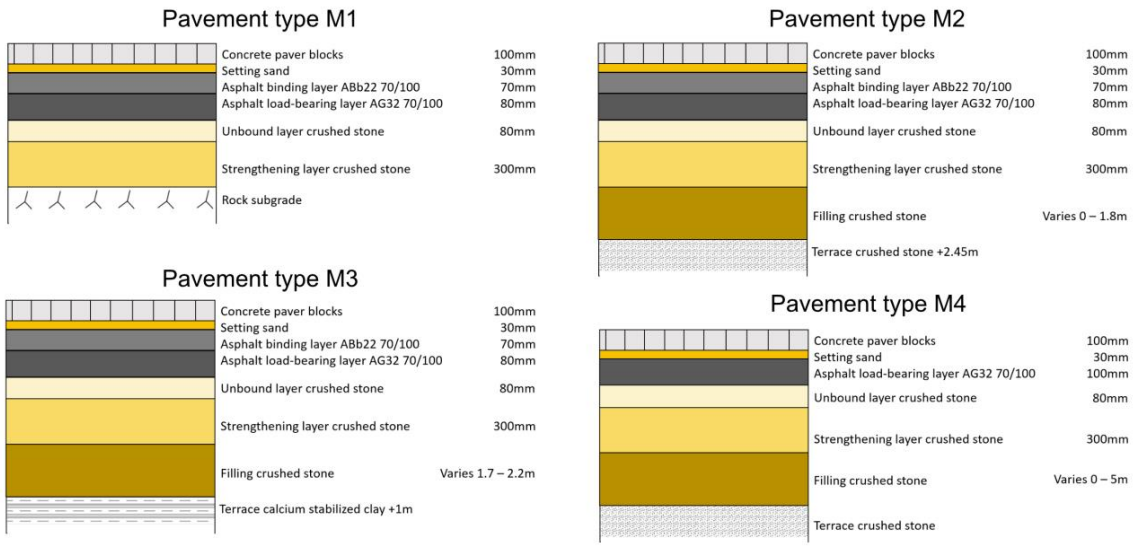

Figure 3.2.3:Port pavements design(J. D. Rodriguez Millan, 2024)

As it is possible to see from Figure 3.2.3 the pavements are composed of:

- Concrete block surface of 100 mm
- Bedding layer made of sand of 30 mm
- Two Asphalt layers, except for M4 which has only one asphalt layer
- Unbound base layer of 80 mm
- Granular subbase layer of 300 mm

The subgrade types are three:

- Rock subgrade
- Clay subgrade
- Terrace subgrade

Depending on the subgrade type there is a presence of a “filling crushed stone layer” which is adapting to the morphology of the terrain. Since the depths of this layer, in each point, are unknown, it has not been included in the LCA calculations.

The first task is to develop the LCA cycle for each layer of the pavements in the construction phase. Starting with the surfacing concrete layer the LCA follows the scheme in Figure 3.2.4:

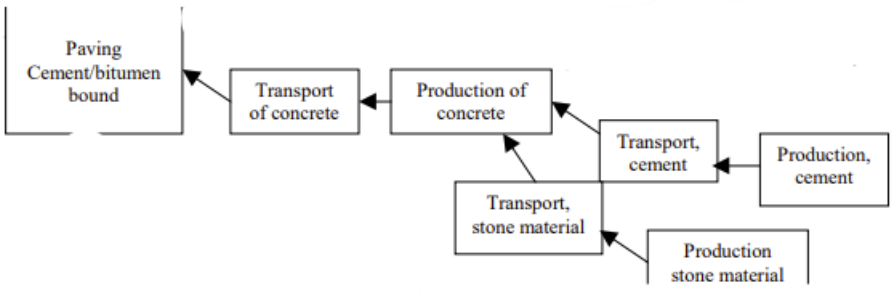

Figure 3.2.4:LCA structure for the concrete blocks surface(Stripple, 2001)

Starting from right to left, the first step is to compute the CO_2outflow of the production of cement and production of stone materials, which are the aggregates in the concrete mix. In order to do that it is necessary to determine the concrete mix design to be used. The mix design shown in "Table 4.2.17.1 Basic material and energy usage in production of cement based road concrete" page 53 of the IVL report "Life Cycle Assessment of roads"(Stripple, 2001) has been taken as a reference, and its characteristics are shown in Table 3.2.1:

Table 3.2.1:mix design of concrete used in the surface of the port pavements M1, M2, M3, M4

Mix design of concrete (amount per m^3produced concrete)		
Cement	kg/m^3	400
Crushed aggregates	kg/m^3	1200
Pit-run gravel/sand	kg/m^3	700

The water cement ratio is 0.6 according to SS-EN 206:2013+A2:2021. Once the mix design properties are established, it is necessary to determine some geometrical data, such as the volume of concrete to be used. This value is obtained as a product of the thickness of the layer, 100 mm, and the area where the pavement is used. As shown in Figure 3.2.2 the pavements cover different areas of the port, therefore this variable will change for each pavement analysed. The areas where the pavements are used are shown in Table 3.2.2:

Table 3.2.2:Areas where the pavements are used, according to Figure 2.2.2 (J. D. Rodriguez Millan, 2024)

Area of the whole port	m^2	2.77E+05
Area of M1	m^2	7.61E+04
Area of M2	m^2	8.75E+04
Area of M3	m^2	2.86E+04
Area of M4	m^2	8.87E+04

As a result the volume of concrete needed varies. Once the geometric characteristics of the port, and the mix design of concrete have been established, it is necessary to evaluate the eq. CO_2outflow for every step of the LCA cycle. Therefore it is necessary to conduct an inventory analysis to gather the data needed in the LCA calculations. Those were taken from the IVL report and they are summarized in the table below:

Table 3.2.3:Outflow data for the concrete block layer of the pavement(Stripple, 2001)

Data	**Functional Unit**	**Value**
Production of concrete	g/m^3	3.28E+05
Concrete road paving (without dowels)	g/m^2	3.30E+02
Production of cement	g/m^3	3.23E+05
Excavation of crushed aggregate	g/m^3	1.71E+03
Excavation of pit-run gravel/sand	g/m^3	5.09E+01
truck emissions	g/km	943
tonnes the trucks can transport	tons	14

Sawing ad sealing of joints	g/m^2	213

The steps to follow to evaluate the CO_2 eq. in the construction phase of the concrete blocks are 7:

1. Production of cement
2. Transportation of cement to the area of production of concrete
3. Production of stone material (crushed aggregates and gravel/sand)
4. Transportation of stone material to the production of concrete area
5. Production of concrete
6. Transportation of concrete to the construction site
7. Paving concrete

Several steps account for environmental impact due to transportation of materials. All the data regarding travel distances can be found in the Appendix " Road parameters " page 1 to 2 of the IVL report (Stripple, 2001), and are shown in the following table

Table 3.2.4:Travel distance data used in the LCA cycle calculations (Stripple, 2001)

Transport data		**unit**
Transport distance of excavated materials that has to be moved within construction site	0.5	km
Transport distance of excavated materials from external pit	2	km
Concrete paving, wearing course, transport distance for crushed aggregates from production site to concrete production site	10	km
Concrete paving, wearing course, transport distance for pit-run gravel/sand from production site to concrete production site	10	km
Concrete paving, wearing course, transport distance for cement from production site to concrete production site	300	km
Concrete paving, wearing course, transport distance for road concrete from concrete production to road construction site	2	km

The first step is to evaluate the CO_2 outflow due to the production of cement. This is done multiplying the value of "CO_2 outflow due to the production of cement" which is 3.23E+05 g/m^3, by the volume of concrete needed.

The second step accounts for the transportation of cement to the mixing area, this is computed considering the distance between the facility where the cement is produced, and the mixing area. This is estimated to be 300 km (Stripple, 2001). The environmental impact is due to the emissions of trucks moving the material from one location to another. These are 9.43E+02 g/km. Lastly it is fundamental to evaluate the number of trucks needed to complete the operation. Knowing that each truck can transport 14 tons of material, it will be sufficient to divide the mass of cement needed, by the capacity of each truck. Finally the total CO_2 eq. outflow in this step will be the product of the truck emission by the number of trucks used and by the travel distance.

The third and fourth steps follow the same procedure as the ones already explained, the only difference is in the travel distance, which is 10 km (Stripple, 2001), and the type of material. In this case the focus is on stone materials, so aggregates used in the design mix. The difference in material results in a change in the mass of material.

Once the aggregates and the cement are both in the mixing area it is time to produce concrete. The environmental impact of this step is expressed in terms of eq.CO_2 outflow equal to 3.28E+05 g/m^3, because it has to account for the carbon footprint of the production of cement and the aggregates, as well as the electricity needed for the mixing procedure. To determine the total outflow it is enough to multiply this value by the volume of concrete needed.

Then the mix needs to be transported to the site, the travel distance is considered equal to 2km, as per Table 3.2.4.

The last step involves paving operations, the emissions are expressed in terms of eq. CO_2, ad they are equal to 3.3E+02 g/m^2.

These steps are applied to all four pavements, and they summed up in Table 3.2.5:

Table 3.2.5: CO_2 outflow concrete block pavements

concrete block pavement eq.CO2 outflows [g/m^2]				
Steps	**M1**	**M2**	**M3**	**M4**
Production of cement	3.23E+04	3.23E+04	3.23E+04	3.24E+04
Transportation to the mixing area	8.08E+02	8.08E+02	8.08E+02	8.08E+02
Production of aggregates	1.76E+02	1.76E+02	1.76E+02	1.76E+02
Transportation to the mixing area	1.28E+02	1.28E+02	1.28E+02	1.28E+02
Production of concrete	3.29E+04	3.28E+04	3.28E+04	3.28E+04
Transportation to the construction site	3.43E+01	3.42E+01	3.42E+01	3.42E-05
Paving	3.30E+02	3.30E+02	3.30E+02	3.31E+02
Total	**6.66E+04**	**6.65E+04**	**6.64E+04**	**6.66E+04**

In order to evaluate the environmental impact of the construction of the port pavements in concrete blocks, it is necessary to compute the CO_2 outflow of the rest of the layers for each pavement type.

The surface is laid on a sand layer, also referred as bedding layer. The LCA cycle in this case is composed by the following steps:

1. Excavation of sand
2. Transportation to the construction site

The input data are:

Table 3.2.6:CO_2 outflow for the LCA cycle of the sand layer (Stripple, 2001)

CO_2 outflow data		**Functional unit**
CO_2 outflow of the trucks	9.43E+02	g/ton
Truck capacity	14	ton
CO_2 outflow Excavation of sand	0.078	g/ton

The characteristics of the layer are:

Table 3.2.7: Characteristics of the sand layer

Layer characteristics		**Unit**
Layers thickness	30	mm
Sand density	1602	kg/m^3
CO_2 outflow Excavation of sand	0.078	g/ton

As explained previously the aim is to obtain the total outflow in grams. The total outflow will change as the pavement type changes, as the volume of sand used it's variable, as it depends on the thickness of the layer and the area that the pavement covers. The variable volume implies a change in the mass of sand, which is necessary in order to compute the total CO_2 outflow. Therefore every pavement type will have a slightly different value.

As per Figure 3.2.3, the pavements are composed of two bituminous layers. The LCA cycle in this case is structured this way:

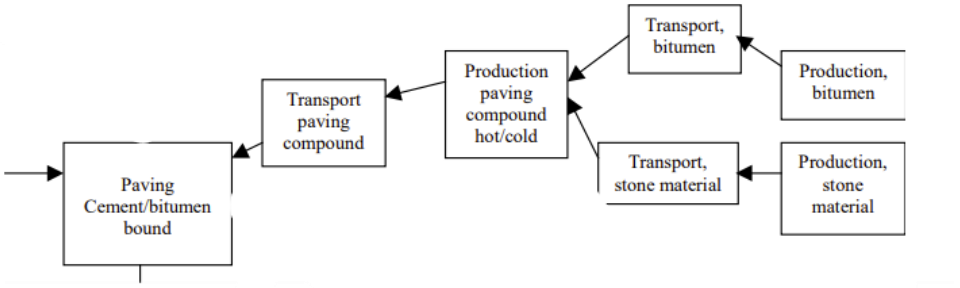

Figure 3.2.5: structure of an LCA for a bituminous material(Stripple, 2001)

From the right to the left the steps are (Stripple, 2001):

1. Production of bitumen
2. Production of stone material
3. Transport of bitumen
4. Transport of stone material
5. Production of paving compound, in this case hot mixing asphalt
6. Transport of paving compound
7. Paving operations

The types of asphalts used are ABb22, and AG32. The mix design has been taken from the Swedish standard TDOK 2013:0529, (Kenneth, 2020).

The mix designs of ABb22 is:

- 4% filler
- 22% sand
- 74% other aggregates
- 4.8% binder

The mix design of AG32 is:

- 4.5% filler
- 25% sand
- 70.5% other aggregates
- 4.4% binder

The input data, in terms of $eq.\,CO_2$ outflow are:

Table 3.2.8: $eq.CO_2$ outflow for the LCA cycle of the bituminous layers (Stripple, 2001)

Input Data		
CO2 outflow	**Value**	**Functional unit**
Production of sand	0.0728	kg/ton
Production of bitumen	173	kg/ton
Production of filler	0.806	kg/ton
aggregates	1.42	kg/ton
Hot Mix Asphalt (HMA) operations	22637	g/ton
Asphalt paver	4.69E+01	g/m^2
Asphalt roller	6.32E+01	g/m^2
Trucks capacity	14	tonnes
Trucks emissions	943	g/km

The travel distances covered are:

Table 3.2.9:Travel distances covered in the LCA cycle for bituminous layers (Stripple, 2001)

Transport distance for excavated materials that has to be moved within the construction site	km	0.5
Transport distance of excavated materials from external pit	km	2
Transport distance of excavated material from road construction site to landfill	km	2
Transport distance of aggregates from production site to asphalt plant	km	5
Transport distance of filler from production site to asphalt plant	km	200
Transport distance of bitumen from production site to asphalt plant	km	100
Transport distance of asphalt from asphalt plant to road construction site	km	200

In order to obtain the overall CO_2 outflow for each asphalt layer, the analysis' method is analogous to the one for the surface layer. The estimated CO_2 outflow for each step for the different layers are shown in Table 3.2.10:

Table 3.2.10: CO_2 eq. outflow for concrete block pavements, asphalt layers

CO_2 eq. outflow asphalt layers [g/m^2]				
Steps	**M1**	**M2**	**M3**	**M4**
Production of bitumen	1.64E+03	1.63E+03	1.64E+03	1.86E+03
Transportation to the mixing area	3.93E+03	3.93E+03	3.94E+03	7.25E+01
Production of stone material	2.41E+02	2.37E+02	2.99E+02	2.58E+02
Transportation to the mixing area	2.97E+02	2.92E+02	2.92E+02	2.28E+02

Production of HMA	1.03E+04	1.03E+04	1.03E+04	5.54E+03
Transportation to the construction site	3.48E+01	3.02E+01	9.25E+01	3.11E+01
Paving	1.10E+02	1.10E+02	1.10E+02	1.10E+02

Due to the presence of binder and cement the asphalt layers and the concrete pavers procedures are the most significative in terms of environmental impact. Therefore the results are shown in detail for each step.

As shown in Figure 3.2.3, base and subbase don't vary significantly for each pavement type, when the "crushed stone layer" is not considered. Both layers are unbound, therefore there is no binding material in use. The structure of the LCA cycle for the base is:

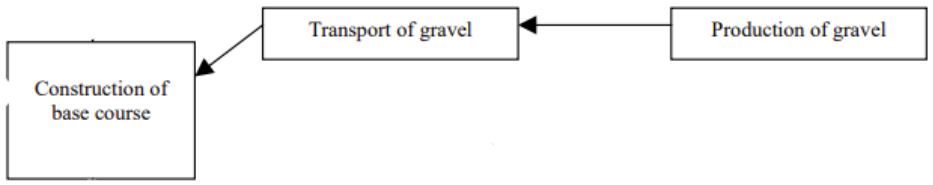

Figure 3.2.6: Structure of the LCA cycle of a generic unbound base of a road infrastructure(Stripple, 2001)

From right to left the steps are (Stripple, 2001):

1. Production of gravel material
2. Transport of gravel material
3. Construction of base, which involves compaction operations

The CO_2 outflow input data are:

Table 3.2.11:Input data for a generic unbound base(Stripple, 2001)

Input data		
CO_2 outflow	**value**	**Functional unit**
production of gravel	7.29E+01	g/ton
Compactor	5.55E+01	g/m^2
dumper trucks	5.35E+02	$g/m^3/km$
transport distance	2	km

The characteristics of the layer are:

Table 3.2.12:Charcteristics of the base layer (Balieu, 2022; J. D. Rodriguez Millan, 2024)

Characteristics of the layer		
Material density	2160	kg/m^3
Thickness of base layer	80	mm

The subbase LCA cycle is realized in the following way:

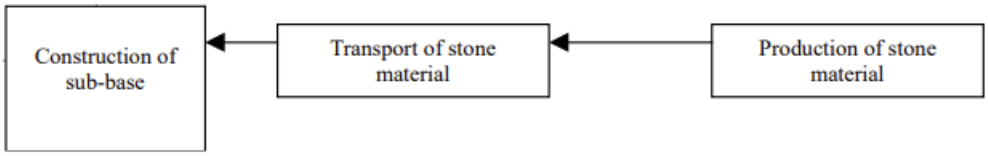

Figure 3.2.7:LCA cycle of a generic granular subbase (Stripple, 2001)

From right to left the steps are:

1. Production of stone material
2. Transport of stone material
3. Construction of subbase, involving compaction operations

The subbase input values are:

Table 3.2.13: Input data for a generic granular subbase (Stripple, 2001)

Input data		
CO_2 outflow	**value**	**Functional unit**
production of stone material	1420	g/ton
Compactor	5.55E+01	g/m^2
dumper trucks	5.35E+02	$g/m^3/km$
transport distance	5	km

The characteristics of the layer are:

Table 3.2.14: Characteristics of the subbase layer(Balieu, 2022; J. D. Rodriguez Millan, 2024)

Characteristics of the layer		
Material density	1920	kg/m^3
Thickness of subbase layer	300	mm

The overall total outflow for each layer for the different pavements is:

Table 3.2.15: CO_2 eq. total outflow for concrete block pavements

CO_2 eq. Outflow concrete block pavements [g/m^2]				
layers	**M1**	**M2**	**M3**	**M4**
Concrete blocks	6.66E+04	6.67E+04	6.68E+04	6.66E+04
Sand	3.25E+01	3.23E+01	3.24E+01	3.24E+01
Asphalt layer	1.23E+04	1.23E+04	1.24E+04	8.09E+03
Base	1.54E+02	1.53E+02	9.93E+02	9.82E+01
Subbase	1.68E+03	1.68E+03	8.99E+02	1.67E+03
Total	**8.08E+04**	**8.09E+04**	**8.03E+04**	**7.65E+04**

3.2.2 Construction phase, rigid and flexible pavements

The LCA cycle has been applied to the road designs shown in Chapter 3. The final designs are shown in the Tables below:

Table 3.2.16: Flexible pavement in the Ro-Ro Terminal, Heavy duty pavement manual design 2

Flexible pavement Ro-Ro terminal heavy duty pavement manual design 2		
HRA surface	138	mm
Cement bound Base	200	mm
Subbase	300	mm

Table 3.2.17: Flexible pavement Ro-Ro terminal, Heavy duty pavement manual design 1

Flexible pavement Ro-Ro terminal heavy duty pavement manual design 1		
HRA surface	450	mm
Subbase	150	mm

Table 3.2.18:Rigid pavement in the Ro-Ro Terminal, Heavy duty pavement manual design

Rigid pavement Ro-Ro terminal heavy duty pavement manual design		
concrete surface	234	mm
Subbase	150	mm

Table 3.2.19:Rigid pavement Ro-Ro terminal, AASHTO '93 manual design 1

Rigid pavement Ro-Ro terminal AASHTO manual design 1		
concrete surface	336	mm
Subbase	150	mm

Table 3.2.20: Rigid pavement Ro-Ro terminal, AASHTO '93 manual design 2

Rigid pavement Ro-Ro terminal AASHTO manual design 2		
concrete surface	330	mm
Cement bound base	250	mm
Subbase	150	mm

Table 3.2.21:Flexible pavement Container terminal, Heavy duty pavement manual design 2

Flexible pavement container terminal heavy duty pavement manual design 2		
HRA surface	138	mm
Cement bound Base	300	mm
Subbase	330	mm

Table 3.2.22:Flexible pavement Container terminal, Heavy duty pavement manual design 1

Flexible pavement container terminal heavy duty pavement manual design 1		
HRA surface	588	mm
Subbase	150	mm

Table 3.2.23:Rigid pavement Container terminal, Heavy duty pavement manual design

Rigid pavement container terminal		
Concrete surface	306	mm
Subbase	150	mm

Table 3.2.24:Rigid pavement Container terminal, AASHTO 93 manual design 1

Rigid pavement Container terminal AASHTO manual design 1		
concrete surface	432	mm
Subbase	150	mm

Table 3.2.25:Rigid pavement Container terminal, AASHTO 93 manual design 2

Rigid pavement Ro-Ro terminal AASHTO manual design 2		
concrete surface	406	mm
Cement bound base	250	mm
Subbase	150	mm

The analysis is divided between the two areas, Ro-Ro Terminal and Container terminal, which are respectively:

Table 3.2.26: Container and Ro-Ro areas

Container area	m^2	1.72E+05
Ro-Ro area	m^2	1.06E+05

The structures of the LCA's cycles for each layer are analogous to the ones already used in the interlocking concrete block pavements. The only difference resides in the base layer, because it is cement bound. Therefore the LCA cycle will be structured this way (Stripple, 2001):

1. Production of cement
2. Production of stone material
3. Transportation of cement to the mixing area
4. Transportation of the stone material to the mixing area.
5. Production of concrete, in this case the one used is $C_{8/10}$, as indicated in the Heavy duty pavement manual
6. Transportation of Cement bound granular mixture (CBGM) to the construction site
7. Stabilization operations, using slipform pavers which include compaction of the layer

The concrete used is $C_{8/10}$, which, as stated in the Interpave manual, has 40% of the amount of cement and water in the mix compared to a normal concrete(Knapton, 2008) . The concrete taken as a reference in this case is the one used for the surface of the interlocking concrete blocks pavement. The same CBGM is used in both rigid and flexible designs. The eq. CO_2 emissions data are taken form the IVL report and they are analogous to the ones used in the concrete block pavements. Except for the stabilization of the cement bound base which is 9.48 g/m^2.

The concrete slab in rigid pavements is realized using the same concrete mix design as the concrete block pavement's surface.

Whereas for the flexible the mix is composed of (Balieu, 2022):

- 5.40% binder
- 1% filler
- 93.6% aggregates, of which 37% sand

The results of the LCA analysis are:

Table 3.2.27: Flexible pavement Container area, Heavy duty pavement manual design 2

Total Outflow Flexible pavement container terminal, Heavy duty pavement design 2		**Unit**
Hot rolled asphalt (HRA)	1.16E+04	g/m^2
Cement bound base	2.06E+05	g/m^2
Subbase	1.84E+03	g/m^2
Total outflow	**2.08E+05**	**g/m^2**

Table 3.2.28:Flexible pavement container area, Heavy duty pavement manual design 1

Total Outflow Flexible pavement container terminal, Heavy duty pavement design 1		**Unit**
Asphalt	4.90E+04	g/m^2
Subbase	8.66E+02	g/m^2
Total outflow	**4.98E+04**	**g/m^2**

Table 3.2.29:Rigid pavement total outflow container area, Heavy duty pavement manual design

LCA results for a rigid pavement container terminal, Heavy duty pavement design		**Unit**
Concrete	2.03E+05	g/m^2
Subbase	8.66E+05	g/m^2
Total outflow	**2.04E+05**	**g/m^2**

Table 3.2.30: Rigid pavement container terminal, AASHTO '93 manual design 1

Total Outflow Rigid pavement container terminal, AASHTO 93 design 1		**Unit**
Concrete	2.85E+05	g/m^2
Subbase	8.66E+02	g/m^2
Total outflow	**2.86E+05**	**g/m^2**

Table 3.2.31: Rigid pavement container terminal, AASHTO '93 manual design 2

Total Outflow Rigid pavement container terminal, AASHTO 93 design 1		**Unit**
Concrete	2.68E+05	g/m^2
Cement bound base	1.72E+05	g/m^2
Subbase	8.66E+02	**g/m^2**
Total outflow	**4.41E+05**	**g/m^2**

Table 3.2.32:Fleixble pavement total outflow Ro-Ro terminal, heavy duty manual design 2

Total Outflow Flexible pavements Ro-Ro terminal, Heavy duty pavement manual design 2		**Unit**
Asphalt	1.18E+04	g/m^2
Cement bound base	1.38E+05	g/m^2
subbase	1.68E+03	g/m^2
Total outflow	**1.39E+05**	**g/m^2**

Table 3.2.33: Flexible pavement Ro-Ro terminal, Heavy duty pavement design 1

Total Outflow Flexible pavement Ro-Ro terminal, Heavy duty pavement design 1		**Unit**
Asphalt	3.76E+04	g/m^2
Subbase	8.66E+02	g/m^2
Total outflow	**3.85E+04**	**g/m^2**

Table 3.2.34:Rigid pavement total outflow Ro-Ro terminal, Heavy duty pavement manual design 1

Total outflow rigid pavement Ro-Ro terminal, heavy duty pavement manual design		**Unit**
Concrete	1.55E+05	g/m^2
Subbase	8.66E+02	g/m^2
Total outflow	**1.56E+05**	**g/m^2**

Table 3.2.35: Rigid pavement total outflow Ro-Ro terminal, AASHTO 93 manual design 1

Total Outflow Rigid pavement container terminal, AASHTO 93 design 1		**Unit**
Concrete	2.35E+05	g/m^2
Subbase	8.66E+02	g/m^2
Total outflow	**2.36E+05**	**g/m^2**

Table 3.2.36: Rigid pavement total outflow Ro-Ro terminal, AASHTO 93 manual design 2

Total Outflow Flexible pavement Ro-Ro terminal, AASHTO 93 design 2		**Unit**
Concrete	2.35E+05	g/m^2
Cement bound base	1.72E+05	g/m^2
Subbase	8.66E+02	**g/m^2**
Total outflow	**4.07E+05**	**g/m^2**

3.2.3 Maintenance phase

The LCA cycle has been developed for both the phase of construction and maintenance. This is usually the usage stage of the pavement, and it includes both maintenance and general operations conducted in the pavement's surface. In order to organize the maintenance works a detailed plan was developed. The general operations are realized to keep the road clean, to guarantee safety and comfort to the drivers. These activities are conducted every year, for each pavement type, and they include (Stripple, 2001):

1. Snow clearance
2. Sand gritting in winter road maintenance
3. Salt ratting of road in winter road maintenance
4. Washing of pavement's signs
5. Erection and removal of snow posts

The structural maintenance of the pavements depends on the type of pavement considered. The plan for flexible pavements includes:

1. Milling of asphalt layer every five years
2. Reconstruction of the asphalt layer every five years

Since the lifespan of the pavements is considered equal to ten years, those activities will be repeated twice during the time period, and then summed to the operations on the pavements surface, which occur every year.

Regarding rigid pavements, their maintenance is less frequent with respect to flexible pavements. Therefore the plan includes the following steps:

The maintenance operations for concrete pavements includes (Stripple, 2001):

1. Milling of wearing course
2. Resealing of joints, use of EPDM rubber
3. Road tracking milling for concrete filling
4. Concrete production for concrete filling
5. Machine operation for concrete production
6. Transport of crushed aggregated to concrete production
7. Transport of pit-run gravel/sand to concrete production
8. Transport of cement to concrete production
9. Transport of concrete to concrete production site to construction site

All of the activities above occur once every ten years, and summed with the operations, which are carried out once every year.

The pavement's technology currently employed in Norvik port is composed of a surfacing layer in concrete blocks, and one or two bituminous layers. Therefore the maintenance plan is derived from the sum of the schemes drawn for rigid and flexible pavements, without considering the "resealing of joints" activity, because the blocks are generally pressed against each other onto a layer of sand. Therefore there is no need to account for the presence of a sealant material.

The outcomes of the overall maintenance activities, as described in the plans, for each pavement typology, considering a lifetime of 10 years are:

Table 3.2.37: CO_2 eq. outflow flexible pavements

CO_2 eq. Flexible pavements [g/m^2]	
Ro-Ro terminal (design 1)	8.14E+04
Ro-Ro terminal (design 2)	2.97E+04
Container terminal (design 1)	9.96E+04
Container terminal (design 2)	2.70E+04

Table 3.2.38: CO_2 eq. outflow concrete block pavements

CO_2 eq. Concrete block pavement [g/m^2]	
Ro-Ro terminal, Heavy duty pavement design	1.60E+04
Ro-Ro terminal, AASHTO 1	2.03E+04
Ro-Ro terminal, AASHTO 2	1.94E+04
Container terminal, Heavy duty pavement design	1.54E+04
Container terminal, AASHTO 1	1.98E+04
Container terminal, AASHTO 2	1.88E+04

Table 3.2.39: CO_2 eq. Concrete block pavements

CO_2 eq. Concrete block pavements [g/m^2]	
M1	4.93E+04
M2	4.97E+04
M3	6.94E+04
M4	3.73E+04

4 Chapter 4

This chapter is dedicated to the results and discussions of the structural design of pavements and the LCA fundings.

4.1 Pavement designs

This chapter reports the results obtained from the pavements designs calculation in Chapter 3, and the concrete block pavements.

The pavements on which the Life Cycle Assessment has been conducted are:

- Concrete block pavements, M1, M2, M3 and M4
- Rigid and flexible pavements designed with the AASHTO 1993 method and the Heavy duty pavement manual

The pavements M1, M2, M3 and M4 are currently used in the Swedish port. The designs are composed of:

- Surfacing layer made of concrete blocks, thickness 100 mm
- Bedding layer made of sand, thickness of 30 mm
- Two asphalt layers one of thickness 80mm and the other 70mm. Except for pavement M4 where there is only one asphalt layer, thickness 100mm
- Unbound base layer, thickness 80 mm
- Granular subbase layer, thickness 300mm

The design of these pavement was conducted by previous studies, and the focusing element was the subgrade type. In actuality the pavements M2, M3 and M4 don't have a rock subgrade, therefore a layer of granular material has been added between the subbase and the subgrade. The thickness of this layer varies in each pavement type, and it follows the terrain's morphology. All four pavement are distributed in the port area based on the location of the subgrade type, as shown in Figure 4.1.1:

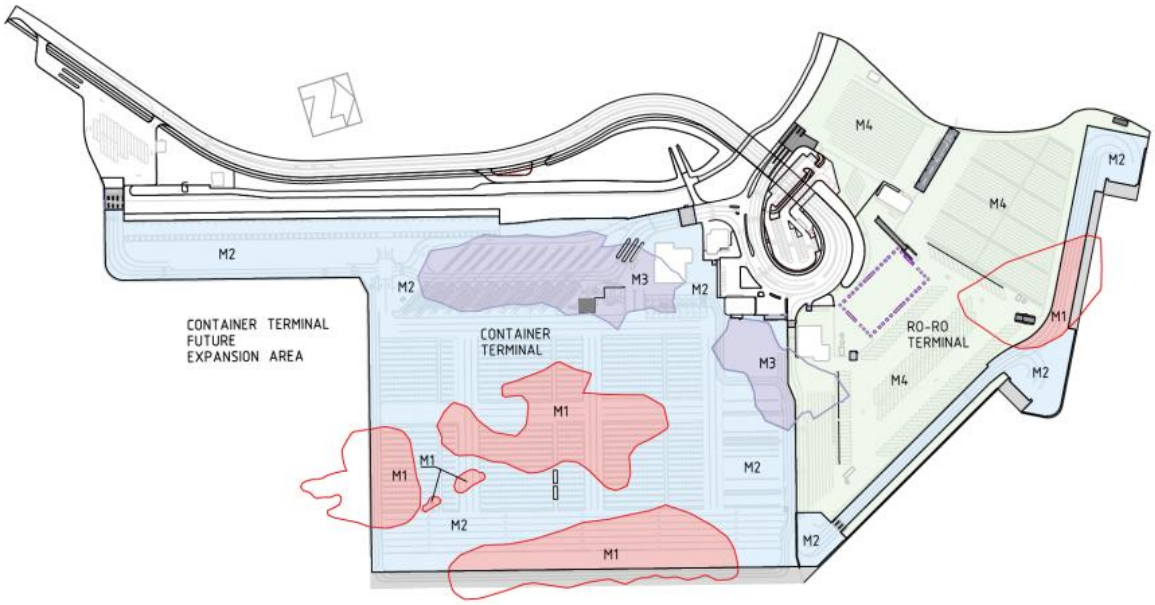

Figure 4.1.1: Distribution of concrete block pavements in Norvik port

They are distributed in the two terminals in this way:

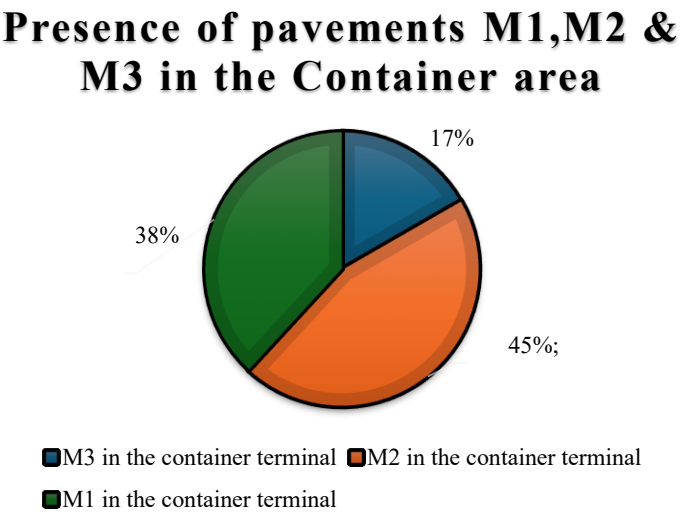

Figure 4.1.2: Distribution of concrete block pavement in the container Terminal

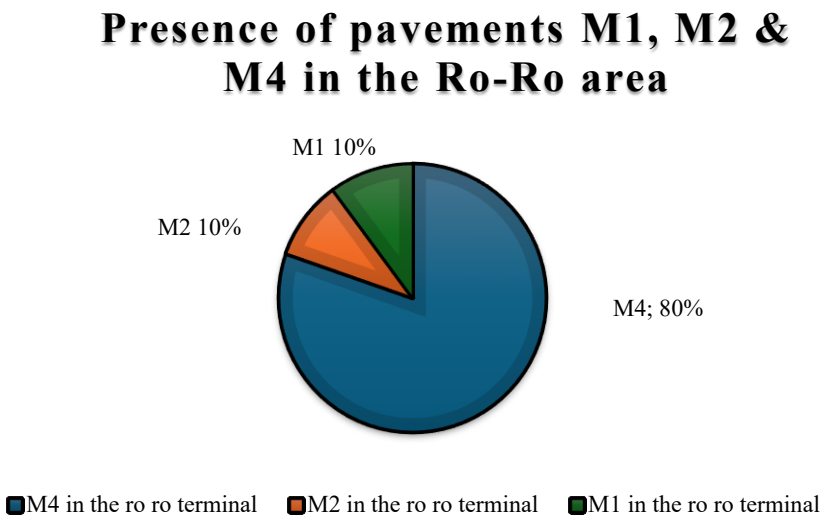

Figure 4.1.3: Distribution of concrete block pavement in the Ro-Ro Terminal

Meanwhile the flexible and rigid pavement have been designed focusing on the traffic. As mentioned the port is divided into two areas, the container terminal and the Ro-Ro terminal. The first is operated by container straddle carriers and trucks, whereas the second one is trafficked only by trucks. Therefore different pavement designs have been realized, considering the different loads they had to withstand. The manuals used for the design are the AASHTO 1993, and the Heavy duty pavement. Since the AASHTO manual was conceived mainly for the design of highways, it doesn't account for the presence of heavy vehicles, such as the container straddle carriers. Therefore the Heavy duty pavement manual method has been taken as a reference in the design process. The rigid and flexible designs using this method are:

Table 4.1.1: Rigid pavement Heavy duty pavement manual design (HDP)

Container terminal			**Ro-Ro terminal**		
Concrete slab	306	mm	Concrete slab	234	mm
subbase	150	mm	subbase	150	mm

Table 4.1.2: Flexible pavement design 2, Heavy duty pavement manual (HDP 2)

Container terminal			**Ro-Ro terminal**		
Hot rolled Asphalt	138	mm	Hot rolled asphalt	138	mm
Cement bound base	300	mm	Cement bound base	200	mm
Subbase	300	mm	Subbase	300	mm

Table 4.1.3: Flexible pavement design 1, Heavy duty pavement manual (HDP 1)

Container terminal			**Ro-Ro terminal**		
Hot Rolled asphalt	588	mm	Hot rolled asphalt	450	mm
Subbase	150	mm	Subbase	150	mm

The rigid pavement design includes a thick slab of concrete, over a granular subbase. This is due to the fact that with the presence of a cement bound base the concrete slab would have been under 10 cm thickness. This is not enough to withstand heavy loads. Whereas it was possible to realize both designs for the flexible pavement. It is of interest to evaluate how the thickness of the asphalt impacts the CO2 eq. emissions.

The AASHTO designs are shown below:

Table 4.1.4: Rigid pavement design 1, AASHTO 1993 manual (A1)

Container terminal			**Ro-Ro terminal**		
Concrete slab	432	mm	Concrete slab	356	mm
subbase	150	mm	subbase	150	mm

Table 4.1.5: Rigid pavement design 2, AASHTO 1993 manual (A2)

Container terminal			**Ro-Ro terminal**		
Concrete slab	406	mm	Concrete slab	330	mm
Cement bound base	250	mm	Cement bound base	250	mm
Subbase	150	mm	Subbase	150	mm

Using the AASHTO manual it is possible to obtain the thickness of the concrete slab, knowing the thickness of the base and subbase. Therefore using this method it was possible to obtain two different designs, both of which with a plausible stratigraphy. Whereas for the flexible pavement design the AASHTO ’93 manual presented some limitations, as both the roadbed resilient modulus and the loads considered where considerably exceeding the suggested values in the manual. Therefore the designs produced are considered to be inadequate for their purpose. The flexible pavement design is shown below:

Table 4.1.6: Flexible pavement design, AASHTO '93 manual

Container terminal			**Ro-Ro terminal**		
Asphalt concrete	88	mm	Asphalt concrete	52	mm
Cement bound base	687	mm	Cement bound base	467	mm
Subbase	247	mm	Subbase	189	mm

As shown in Table 4.1.6 the asphalt concrete surface is not sufficient to withstand heavy loads, and it is not even complaint with the minimum thickness required by the AASHTO ’93 manual. Therefore this design has not been considered in the LCA calculation.

4.2 LCA results

This chapter discusses the results obtained in the construction and maintenance phase of the LCA cycle.

4.2.1 Construction phase

The LCA cycle includes two phases:

- Construction phase
- Maintenance phase

The construction phase is the one with the highest impact on the environment. The environmental impact is measured as emissions of CO_2 eq., in g over a square meter of pavement. The functional unit is one m^2 of pavement. This phase includes the emissions due to the construction of each layer of the pavements. Depending on the layer the steps included in the construction phase are different. Usually for a flexible or rigid pavement' surface the steps include:

- Production of binder, cement or bitumen, and aggregates
- Transportation of binder and aggregates to the mixing plant
- Production asphalt or concrete
- Transportation of the final product to the construction site
- Paving operations

The steps for the construction of the cement bound base are similar to the ones used for the construction of the wearing courses, because they include the production of cement and then the production of concrete. However the last step includes stabilizing operations instead of paving.

For a granular base or subbase the steps are:

- Production of the stone material
- Transportation of the stone material to the construction site
- Compaction of the layer

The pavements examined can be divided into two groups:

1. Port pavements currently employed in Norvik Port; M1, M2, M3 and M4, which are distributed in the port dependently on the type of subgrade in the various locations.
2. Port pavements designed with the Heavy duty pavement manual and the AASHTO '93 manual, focusing on the traffic loads in the container terminal and Ro-Ro terminal of Norvik port.

Within the second group it is possible to distinguish between rigid pavement, with a concrete surface, and flexible ones, with an asphaltic surfacing layer. The LCA analysis has been carried out for all the pavements categories. First of all the results of the LCA construction phase, for each pavement category are:

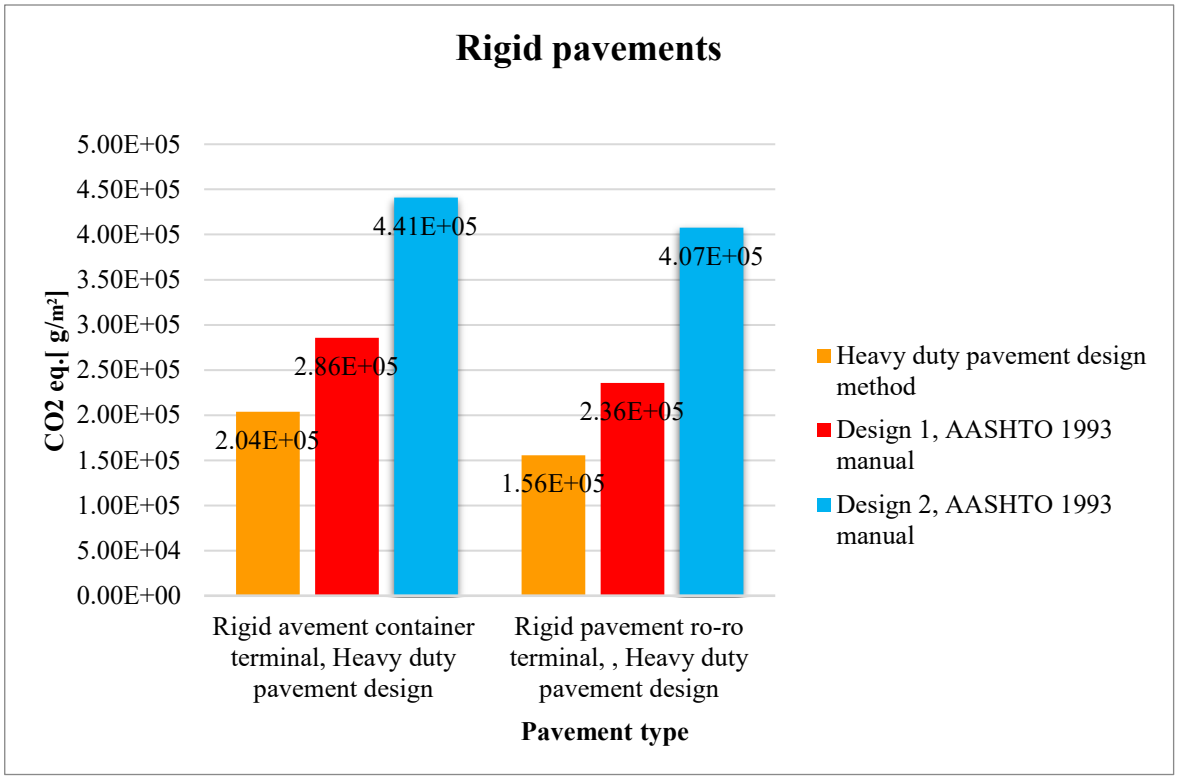

Figure 4.2.1: Results of the LCA construction phase cycle on rigid pavements

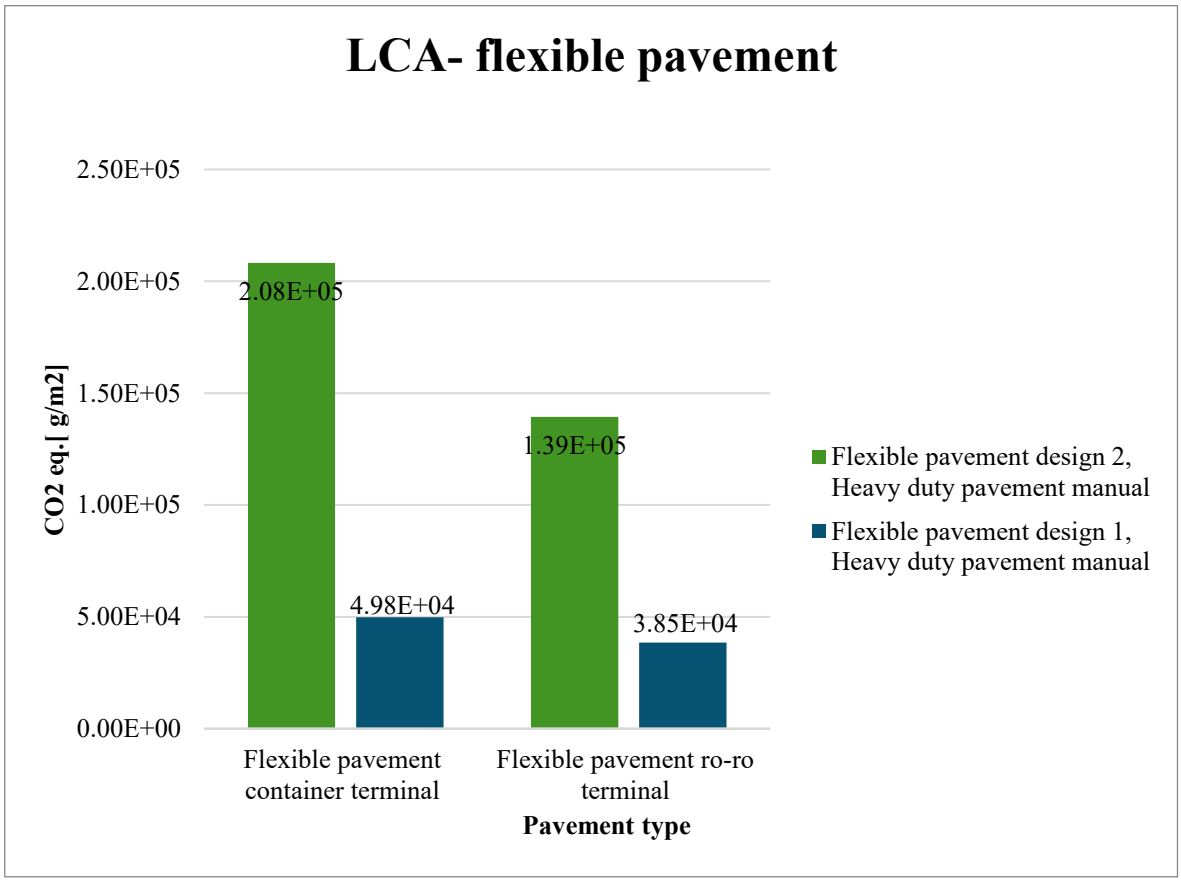

Figure 4.2.2: Results of the LCA construction phase cycle on flexible pavements

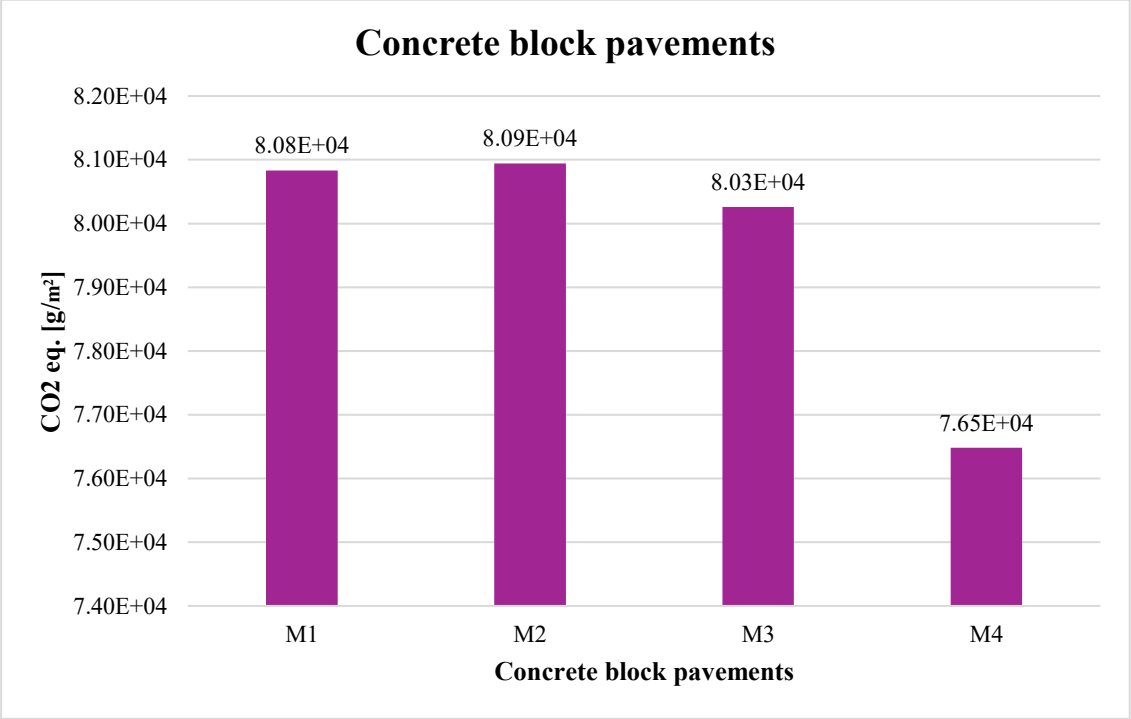

Figure 4.2.3: Results of the LCA, construction phase on concrete block pavements

These graphs show the CO_2 eq. emitted in the construction phase of the various pavements designed. The emissions indicated are the sum of the ones coming from each layer composing the pavement. The major contribution is given by the rigid pavements, and the flexible pavement design that has a cement bound base. Overall the highest ones come from the rigid pavement design 2, which has a concrete slab and a cement bound base. Therefore it is safe to assume that the major impact is due to the presence of concrete in the pavements. The highest the presence of this material the highest the CO_2 eq. are. The lowest emissions are coming from the block pavement designs, and the flexible pavement design 1, which doesn't have a cement bound base. In order to further analyse the results it is possible to compare them in a single graph:

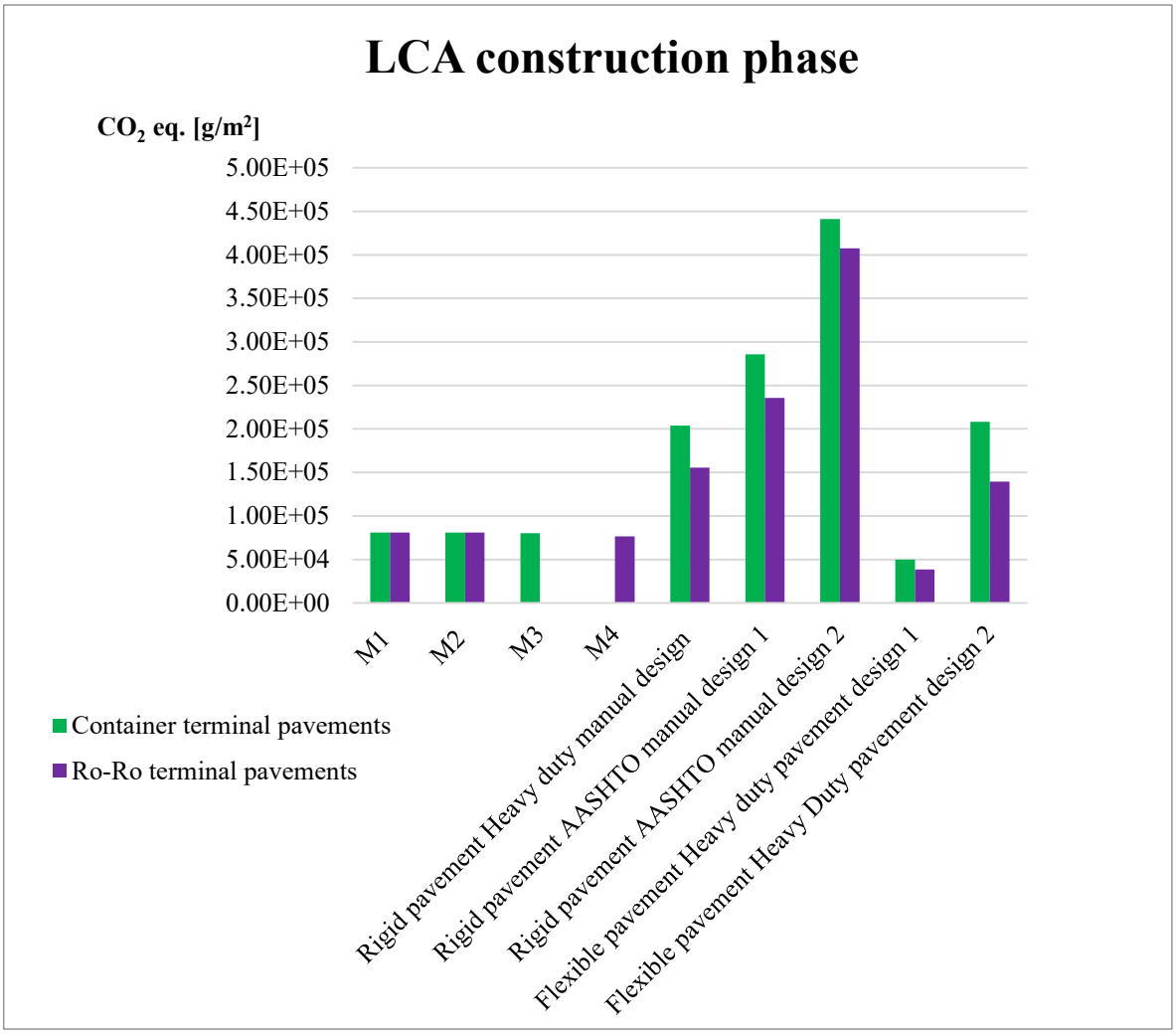

Figure 4.2.4: Results of LCA, construction phase of all pavement's designs

This graph compares all the pavement designed. The green columns refer to the rigid and flexible pavements designed for the container terminal. The purple ones refer to the rigid and flexible pavements realized for the Ro-Ro terminal. Since the block pavements where not designed following this criteria they are distributed in both areas. Therefore the emissions in both terminals are constant. The overall highest emissions are reached with the rigid pavement design 2, from AASHTO manual. This is due to the fact that this design has a presence of cement both in the slab and in the base. This finding asserts the hypothesis that the highest environmental impact is due to the volume of cement. This value depends on two variables:

- Area covered by the pavements
- Thickness of the concrete slab or cement bound base

Since the results are expressed grams of CO_2 eq. per meter square of pavement, the only real variable is the thickness of the layer. In actuality the rigid pavement design 2, is the one with the highest thickness of the concrete slab, in both terminals. Consequently the emissions of the concrete block pavements are among the lowest because the thickness of the concrete block layer is the lowest among all the results. Moreover the lowest emissions are the one due to the flexible pavement design 1, that doesn't have any presence of cement. On the same note the flexible pavement design 2, with the cement bound base, has higher emissions than the other flexible pavement design. The difference in emissions is highlighted by a different order of magnitude, in

the design 1 the order of magnitude is 10^4 g/m^2, and in the design 2 it is 10^5 g/m^2. Therefore it is safe to assume that the production processes that involves cement has a more negative impact on the environment, compared to those processes that involve bituminous binders.

Regarding this matter it is interesting to further analyse how flexible or rigid pavement's designs influence the environmental impact. Therefore the rigid pavement design realized with Heavy duty pavement has been compared with the corresponding one evaluated using AASHTO '93 method. Both of them are subjected to comparative analysis with the flexible design 1, as all of these designs are composed of:

1. Surfacing layer of asphalt concrete or concrete
2. Granular subbase of 150 mm thickness

The results of this analysis are shown in:

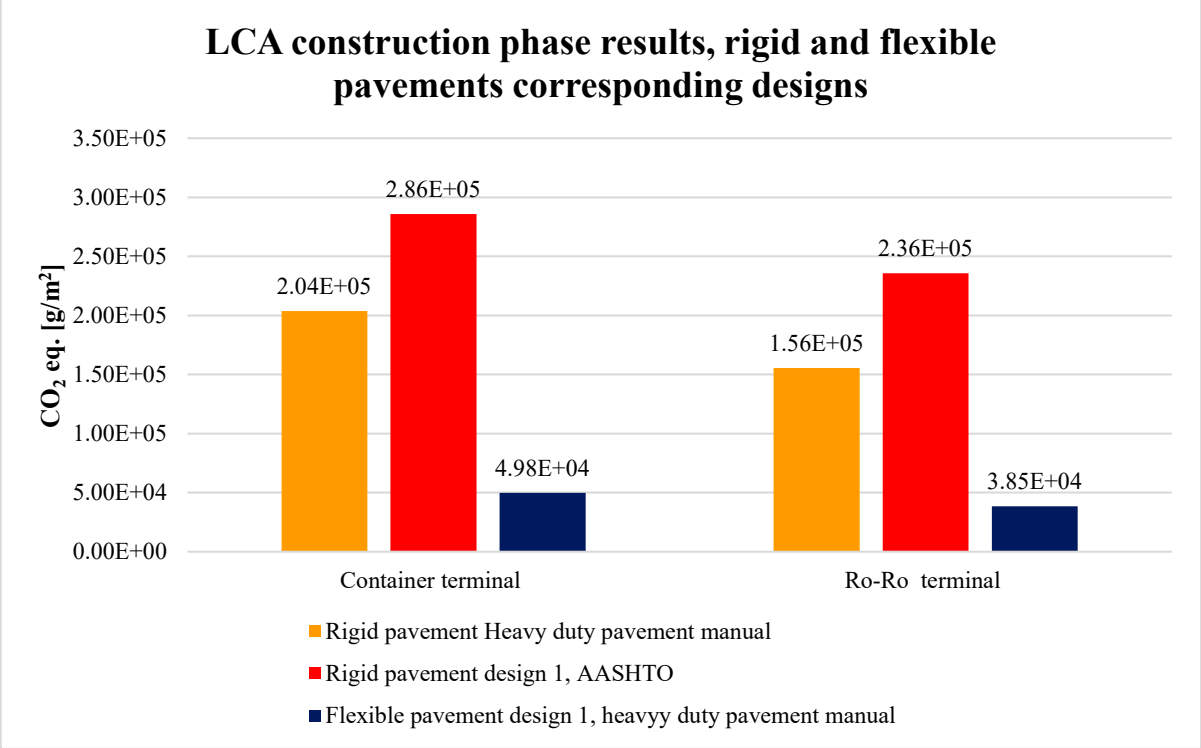

Figure 4.2.5: Results of the rigid pavements and the flexible pavements without a cement bound base

Since the three pavement's designs have the same subbase thickness and material composition, it is possible to confirm that the designs that have to account for the presence of cement have the highest environmental impact. The order of magnitude of the CO2 eq. emitted through the construction processes of the asphaltic pavements are significantly lower than those of the rigid designs. This is considering that the asphalt layer is considerably thicker than one of the concrete slab, in both terminals, as it is:

- In the container terminal the asphalt layer is 588 mm thick, compared to the AASHTO rigid design with a concrete slab of 432mm and the Heavy duty pavement one with a slab of 310 mm.
- In the Ro-Ro termina the asphalt layer is 450 mm thick, compared to the AASHTO rigid design which is 356mm thick and the Heavy Duty pavement one is 240 mm.

Particularly it is engaging to observe how the pavements designed following the guidelines of the heavy duty pavement manual result in surfacing layers made of asphalt that are almost double the concrete slab, in the corresponding rigid designs. In the container terminal the concrete slab is 310 mm, whereas the asphalt surface is 588mm. The same can be reported about the ro-Ro terminal, where the concrete slab is 240 mm, and the asphalt surface is 450 mm. However, as shown in the graph above, the rigid designs have a more negative impact on the environment than the flexible ones, even when the design method is analogous and the thickness of the layers is half the others.

In light of this it is pertinent to scrutinize the steps with most pronounced negative impact on the environment, the results of this analysis are shown in:

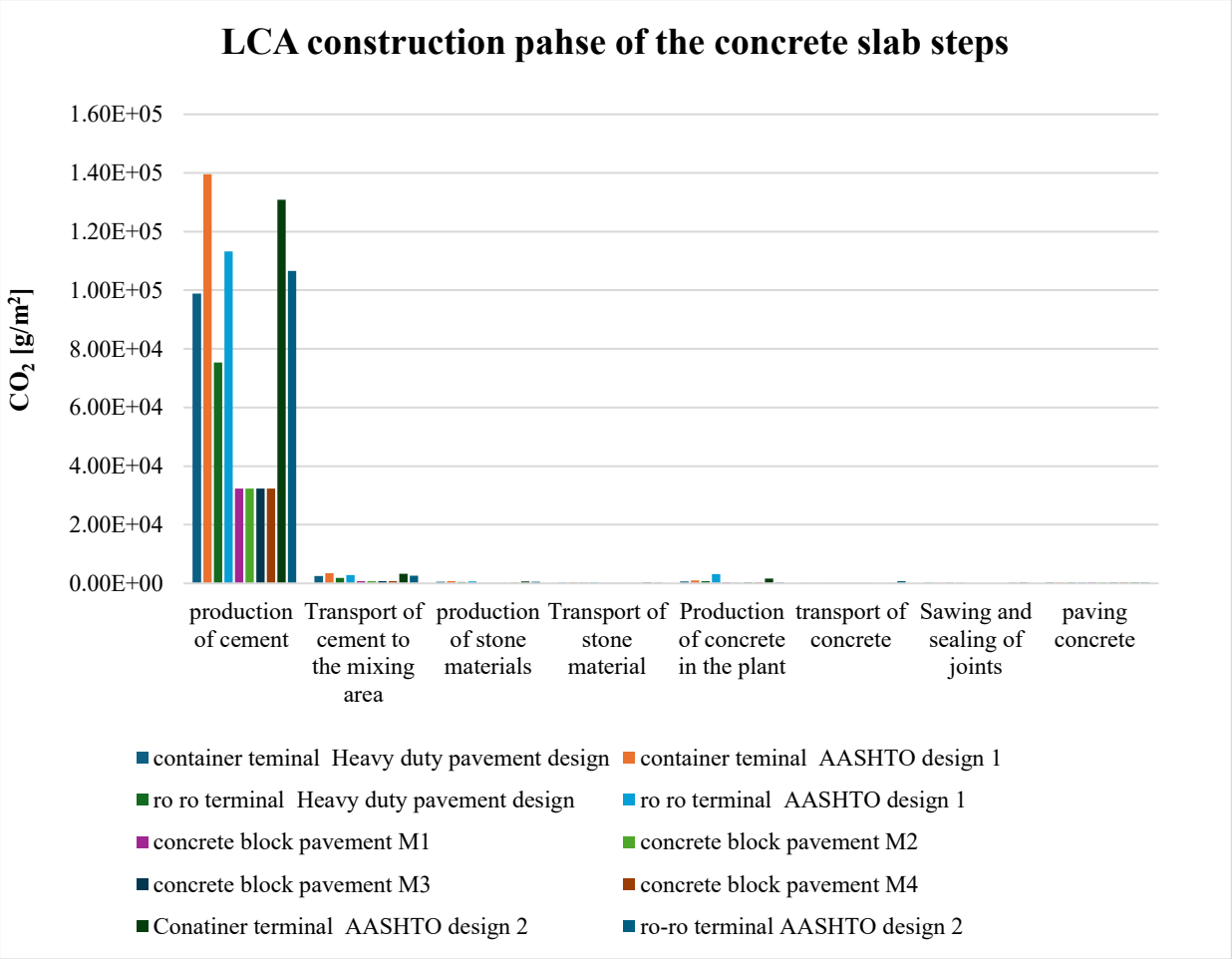

Figure 4.2.6: Results of the construction of concrete slabs and blocks

This graph collects the CO2 eq. emitted through each step of the construction of the concrete slab, in each pavement design analysed. The steps in the construction phase are 8:

1. Production of cement
2. Transportation of cement to the mixing area
3. Production of crushed aggregates and sand/gravel
4. Transportation of crushed aggregates and sand/gravel to the mixing area
5. Production of concrete
6. Transportation of concrete to the construction site
7. Sawing and sealing of joints
8. Paving operations

The highest contribution is due to the:

1. Production of cement

Therefore the most critical phase is the production of cement. As expected the results show that the highest CO_2 emissions in the most crucial step are due to the AASHTO design 1, which is the one with the thicker concrete slab. Whereas the lowest results are due to the concrete block pavements, as they have the lowest slab thickness.

The order of magnitude of the emissions due to the other steps, such as transportation or sawing and sealing of joints or paving operations, is significantly lower than the most crucial steps.

An analogous analysis can be carried out for the flexible pavements, account for all the steps included in the construction process of the asphaltic layer:

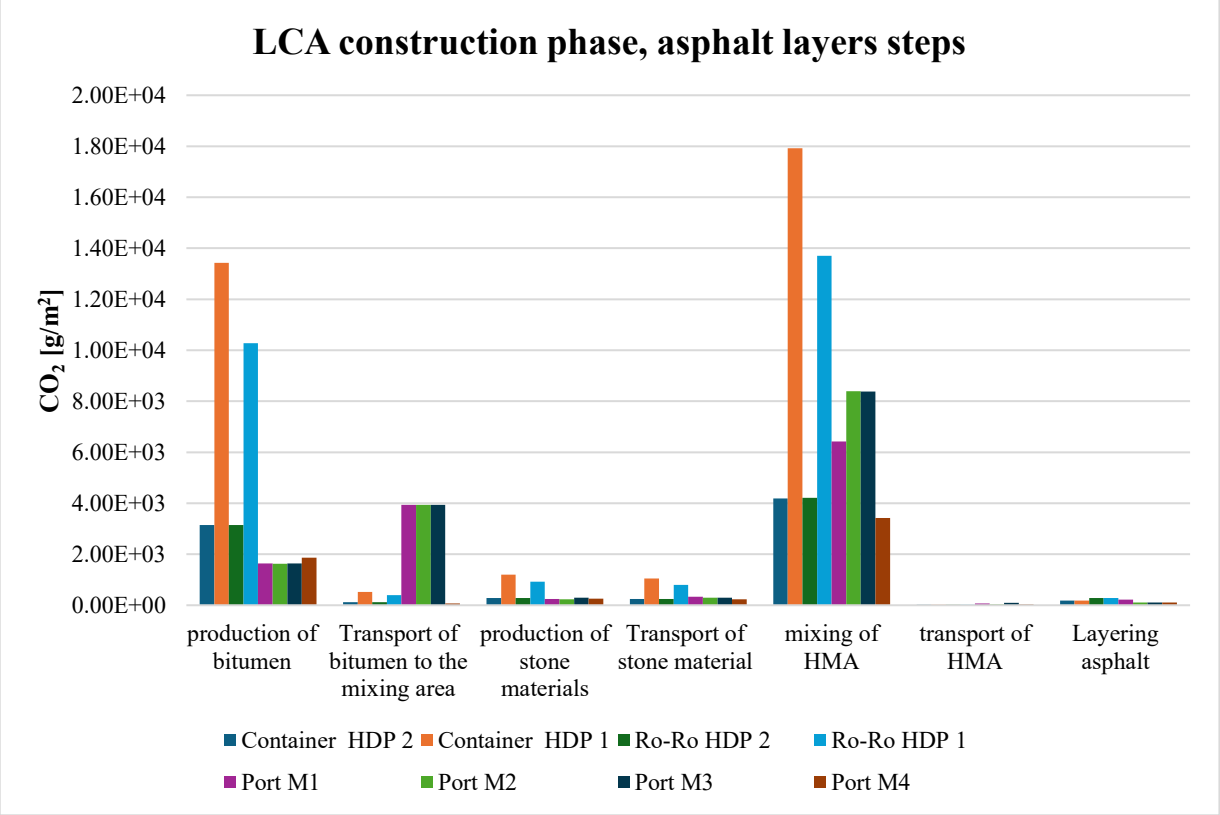

Figure 4.2.7: results of the construction of the asphalt layers

This graph collects the CO_2 eq. emitted through each step of the construction of the concrete slab, in each pavement design analysed. The steps in the construction phase are 7:

1. Production of bitumen
2. Transportation of bitumen in the mixing area
3. Production of stone materials
4. Transportation of stone materials into the mixing area
5. Mixing of Hot Mix Asphalt
6. Transportation of HMA into the construction site
7. Layering operations

As expected the highest carbon footprint is due to:

- Mixing of HMA, which accounts only for the mixing operation in the graph above

The mixing of hot asphalt has a higher environmental impact than the production of concrete, because it includes a number of steps, that need to be executed in a controlled environment, using specific tools. The steps include the heating of aggregates and of bitumen, employing a specialized laboratory oven, then the mixing in a plant, making us of a specialized mixing machine. The same process doesn't apply to the production of concrete, which could be executed manually or with the aid of a machine, which uses a specific amount of electricity.

The highest carbon footprints are related to the Heavy duty pavement design 2, which is the one with the thicker asphalt layer. In light of this results it is possible to identify a pattern, whenever the higher the binder layer is the higher is the negative impact it has on the environment.

The concrete block pavement design includes two layers of asphalt, in the M1, M2 and M3 designs, and only one in the M4 pavement. Therefore those have been inserted in the graph above. Since the thickness of these layers is the smallest compared to the others, the related emissions are the more environmentally friendly.

Therefore it is possible to conclude that the rigid pavements are the first contributors to CO_2 eq. emissions in the environment, and that is due to the production of cement which depends on the volume of material needed, which relies on the thickness of the concrete slab. Therefore the thicker the slab is the highest the CO_2 eq. emissions will be. Whereas the impact of the production of bitumen, in asphalt concrete pavements, is significantly lower than the concrete ones. Even when the thickness of the asphaltic layer is double the one in concrete. Now it remains to analyse what happens in the maintenance phase.

4.2.2 Maintenance phase

The maintenance phase includes both operations carried out on the pavement's surface, which are analogous for all pavements designed, and specific maintenance operations of concrete or asphalt layers. The first ones include:

- Snow clearance
- San gritting of the pavement, as a part of winter operations
- Salt gritting of the pavement
- Sweeping
- Washing of roadsides posts
- Washing of pavement's sings
- Erection and removal of snow posts
- Electric power production for traffic lights and lightings
- Vehicles used in complementary operations

The operations are carried out every year for the lifetime of the pavements, which is 10 years.

The structural maintenance operations for flexible pavements are scheduled once every 5 years, and comprehend:

- Milling of asphalt layer
- Reconstruction of the asphalt layer

For a rigid pavement the structural maintenance activities occur once every 10 years, and they include:

- Milling of wearing course
- Resealing of joints operations
- Pavement milling for concrete filling
- Concrete production for concrete filling
- Machine operations for concrete filling
- Transportation of crushed aggregates, sand and cement to concrete production site
- Transportation of concrete to construction site

The activities for the concrete block pavements, in use at Norvik port, are the sum of the maintenance operations for rigid pavements, excluding the "resealing of joints", because no sealant is employed in this operation, and the activities for the structural maintenance of flexible pavements. This is a consequence of the stratigraphy of the concrete block pavements, which are composed of a surface in concrete blocks, and one or two layer of asphalt.

The resulting maintenance phase is considered as the sum of the structural maintenance activities, for each pavement type, and the operations. The results, for reach pavement type, are shown in the graphs below.

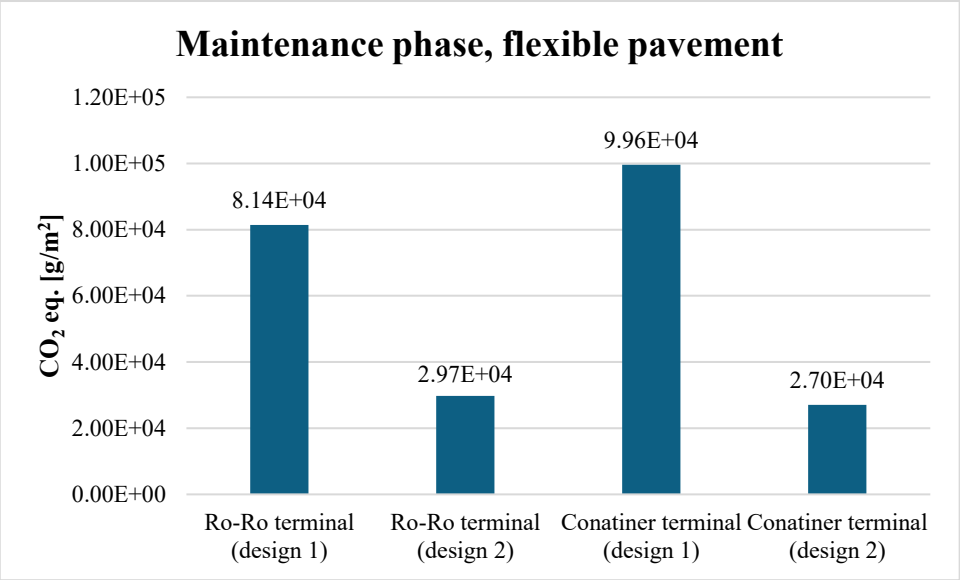

Figure 4.2.8: Results of the maintenance phase of flexible pavements

The results show that the "design 2" have the highest emissions, this is due to the fact that these designs are composed of a thick layer of asphalt concrete, laid over an unbound granular subbase layer. Whereas the designs 1 are composed of a layer of asphalt concrete, a cement bound layer and a subbase unbound layer. Therefore the thicknesses of the asphalt layers in "design 2" are the highest ones, compared to "design 1". This is reflected in the structural maintenance calculations, which include the reconstruction of the asphalt layers every 5 years.

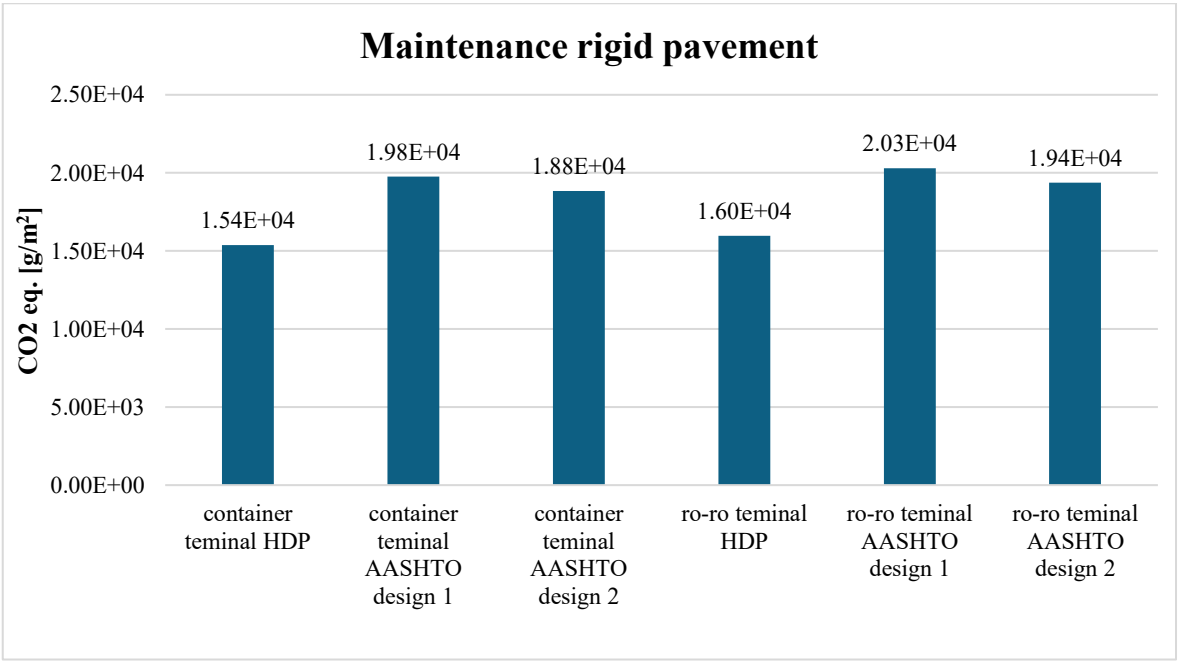

Figure 4.2.9: Results of the maintenance phase of concrete pavements

The results show that the CO2 eq. emissions are similar across the different terminal designs. The highest values are found in AASHTO design 1. This is attributed to the "production of concrete for filling", which is the most crucial contributor in the maintenance phase. The Production of concrete for filling accounts for 10% of the CO2 eq. emissions of the production of concrete, in the construction phase. This is based on the grams of CO2 eq. emitted per m^3 of concrete produced.

Therefore it is linked to the volume of concrete produced. Thus each design will show different results, based on the thickness of the concrete layer, and its extension. Since the AASHTO design 1 are the ones with the thicker layer of concrete, this is reflected in the overall maintenance results.

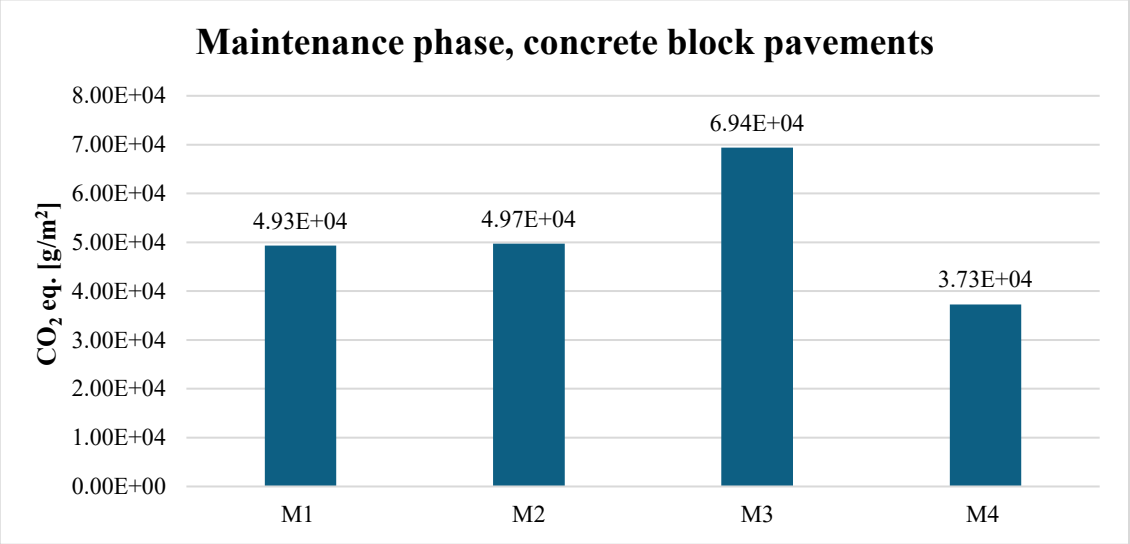

Figure 4.2.10: Results of the maintenance phase of concrete block pavements

The concrete block pavements maintenance plan included both the milling and reconstruction of asphalt layer, every 5 years, and the maintenance of concrete blocks layer every 10 years, and the general operations every year. Consequently the results are higher than the rigid pavements ones, because of the asphalt layers activities, but lower than the flexible pavements, design 2. This is due to the fact that the asphalt layers thicknesses are less than half on the ones in the flexible pavements “design 2”. Furthermore, the thickness of the concrete block layer is one third of the ones used in the rigid pavements designs. In light of these considerations, the overall results for the concrete block pavements are appropriately position halfway between the most impactful in the flexible and rigid pavements.

The overall results for the maintenance phase of all the pavement's designs are collected in the graph below:

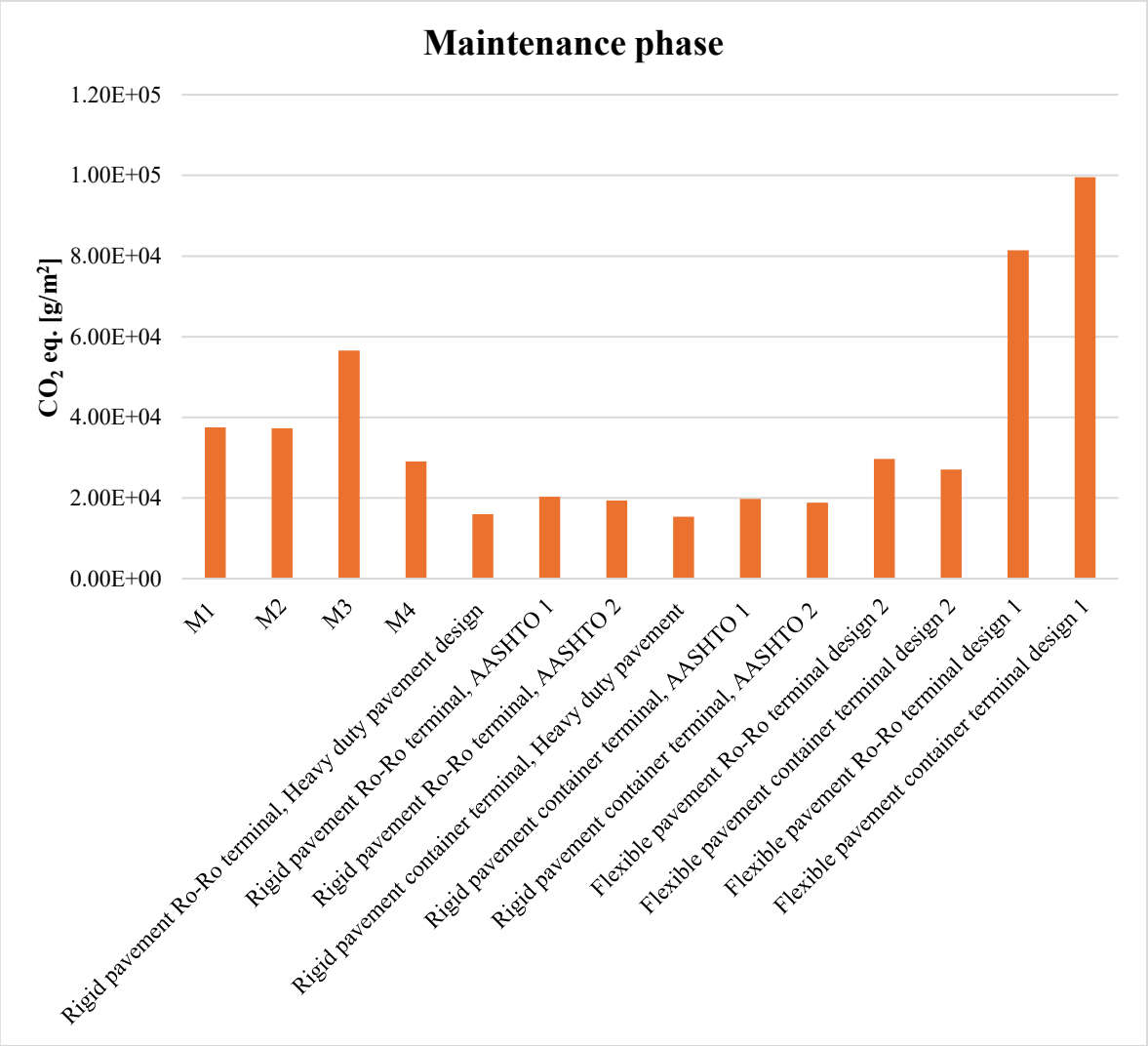

Figure 4.2.11: Results of the maintenance phase of rigid, flexible and concrete block pavements

This graph highlights previous considerations, confirming that the highest carbon footprint is due to the flexible "design 2", compared to the other designs, followed by the concrete block pavements, as they are composed of two layer of asphalt, underneath the concrete block one. The rigid pavement designs are the less impactful. This result is aligned with literature fundings that state that rigid pavements require a less frequent maintenance, which is also more economical, and as a result of this analysis, more environment friendly, when compared to the other designs analysed. However it is necessary to mention that the activities reported are not specific to port pavements, and are based on the ones indicated in the IVL Swedish report. Hence on other regions of Europe, or globally, maintenance activities or surface clearing operations, may vary based in weather conditions. Furthermore the accuracy of the results could be enhanced when considering activities that are strictly related to the pavement's purpose. Ultimately while these findings provide valuable insight into the environmental impact of maintenance operations, it is essential to acknowledge that they may fluctuate based on the multitude of variables outlined above.

4.3 Final results

The final results of the LCA cycle, accounting for construction and maintenance phase, are:

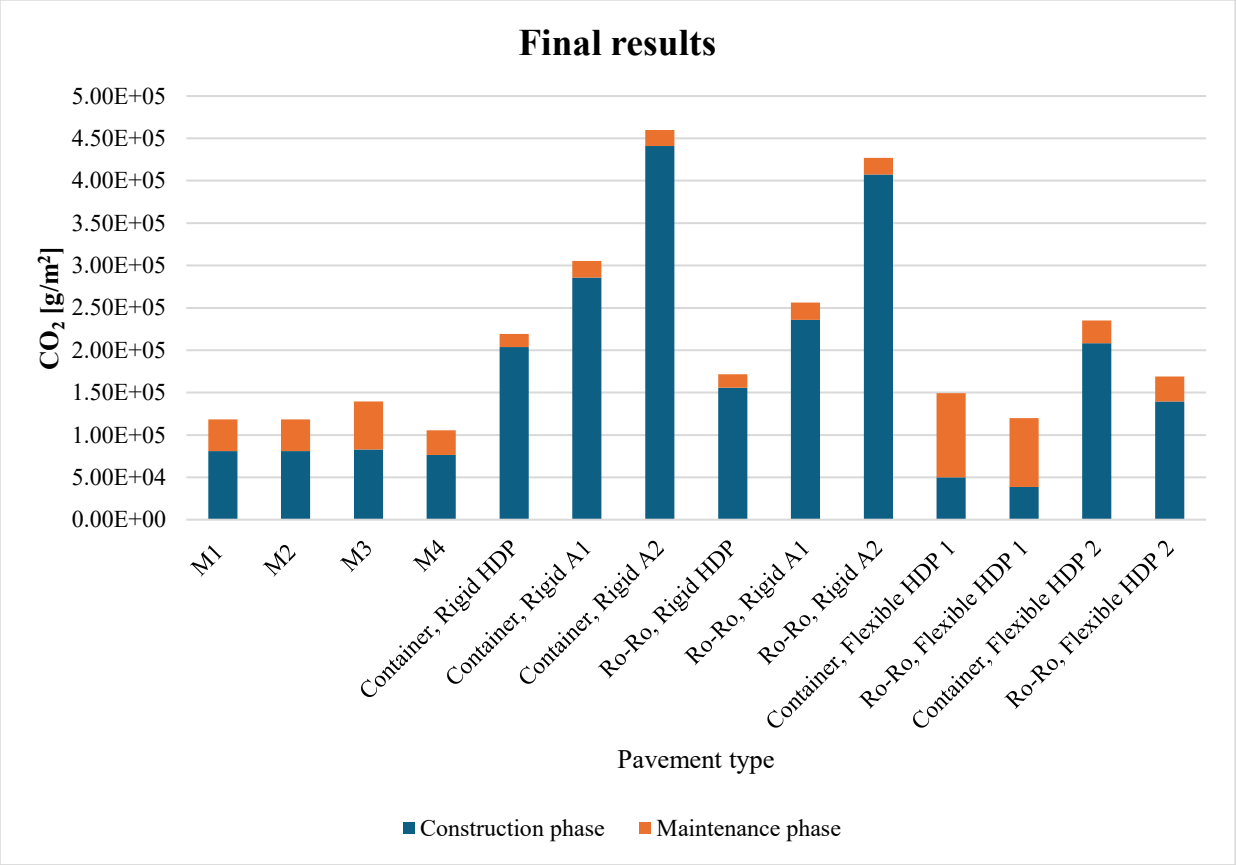

Figure 4.3.1: Results of the complete LCA cycle

Overall the maintenance phase results have lower impacts compared to the construction phase. The only exception is represented by the "design 2", across the two terminals, of the flexible pavements. As previously stated the maintenance plan includes the reconstruction of the asphalt layer every 5 years, since the layers are very thick, this results in a lack of balance between the construction phase and maintenance one. For analogous reasons the maintenance has a greater impact when considering the concrete block pavements, M1 to M4, compared to the rigid ones.

In conclusion, the construction phase is the one with the highest carbon footprint, in the LCA analysis, with the exception of "design 2" of the flexible pavement.

5 Conclusions

The present thesis study aimed at analysing, and comparing the carbon footprint of three different pavement technologies through the use of the LCA cycle. The initial task was to design two alternative pavement designs, to the concrete block pavements in use in Norvik port. The pavements designed are both rigid and flexible. They have been designed using the Heavy duty pavement manual, and, subsequently with a widely known method, the AASHTO '93 manual, in order to compare the different analysis methodologies.

Overall both methodologies show valid results, with the exception of the flexible pavement designed following the AASHTO ’93 indications, which is not consistent with the minimum requirements indicated in the manual. Therefore it has not been included in the LCA analysis.

Generally, the Heavy duty pavement’s designs resulted in a lower thickness in the surfacing layers, compared to the AASHTO ’93 designs, considering the same subbase thickness.

The rigid and flexible designed were compared to the concrete block pavements, currently used in Norvik port, Sweden, through the LCA. This analysis included two phases:

- Construction phase
- Maintenance phase

The first one accounted for the production of the materials used in the pavement’s layers, and their transportation to mixing areas, when necessary, and to the construction site. Furthermore specific operational procedures such as paving of asphalt and concrete layers, stabilization of cement bound base and compaction of granular subbase were taken into account.

The second phase was evaluated considering distinct maintenance operations of concrete or asphaltic layers, combined with surface operations aimed at maintaining the cleanliness of the pavement.

The environmental impact of those processes was evaluated through CO_2 equivalent emission, in g per one meter square of pavement

The results of the LCA analysis, in the construction phase, show:

- The overall highest environmental impact, in terms of CO_2 eq. is due to the rigid pavements
- The overall lower environmental impact, in terms of CO_2 eq. is due to the flexible pavement HDP 1 design
- In the construction phase of the cycle, the highest emissions are due to the “production of cement” step, followed by the “production of bitumen”.
- The production of binder is increasing with the thickness of the layer, where the binder is employed. Therefore thick concrete slabs do not result in an optimal design.

Whereas the conclusions of the maintenance phase analysis are:

- Overall the maintenance phase has a lower environmental impact than the construction phase
- The only exception is represented by the flexible pavement design 1, across both terminals, which shows higher carbon footprint during maintenance, than during construction. This result is a consequence of the thickness of the asphalt layer, which is reconstructed twice during the lifetime of the pavement

The overall conclusions across both phases show:

- The construction phase has the overall higher emissions compared to the maintenance phase
- Observing the outcomes in the construction phase only, which is the one with the highest emissions between the two phases, the optimum result would be the flexible pavement design HDP 1, as stated in the abstract. However the addition of the maintenance phase, constituted as assumed in this thesis, has a significant impact on this design. Therefore the

real optimum solution is represented by the concrete block pavements currently employed in the port.

It is recommend to integrate a more detailed performance analysis to the LCA cycle, to have a more comprehensive evaluation of the results. Studies show that there are numerous concerns when it comes to the employment of flexible pavements in heavy duty areas. The surfacing layer of asphalt pavements is composed of a bituminous mixture. Bitumen is a viscous-elastic material, and its characteristics are contingent upon temperature variations. Therefore this pavement is likely to experience rutting and thermal cracking. Another factor influencing bitumen's performance is loading time, therefore studies strongly suggest to not employ flexible pavements in areas where they will have to sustain prolonged heavy loads. This applies to container areas in ports, where the static loads transferred to the pavement are significantly heavy, especially because containers are often stacked. (Di Mascio et al., 2019) However various ports employ flexible pavements in ports, such as Hamburg port, in Germany. This is possible because studies show that the resilience of asphalt pavements can be increased when the bitumen mixture is modified with polymers. The addition of polymers in bitumen mixtures can increase stiffness, which results in a significant performance improvement compared to standard bituminous mixtures.

Conversely, concrete pavements do not experience rutting, however they are overall more costly to implement. Furthermore, they have a significant negative impact on the environment.

As previously stated the use of concrete block pavements is increasing throughout the world, this is due to several benefits like the easy and rapid maintenance, the presence of a stiff surface made of concrete blocks, which is able to withstand heavy static loads, costs of production. This pavement technology is recommended by the heavy duty pavement manual, as it is considered as the reference pavement, from which other designs can be derived.

In conclusion, it is recommended to include a more detailed performance analysis, including variations of the traditional pavements analysed, obtained using recycled materials, such as reclaimed asphalt pavement or construction demolition waste. Furthermore, a thorough evaluation should comprehend a cost analysis, as the pavement's costs can lead up to 25% of the total construction cost (Di Mascio et al., 2019).

Bibliography

AASHTO. (2001). *AASHTO guide for design of pavement structure 1993*.

A.Guarin. (2023). *AF2901, Road and Railway Engineering, 2.10 AASHTO design example* .

Airport Engineering Division, F. (2010). *AC 150/5320-6F, Airport Pavement Design and Evaluations, 10 November 2016*.

Balieu, R. (2022). *LCA analysis for road construction*.

B.Shackel. (1990). *Design and construction of interlocking concrete block pavements* . ELSEVIER SCIENCE PUBLISHERS LTD.

Di Mascio, P., Loprencipe, G., & Moretti, L. (2019). Technical and economic criteria to select pavement surfaces of port handling plants. *Coatings*, *9*(2). https://doi.org/10.3390/coatings9020126

Fastställd. (2006). *SVENSK STANDARD*. www.sis.se

Huang, Y., Bird, R., & Heidrich, O. (2009). Development of a life cycle assessment tool for construction and maintenance of asphalt pavements. *Journal of Cleaner Production*, *17*(2), 283–296. https://doi.org/10.1016/j.jclepro.2008.06.005

J. D. Rodriguez Millan. (2024). Smart pavement maintenance infrastructure operation through digital twins,case study for Norvik port Sweden. In *Smart pavement maintennace and infrastructure operation thorugh digital twins*.

Jamshidi, A., Kurumisawa, K., White, G., Nishizawa, T., Igarashi, T., Nawa, T., & Mao, J. (2019). State-of-the-art of interlocking concrete block pavement technology in Japan as a post-modern pavement. In *Construction and Building Materials* (Vol. 200, pp. 713–755). Elsevier Ltd. https://doi.org/10.1016/j.conbuildmat.2018.11.286

Kenneth, L. (2020). *KRAV 1 (1 4 1) Skapat av (namn och organisatorisk enhet) Dokument-ID Version Bitumenbundna lager*.

King, D., & Taylor, P. (2023). Concrete Overlay Strategies for Improving Pavement Resilience. *Transportation Research Record*, *2677*(8), 259–269. https://doi.org/10.1177/03611981231156570

Knapton, J. (2008). *THE STRUCTURAL DESIGN OF HEAVY DUTY PAVEMENTS FOR PORTS AND OTHER INDUSTRIES EDITION 4 heavy duty Uniclass L534 THE STRUCTURAL DESIGN OF HEAVY DUTY PAVEMENTS FOR PORTS AND OTHER INDUSTRIES EDITION 4*. www.paving.org.uk

LIebherr Container Cranes Ltd. (n.d.). *Liebherr Straddle Carrier*.

Sengun, E., Kim, S., & Ceylan, H. (2024a). A comparative study on structural design of plain and roller-compacted concrete for heavy-duty pavements. In *Road Materials and Pavement Design* (Vol. 25, Issue 2, pp. 392–422). Taylor and Francis Ltd. https://doi.org/10.1080/14680629.2023.2209194

Sengun, E., Kim, S., & Ceylan, H. (2024b). A comparative study on structural design of plain and roller-compacted concrete for heavy-duty pavements. In *Road Materials and Pavement*

Design (Vol. 25, Issue 2, pp. 392–422). Taylor and Francis Ltd. https://doi.org/10.1080/14680629.2023.2209194

Siverio Lima, M. S., Hajibabaei, M., Hesarkazzazi, S., Sitzenfrei, R., Buttgereit, A., Queiroz, C., Haritonovs, V., & Gschösser, F. (2021). Determining the environmental potentials of urban pavements by applying the cradle-to-cradle lca approach for a road network of a midscale German city. *Sustainability (Switzerland)*, *13*(22). https://doi.org/10.3390/su132212487

Sol-Sánchez, M., Moreno-Navarro, F., Hidalgo, M. E., Pérez, V., & Rubio-Gámez, M. C. (2020). Laboratory study on asphalt mixtures for application in port pavements. *Construction and Building Materials*, *235*. https://doi.org/10.1016/j.conbuildmat.2019.117513

Stripple, H. (2001). *Life Cycle Assessment of Road A Pilot Study for Inventory Analysis Håkan Stripple*. www.ivl.se

Wintruff, N. C., & Fernandes, J. L. (2023). A Review on Life Cycle Assessment of Pavements in Brazil: Evaluating Environmental Impacts and Pavement Performance Integrating the International Roughness Index. In *Sustainability (Switzerland)* (Vol. 15, Issue 19). Multidisciplinary Digital Publishing Institute (MDPI). https://doi.org/10.3390/su151914373